

**CUSTOMIZATION OF MODFLOW AND MT3DMS  
MODELS FOR INTEGRATED WATER RESOURCE  
MANAGEMENT IN COASTAL AQUIFERS IN THE  
SULTANATE OF OMAN**

A thesis submitted to the  
*UPES*

For the Award of  
*Doctor of Philosophy*  
in  
*Civil Engineering*

**By**  
**Javed Akhtar**

**October 2023**

**SUPERVISORS**

**Dr. Syed Mohammed Tauseef**  
**Dr. Ahmed Sana**



**Sustainability Cluster**  
**School of Advanced Engineering**  
**UPES**  
**Dehradun-248007; Uttarakhand**

**CUSTOMIZATION OF MODFLOW AND MT3DMS  
MODELS FOR INTEGRATED WATER RESOURCE  
MANAGEMENT IN COASTAL AQUIFERS IN THE  
SULTANATE OF OMAN**

A thesis submitted to the  
**UPES**

For the Award of  
***Doctor of Philosophy***  
in  
***Civil Engineering***

**BY**  
**Javed Akhtar**  
**(SAP ID:500055804)**

**October 2023**

**Supervisor**

**Dr. Syed Mohammed Tauseef**  
***Professor & Associate Dean (R&D)***  
**UPES**

**External Co-Supervisor**

**Dr. Ahmed Sana**  
***Associate Professor***  
**Department of Civil & Architectural Engineering,**  
**Sultan Qaboos University, Muscat, Oman**



**Sustainability Cluster**  
**School of Advanced Engineering**  
**UPES**  
**Dehradun-248007; Uttarakhand**

## **DECLARATION**

I declare that the thesis entitled “**Customization of MODFLOW and MT3DMS Models for Integrated Water Resource Management in Coastal Aquifers in the Sultanate of Oman**” has been prepared by me under the guidance of **Dr. Syed Mohammed Tauseef, Professor & Associate Dean (R&D), UPES and Dr. Ahmed Sana, Associate Professor, Sultan Qaboos University, Muscat**. No part of this thesis has formed the basis for the award of any degree or fellowship previously.



**(Javed Akhtar)**

**Sustainability Cluster,  
School of Advanced Engineering,  
UPES  
Dehradun-248007; Uttarakhand  
October 2023**

## **CERTIFICATE**

I certify that Javed Akhtar has prepared his thesis entitled “**Customization of MODFLOW and MT3DMS Models for Integrated Water Resource Management in Coastal Aquifers in the Sultanate of Oman**”, for the award of PhD degree of the UPES, Dehradun, India under my guidance. He has carried out the work at the Sustainability Cluster (Formerly Department of Health, Safety, Environment and Civil Engineering), UPES, Dehradun, India.



Supervisor

**Dr. Syed Mohammed Tauseef**

**Professor and Associate Dean (R&D)**

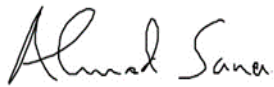
**UPES**

**Dehradun-248007; Uttarakhand**

**October 2023**

## **CERTIFICATE**

I certify that Javed Akhtar has prepared his thesis entitled “**Customization of MODFLOW and MT3DMS Models for Integrated Water Resource Management in Coastal Aquifers in the Sultanate of Oman**”, for the award of PhD degree of the UPES, Dehradun, India under my guidance. He has carried out the work at the Sustainability Cluster (Formerly Department of HSE & Civil Engineering), UPES, Dehradun, India.



External Co-Supervisor

**Dr. Ahmed Sana**

**Department of Civil & Architectural Engineering**

**Sultan Qaboos University, Muscat**

**Sultanate of Oman**

**October 2023**

## ABSTRACT

Countries with arid and semi-arid climates, which have low surface water resources and limited rainfall, are constantly exposed to the danger of excessive exploitation of their groundwater aquifers. The management of groundwater is crucial for the current and future development of the Sultanate of Oman, as it serves as the primary water source for agriculture and industrial purposes. Accurately estimating aquifer properties, water levels, and rates of groundwater abstraction is essential for effective management of groundwater resources. Numerical model is an accurate and economical tool to simulate and predict the head and quality of groundwater in the coastal aquifers if fed properly with the available data of observation head, pumping rates, geo-hydrological parameters, boundary conditions, etc.

The study focused on the coastal aquifer of Wadi Al-Jizi in Sohar wilayat of Al Batinah region, Sultanate of Oman. The aquifer is facing a chronic water deficit caused by over-abstraction for domestic, industrial, and agricultural activities, which has led to a continuous decline in water levels. The three-dimensional groundwater modelling system (GMS) which includes MODFLOW and MT3DMS was employed to simulate groundwater flow and seawater intrusion. The steady-state condition of the year 2000 was used to manually calibrate the model using observed groundwater elevations. The parameters used for calibration are the hydraulic conductivity and vertical anisotropy of a two-layered model. Computed groundwater elevations showed a good agreement with the observed values in the study area. Field data in the form of the observed water elevations was available and hydrogeological data from the previous studies was used for calibration of the model. A sensitivity analysis was carried out on the hydraulic conductivity of both layers to estimate the impact of uncertainties in this model parameter on the numerical results.

Twenty- two abstraction wells were used to study the water abstraction from the study area having the similar location as the previous work. The groundwater elevation data from a set of nine monitoring wells was used in the calibration process. After calibration, the model was validated in the transient state from 2000 to 2017.

The groundwater elevation data and model results indicated that the water levels will rise and fall according to the expected wet and dry recharge periods with significant decline and substantial seawater intrusion in the dry periods. The groundwater elevations in the aquifer then recovered in the wet years.

Various management scenarios were considered for predictions using the validated model. Two sets of scenarios of increased pumping rates by 10 %, 20 % and 30 % and reduced pumping rates by 5 % and 10 % with respect to the year 2017 pumping rates were considered in the predictive simulation. If the current rate of groundwater abstraction continues, the study area's water table is expected to fall by an average of 2.0 m by the year 2040, according to the model's predictions. For the pumping rates reduced by 10% from the 2017 base pumping rates, water level, though lower than the one computed in 2017, could improve water levels and mitigate saline intrusion.

Twenty salinity monitoring wells and same number of pumping wells were used for calibration of the mass transport model. Model simulation shows, if the base pumping of 2017 will be continued until year 2040, salinity intrusion (TDS >12800 mg/L) will intrude by a distance of 0.80 km inland. The condition is anticipated to deteriorate in the following years with increasing pumping rates. Two scenarios were considered to study the effects of pumping and sea level rise due to climate change on seawater intrusion in Wadi Al-Jizi aquifer: increased and decreased pumping rates and sea level rise due to climate change. According to the findings, even a slight rise of 0.5 meters in the current sea level would considerably impact the location of the interface zone, leading to an additional seawater intrusion of 0.50 km towards the land in the study region. Increase in the pumping rate by 30% with respect to baseline value may result in further transgression of salinity (nearly 1.0 km) whereas reducing the pumping rates by 10% may push back salinity intrusion by 0.60 km.

The results of this study may be valuable to decision-makers and engineers working to improve the management of groundwater resources in arid regions.

*Key words: Al Batinah region, Coastal aquifers, Numerical modelling, Groundwater flow, Sea water intrusion*

## **ACKNOWLEDGEMENT**

I would like to express my sincere gratitude and appreciation to my supervisors, Dr. Syed Mohammed Tauseef, Professor & Associate Dean (R&D), UPES, Dehradun, India and Dr. Ahmad Sana, Associate Professor, Civil & Architectural Engineering Department, Sultan Qaboos University (SQU), Muscat for their invaluable guidance and continuous support, that have led me throughout the period of my research. Without their in-depth knowledge, positive approach and psychological support from the inception of the work, this thesis could never be completed.

I would also like to thank all the panel members of the School research committee and the Departmental research committee, UPES for their constructive comments, suggestions, and salient advice during progress presentations which helps a lot to improve this study. My gratitude goes to all the anonymous reviewers who commented on my articles, which aided in the refinement of the work. I am thankful to the examiners for their constructive comments to improve the quality of this thesis.

I would like to gratefully acknowledge the support extended by the Ministry of Regional Municipality & Water Resources (MRMWR) and DEIM both for providing the relevant data and Ministry of Defence (MOD) for providing the topo sheets of the study area.

Finally, my sincere warm-hearted gratitude goes to my wife; Shakila Javed, my son; Mohammed Uzair, my daughter; Zainab and my mother for their endless love, understanding, and patience not only to complete this thesis but also to take a journey of my life this far and to the rest of my life. Finally, I wish to thank all my friends and colleagues who have supported me in any respect during the completion of this thesis.



## TABLE OF CONTENTS

ABSTRACT.....	v
ACKNOWLEDGEMENT .....	vii
TABLE OF CONTENTS.....	viii
LIST OF FIGURES .....	xi
LIST OF TABLES .....	xv
LIST OF ABBREVIATIONS & SYMBOLS .....	xvi
Chapter 1        INTRODUCTION .....	1
1.1    General.....	1
1.2    Background of the research work .....	2
1.3    Salinity intrusion.....	3
1.4    Objectives of the study .....	5
1.5    Novelty of this study.....	7
1.6    Report structure and its outline .....	7
Chapter 2        LITERATURE REVIEW .....	9
2.1    Introduction.....	9
2.2    Water management in Sultanate of Oman .....	10
2.3    National and International studies on Numerical modelling .....	14
2.3.1 Summary of Literature review .....	22
Chapter 3        METHODOLOGY .....	28
3.1    Introduction.....	28
3.2    Geographical location .....	28
3.3    Climate of the region .....	29
3.4    Topography of Al Batinah region.....	30
3.5    Rainfall in the region .....	30
3.6    Hydrogeology of the Al Batinah region .....	32
3.7    Description of the study area .....	33
3.8    Water Balance.....	34
3.9    Groundwater level.....	35
3.10    Saline intrusion in Sultanate’s Coastal Aquifers .....	36
3.10.1 Adverse effects of saltwater intrusion in Al Batinah .....	38

3.11	Secondary Data .....	41
3.11.1	Soil.....	41
3.11.2	Land Surface characteristics.....	42
3.11.3	Geology .....	43
3.11.4	Slope .....	45
3.11.5	Geomorphology.....	45
3.12	Groundwater modelling .....	47
3.13	Model Development .....	47
3.14	Three-Dimensional Mass Transport Multi species (MT3DMS).....	48
3.15	Governing Equations .....	49
3.16	Simulation Hypothesis.....	50
3.17	Hydrogeological conceptual model .....	51
3.18	Model Domain, Grid and Zoning .....	53
3.19	Boundary Conditions .....	54
3.20	Recharge .....	54
3.21	Groundwater abstraction.....	55
3.22	Groundwater levels .....	57
3.23	Hydrogeological Parameters.....	59
3.24	Model Calibration and Validation .....	59
Chapter 4	<b>RESULTS AND DISCUSSIONS</b>	<b>61</b>
4.1	Introduction.....	61
4.2	Steady-State Groundwater Flow simulation.....	61
4.3	Sensitivity to the Hydraulic conductivity value.....	65
4.4	Transient Model calibration and validation for Groundwater Flow.	67
4.5	Predictive simulation .....	70
4.5.1	Scenario 1: Incremental Pumping rates .....	71
4.5.2	Scenario 2: Reduced Pumping rates .....	72
4.5.3	Scenario 3: Effect of Sea level rise due to Climate change .....	73
4.6	Solute Transport Model .....	73
4.6.1	Steady State Transport Calibration and Validation .....	75
4.7	Impact of Pumping rates on Sea Water intrusion .....	83
4.7.1	Pumping @ baseline pumping rate of 2017.....	83

4.7.2 Pumping Increment @ 10% .....	87
4.7.3 Pumping Increment @ 20% .....	89
4.7.4 Pumping Increment @ 30% .....	91
4.7.5 Pumping Reduction @ 5% .....	93
4.7.6 Pumping Reduction @ 10% .....	95
4.8 The Impact of Climate Change on the Intrusion of Seawater.....	97
4.8.1 Sea level rise as per IPCC prediction.....	97
4.8.2 Sea level rise @ +0.25m to the base sea level .....	99
4.8.3 Sea level rise @ +0.50 m to the base sea level .....	101
4.8.4 Sea level rise @ -0.25 m to the base sea level .....	103
4.9 Management implications of the research .....	106
Chapter 5 CONCLUSIONS AND SCOPE FOR FUTURE WORK .	108
5.1 Conclusion .....	108
5.2 Future scope for work .....	110
REFERENCES .....	111
APPENDIX -A.....	123

## LIST OF FIGURES

Figure 1-1: Diagrammatical representation of flow of freshwater-seawater interface near a coastal zone (Pristy & Farooq 2020).....	4
Figure 1-2: Damaged and abandoned dates farm due to salinity intrusion (Photograph taken by: Javed Akhtar on 17 <sup>th</sup> December 2021) .....	5
Figure 2-1: Location Map of Sultanate of Oman.....	11
Figure 2-2: The main catchment systems in Al Batinah region (Abulibdeh et al. 2021) .....	14
Figure 3-1: Location map of Wadi Al Jizi Catchment.....	29
Figure 3-2 Rainfall hydrograph (1982-2010) (Chitrakar & Sana, 2016).....	32
Figure 3-3 A satellite image of Al Batinah region displays the mountains and alluvial plain, which creates a suitable environment for water retention. (MRMWR, 2008).....	33
Figure 3-4 Wadi Jizi Catchment area selected for the study .....	34
Figure 3-5 Hydrograph of some selected observation wells.....	36
Figure 3-6 Saltwater intrusion near the coast (Tabinas, 2014 – Accessed 2020, Dec. 5).....	37
Figure 3-7 Soil map .....	42
Figure 3-8 Land use and Land cover map .....	43
Figure 3-9 Geological map .....	44
Figure 3-10 Slope map.....	45
Figure 3-11 Geomorphological map.....	46
Figure 3-12 Conceptual model of Wadi Al Jizi groundwater flow system .....	52
Figure 3-13 Rainfall hydrograph of Al Khan rainfall station .....	55
Figure 3-14 Model domain showing different zones and pumping well location .....	56
Figure 3-15 Observation wells spatial distribution over the model domain.....	58

Figure 4-1: Calibrated water heads in the steady state condition in the year 2000 .....	63
Figure 4-2: Observed versus computed head (m) in steady state conditions in year 2000.....	64
Figure 4-3 Sensitivity of water table to variation of hydraulic conductivity in Layer 1: (a) NJ-1 (b) JA-2 (c) NJ-9 (d) EA-1 and Layer 2: (e) NJ-1 (f) JA-2 (g) NJ-9 (h) EA-1 .....	66
Figure 4-4 Time series plot of selected observation wells (a) NJ-1, (b) JA-2, (c) NJ-9, (d) EA-1, (e) JA-5 and (f) DE-5.....	69
Figure 4-5 Predictive simulation of groundwater elevation in (a) observation well JA-2 (b) observation well EA-1 for different pumping scenarios .....	72
Figure 4-6 Spatial distribution of salinity monitoring wells and zoning in model domain.....	76
Figure 4-7 Salinity contour map year 2000 (a) Ministry map (b) Model simulation.....	79
Figure 4-8 Salinity contour map year 2005 (a) Ministry map (b) Model simulation.....	80
Figure 4-9 Salinity contour map year 2010 (a) Ministry map (b) Model simulation.....	81
Figure 4-10 Salinity contour map year 2016 (a) Ministry map (b) Model simulation.....	82
Figure 4-11: Salinity contour in the Year 2025 during baseline pumping rates of 2017 .....	85
Figure 4-12: Salinity contour in the Year 2030 during baseline pumping rates of 2017 .....	86
Figure 4-13: Salinity contour in the Year 2040 during baseline pumping rates of 2017 .....	86
Figure 4-14: Salinity contour in the Year 2025 during pumping increment @10% .....	87

Figure 4-15: Salinity contour in the Year 2030 during pumping increment @10% .....	88
Figure 4-16: Salinity contour in the Year 2040 during pumping increment @10% .....	88
Figure 4-17: Salinity contour in the Year 2025 during pumping increment @20% .....	89
Figure 4-18: Salinity contour during the Year 2030 pumping increment @20% .....	90
Figure 4-19: Salinity contour in the Year 20240 during pumping increment @20% .....	90
Figure 4-20: Salinity contour in the Year 2025 during pumping increment @ 30% .....	91
Figure 4-21: Salinity contour in the Year 2030 during pumping increment @ 30% .....	92
Figure 4-22: Salinity contour in the Year 2040 during pumping increment @ 30% .....	92
Figure 4-23: Salinity contour in the Year 2025 during pumping reduction @ 5% .....	93
Figure 4-24: Salinity contour in the Year 2030 during pumping reduction @ 5% .....	94
Figure 4-25: Salinity contour in the Year 2040 during pumping reduction @ 5% .....	94
Figure 4-26: Salinity contour in the Year 2025 during pumping reduction @ 10% .....	95
Figure 4-27: Salinity contour in the Year 2030 during pumping reduction @ 10% .....	96
Figure 4-28: Salinity contour in the Year 2040 during pumping reduction @ 10% .....	96

Figure 4-29: Salinity contour in the Year 2025 during Sea level rise as per IPCC	98
Figure 4-30: Salinity contour in the Year 2030 during Sea level rise as per IPCC	98
Figure 4-31: Salinity contour in the Year 2040 during Sea level rise as per IPCC	99
Figure 4-32: Salinity contour in the Year 2025 during Sea level rise @ +0.25m	100
Figure 4-33: Salinity contour in the Year 2030 during Sea level rise @ +0.25m	100
Figure 4-34: Salinity contour in the Year 2040 during Sea level rise @ +0.25m	101
Figure 4-35: Salinity contour in the Year 2025 during Sea level rise @ +0.50m	102
Figure 4-36: Salinity contour in the Year 2030 during Sea level rise @ +0.50m	102
Figure 4-37: Salinity contour in the Year 2040 during Sea level rise @ +0.50m	103
Figure 4-38: Salinity contour in the Year 2025 during Sea level rise @ -0.25m	104
Figure 4-39: Salinity contour in the Year 2030 during Sea level rise @ -0.25m	104
Figure 4-40: Salinity contour in the Year 2040 during Sea level rise @ -0.25m	105

## LIST OF TABLES

Table 2-1 Water deficit in different regions of the Sultanate of Oman (MAF & ICBA 2012).....	13
Table 2-2 Hydrogeological parameters used for various studies in the Arabian Peninsula.....	23
Table 3-1 Water balance in Million cubic meter (Mm <sup>3</sup> ) per year (Sana et al., 2013).....	35
Table 3-2 Classification of groundwater salinity (MAF & ICBA 2012).....	39
Table 3-3 Spatial location of pumping wells in the study area.....	57
Table 3-4 Observation wells detail .....	58
Table 4-1 Hydrogeological parameters used for steady state model simulation .....	62
Table 4-2 Calibrated heads in the year 2000 in Steady state simulation .....	65
Table 4-3 Calibrated hydrogeological parameters used for transient model simulation.....	67
Table 4-4 Observed and computed head of observation wells .....	71
Table 4-5 Location of salinity monitoring well with observed salinity in the year 2000, 2005, 2010 and 2016.....	74
Table 4-6 Observed and computed salinity (Base pumping rates) .....	84
Table 4-7 Predictive scenarios and respective salinity intrusion distance.....	105
Table A-5-1 Al Khan station monthly rainfall data and recharge rates.....	123
Table A-5-2 Abstraction by the pumping wells (2000-2008).....	126
Table A-5-3 Abstraction by the pumping wells (2009-2017).....	126



## LIST OF ABBREVIATIONS & SYMBOLS

<b>ADR</b>	Abstraction Desalination & Recharge
<b>ASR</b>	Aquifer Storage & Recovery
<b>ESCWA</b>	Economic and Social Commission for Western Asia
<b>EC</b>	Electrical Conductivity
<b>FAO</b>	Food and Agriculture Organization
<b>GIS</b>	Geographic Information System
<b>GCC</b>	Gulf Cooperation Council
<b>GMS</b>	Groundwater Modelling System
<b>ICBA</b>	International Centre for Bio saline Agriculture
<b>IPCC</b>	Intergovernmental Panel for climate change
<b>JICA</b>	Japan International Cooperation Agency
<b>MAF</b>	Ministries of Agriculture & Fisheries
<b>MAR</b>	Mean Annual Rainfall
<b>MCM</b>	Million cubic meter
<b>MODFLOW</b>	A modular three-dimensional finite-difference groundwater flow model
<b>MRMWR</b>	Ministry of Regional Municipalities and Water Resources
<b>MT3DMS</b>	A modular three-dimensional multispecies transport models
<b>MWR</b>	Ministry of Water Resources
<b>NWI</b>	National Well Inventory
<b>PAW</b>	Public Authority of Water
<b>RCP</b>	Representative Concentration Pathway
<b>SLR</b>	Sea Level Rise
<b>SWI</b>	Salt /Saline Water Intrusion
<b>TDS</b>	Total Dissolved Solids
<b>UAE</b>	United Arab Emirates
<b>Vani</b>	Vertical anisotropy
<b>WHO</b>	World Health Organisation
<b>°C</b>	Degree Celsius
<b>k</b>	Hydraulic conductivity
<b>km</b>	Kilometre
<b>m<sup>3</sup></b>	Cubic meter

<b><math>\mu\text{S/cm}</math></b>	Micro Siemens per centimetre
<b>mg/L</b>	Milligram per litre
<b>l/sec</b>	Litre per second

## CHAPTER 1 INTRODUCTION

### 1.1 General

Water is rapidly depleting earth's valuable natural resources. As an estimate, 99.4% of the water available as surface water, while groundwater accounts merely 0.6%. Conventional surface water resources were hassled due to growing water demands and led the way to the groundwater extraction to deal with potable water scarcity (Bear, 1999). Since the beginning of the modern Renaissance in the early 1970s, considerable attention has been devoted to water supplies in the Sultanate of Oman, given the country's reliance on groundwater and rain, primarily due to its geographic position and climatic conditions. Water resources are an issue of major importance in the Sultanate, with 98.7% of the population benefiting from safe drinking water services (Supreme council for planning, 2019).

Approximately one-third of the Earth's land surface is categorized as either arid or semi-arid. Available favourable places with water and soil already being utilized in most of the globe, which shift the focus on arid regions to satisfy the growing population demands of portable water and food subjecting these regions under tremendous pressure. Over the past 150 years, the total population of the world has risen four times and may double over the next 30 years. Future estimates show that five billion individuals will be living in nations with mild or serious water stress by 2025 (WHO, 1997).

All the water which is available in the subsoil is termed as groundwater not always accessible in the areas where rainfall is scanty, and abstraction is high. It is a significant resource of water supplying one-third of the world's drinking water. Huge volumes of water are needed for the country's development to cater per capita demand of the increasing population with limited groundwater resources. These depleting resources must be protected from all sorts of contamination. Mostly, population increased in the region having easy access to the coastal groundwater aquifers which can be used for agricultural and domestic supplies thus depleting these resources, resulting salinity intrusion. The utilization of high salinity groundwater for drinking and irrigation purposes

is limited unless it is blended with water of reduced salinity or undergoes desalination. Given the growing demands and diminishing resources, safeguarding groundwater resources has become essential.

## **1.2 Background of the research work**

The word contamination is used because of human activities to add any solute to the hydrological system, whereas the word pollution is limited to a scenario where the contamination reaches concentrations that are deemed objectionable. In the past few decades, the quality of groundwater as well as surface water deteriorated considerably in several areas of the world, triggering fear in the developed and the developing nations. Surface water sources contamination in rivers, lakes and wadis can be easily detected in comparison with pollution of groundwater resources which is slow and non-traceable in the initial stages. Even if traced, usually it becomes challenging with the passage of time to cope with it (Singhal and Gupta 2010).

Over the previous few centuries, water quality has degraded rapidly in many coastal aquifers globally due to salinity intrusion. Over-exploitation of groundwater basins for domestic or agricultural use resulted in dropping water tables and intrusion of saltwater. Hundreds of pumping wells along the shoreline had to be shut down in many nations around the globe, including the Sultanate. Natural brines, leachate from landfill liner system and the seepage of irrigation return water from agricultural farms can also contaminate groundwater apart from seawater intrusion (Bolster et al. 2007).

The quality of groundwater is a significant problem in water resources growth and management. An increase in the population throughout the world leads to the escalation in the potable water requirements, whereas the quality related issues prevent the increase in these resources. On getting polluted surface as well as groundwater resources use to get polluted. Groundwater sources appears to be more protected from the contamination, to deal with due to still can have pollution which later becomes tiring and expensive to deal with.

### **1.3 Salinity intrusion**

In the coastal regions, due to proximity of sea with the aquifers, salt water encroaches fresh groundwater, thus threatening it continually by salinization. The coastal aquifers are more subjected to saltwater intrusion lowering the quality by exceeding standard values of salt content present in water used for drinking or irrigation, thus threatening the quality of the source and polluting to an extent which may be difficult to eliminate and to use the resource in the future (Khublaryan et al, 2008).

Due to the fast disturbances caused by groundwater pumping, the rate of inland saline/saltwater intrusion (SWI) got accelerated. Withdrawal of groundwater more than the recharge capabilities often results in pollution due to salinity intrusion (Bobba 2000). Excessive pumping of groundwater for development in various sectors lower the groundwater head that that of adjacent saline water of the sea resulting in salinity intrusion which will further results in other issues like reduction in the supply of fresh water, human health, and harm to the ecosystem (Kumar et al. 2015).

Use of coastal aquifers as an effective source of potable water needs enhanced methods to predict their behaviour under distinct circumstances. Seawater intrusion models are, therefore, effective means for managing and protecting the coastal aquifers (El Hamidi et al. 2021; Ranjan at el. 2008). Due to non-homogeneous nature of subsoil, geology, topography, land cover features, and land use of the different regions, accurate calculation of groundwater recharge is cumbersome in arid and semi-arid regions. Furthermore, the temporal unpredictability of precipitation and other hydrometeorological factors in these areas may compound these challenges (Izady et al. 2017).

When salt water enters a coastal aquifer, it presents a major environmental and financial danger throughout the globe as even a very tiny amount of marine water mixing with the freshwater makes it unpotable. In the absence of sufficient sources of potable drinking, many countries with hot and humid conditions either looking for another available resource or treating sea water by desalination, producing expensive water not easy for any country to afford (Bolster et al. 2007). Elevated levels of total dissolved solids (TDS), significant cations and anions, as well as selective trace element accumulation are typically

observed in groundwater when the intrusion of seawater is a significant contributor to increased salinity (Mondal et al. 2011).

Intrusion of seawater occurs under natural circumstances when the groundwater density is lower than that of the seawater with which it interacts hydraulically. The water from the sea having high salt content is moving close to the bed floor, while the interface between seawater and groundwater is taking complex form as shown in Figure 1-1. An interface is created where the seawater in meeting with the fresh groundwater, thus making a transition zone. The location and size of this zone depends on seawater density, groundwater discharge rate, and other features.

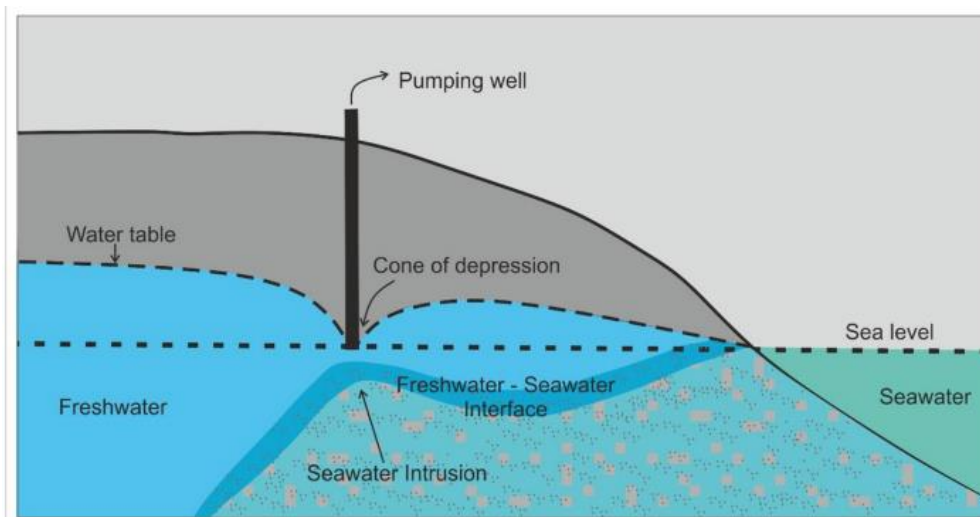


**Figure 1-1: Diagrammatical representation of flow of freshwater-seawater interface near a coastal zone (Pristy & Farooq 2020)**

As the salt content increases, the water becomes unfit for human consumption and drinking water must be brought in by tankers from wells in other areas. As the salinity increases further, crops gradually become less productive, and even the most salt-tolerant plants, such as date palms cannot grow and lands which were used to be productive must be abandoned. In these area collapsing wells and scattered palm trunks as shown in Figure.1-2 are the testimony of the damage caused by the saline intrusion.



**Figure 1-2: Damaged and abandoned dates farm due to salinity intrusion (Photograph taken by: Javed Akhtar on 17<sup>th</sup> December 2021)**

#### **1.4 Objectives of the study**

Acute shortage of portable water resources has been faced by several countries, including Sultanate of Oman. Potable water in Oman and the Gulf region is the most restrictive and strategically significant natural resource. The country's absence of freshwater resources is a significant disincentive to its sustainable development. Although non-renewable, subsurface water in the coastal aquifers contributes as the major means of water supply for different activities in the region. The dynamic equilibrium between freshwater and seawater was upset and the groundwater quality degraded. Rapid increase of population and sea level rise due to climate changes exacerbate the condition, which in turn leads to further intrusion. The issue calls for urgent attention.

In an arid climatic condition and scanty rainfall patterns, if the abstraction rate is higher than the recharge rate of aquifer, the groundwater table depleted resulting in lesser available volume. This reduction results in contamination of groundwater quality with the lower water heads available in the wells increasing costs of pumping (Senanayake et al. 2016). The reduced levels of groundwater will be resulting in the landward movement of seawater, as a result, posing a

serious threat to the quality of groundwater (Abulibdeh et al. 2021; Abd-Elhamid et al.,2015).

In Al-Batinah region the situation is similar to that in other places around the globe. Groundwater quality severely affected in many parts of the region due increase in the salinity level rendering unfit for human consumption. The production of crops, even date palms which are known for their tolerance to higher salinity levels, has been impacted due to increased salinity levels. The demand for groundwater is extremely high, leading to over-exploitation and significant stress on the groundwater resources. As the salinity levels of the soil continue to rise, farms have been abandoned, and in some areas of Al Batinah, up to 750 wells have been left unused within 6 km of the coastline. This emphasizes the urgent attention to use proper conservation measures to protect this valuable natural resource (MRMWR 2008).

This study was conducted to investigate the seawater intrusion problem in Sultanate of Oman using numerical modelling. Considering the serious concerns regarding water security in Sultanate of Oman (and in the world in general), and its significant influence on sustainable development of the country, the present study has strategic importance. Also, the direct relationship between water, energy and food makes tackling this problem and controlling seawater intrusion vital to the economic and social development of the country.

The main objectives of the current study were:

1. Assessment of groundwater potential of Wadi Al-Jizi Aquifer using remote-sensing GIS techniques
2. Customization of model based on MODFLOW and MT3DMS for Al Batinah coastal aquifer for simulation of seawater intrusion and suggesting suitable mitigation measures.
3. Assessment of the water management techniques using the numerical modeling in response to the threats posed by population increase.
4. Study the effect of climate change and sea level rise on coastal freshwater resources in Oman.



## 1.5 Novelty of this study

The area of the Wadi Al Jizi catchment which was chosen for the study is more or less similar to what was studied in the past (Al Sibli, 2002). However, this study is timely and novel with the following inclusions:

- The geological and hydrogeological data from 1988 to 2001 was used in the past study. In the present study, the data collected from 2000 -2017 is used for the model simulation. The data of the year 2000 is used for the steady state calibration. Based on the initial conditions of the steady state results, the transient model simulation was carried out from 2000 -2017. The data from 2000 -2009 was used for the transient state calibration and 2010 -2017 data is used for the validation before using the model for the management scenarios and the salinity intrusion studies.
- Moreover, a finer grid resolution than what was chosen in the past study (270 x 280 m) is considered for this model. The grid is finer (5 x 10 m) at all the pumping well locations and becomes coarser (40 x 80 m) for rest of the model domain.
- A transient calibrated model is used for the various management scenarios to predict the groundwater elevations and the resultant salinity intrusion from 2018 -2040. The increment and the reduction in the base pumping rates and the effect of the climate changes in terms of Sea level fluctuations were used in the present study for the predictive simulation.

## 1.6 Report structure and its outline

To cover the above-mentioned objectives, during course of the research, thesis is designed to cover each one of them which has been presented in the form of chapters which are as follows:

- **Chapter 1** gives the study area's background and highlights the salinity issue, along with the research objectives.
- **Chapter 2** is about the literature review for the salinity intrusion and the groundwater management in the Sultanate of Oman and in the Al Batinah Plain in general, application of numerical modelling using different model codes at the national level and globally to study the groundwater heads and to deal with the salinity intrusion.

- **Chapter 3** presents the research methodology, provides an overview of the study area, including its geology, geomorphology, hydrogeology, and the available groundwater system. Conceptual model with all the details of grid, boundary conditions, layers used with the stress period used and comprehensive three-dimensional groundwater numerical modelling with MODFLOW and MT3DMS.
- **Chapter 4** deals with the results and discussion about the model calibration and validation, various scenarios used for studying the fluctuating groundwater level and extent of salinity intrusion in the coming years and discuss the management implications of the current study.
- **Chapter 5** draws the conclusions of this study, highlighting potential factors to be considered for the future studies and followed by the references and appendix at the end.

## CHAPTER 2 LITERATURE REVIEW

### 2.1 Introduction

The Arabian Peninsula is the largest peninsula in the world with an area of 3.24 million square kilometres. It consists of seven countries: Sultanate of Oman, United Arab Emirates, Saudi Arabia, Qatar, Kuwait, Bahrain and Yemen. These countries are members of Economic and Social Commission for Western Asia (ESCWA) region located in an extremely arid zone and severe climate conditions. (Al Damkhi et al., 2009).

Throughout the Arabian Peninsula, shortage of water supplies currently affecting some parts of the region, which would become more severe and widespread in the coming years (Khorri, 2003). This is exacerbated by the seawater intrusion; sea level rises due to climate changes and population growth. The majority of the Arabian Peninsula's small to medium-sized exploitable fossil aquifer systems will hit maximum depletion by 2050, and in 60-90 years the complete depletion of groundwater supplies in all aquifer systems could be reached (Mazzoni et al. 2018). Since, there is a direct relationship between the available potable water resources, energy and food, managing salinity intrusion is of vital importance to economic and social growth of any country. Therefore, management of groundwater is the need of the hour for sustainable development (Mogren, 2015).

To satisfy growing demands in urban areas, Arab countries are using more treated municipal wastewater. According to an estimate the volume of treated wastewater is around 4.7 billion cubic meters per annum and rising annually. Wastewater treatment and reuse is influenced by water scarcity, financial capability, and the value of the agricultural sector (UN-ESCWA & BGR,2013). The population was found to be the most crucial factor pertaining compared to other variables. As the population increases, salinity intrusion moves further inland due to over-abstraction of water from the subsurface in the absence of proper replenishment due to arid or semi-arid region, which further emphasizes the need for environmental impact mitigation.

## **2.2 Water management in Sultanate of Oman**

Sultanate of Oman is situated on the south-eastern corner of the Arabian Peninsula and considered as the second largest country having a coastline of some 1700 km. It is bordered by the United Arab Emirates (UAE) to the northwest, to the west by Saudi Arabia, and Yemen to the southwest (Figure 2-1). At the foot of the Western Hajar mountains, lies the coastal plain of Al Batinah. The coast of Al Batinah is a general term for the long coastal plain, ranging from 10 to 60 km wide, stretching northwest at Muscat to the Musandam Peninsula (extreme north of Oman) for about 270 km. As an approximate one-third of the country's population lives in Al Batinah which hold second position in terms of population after capital city Muscat and accounts for about 4% of the complete area of the country (Kasimov et al. 2008). This region consists of fertile soil and therefore, is of vital importance to the agricultural yields of the country. The governates of North and South Al Batinah (Al Batinah region) are the most important governates in the field crops, accounting for 34% of the total cultivated area in the Sultanate ([www.omanobserver.om/article/69050](http://www.omanobserver.om/article/69050)). The main cities, in Al Batinah region starting from the north, are Shinas, Liwa, Sohar, Saham, Al Khaburah, As Suwaiq, Musanah, and Barka.

The study area Wadi Al Jizi a coastal plain groundwater aquifer is a part of Al-Batinah, (where, 'Wadi' means a dry riverbed) having same characteristics, particularly in the climate pattern of the region. Sohar city is located on the coastal plain of Al Batinah in north-western Oman (Shibli, 2002). Utilization of groundwater increased in response to the agricultural growth and cultivation intensity. Groundwater demand in the Al Batinah was about 235 Million Cubic Meter (MCM) per annum during 1980 - 84. The projected annual demand of groundwater reached 570 MCM per year (increased by 225%) by the year 1995. The use of groundwater peaked at 600 MCM per year in 1997. Subsequently, there has been a reduction in the cultivated land area leading to a total groundwater demand of 578 million cubic meters per year as of 2010 (ICBA & MAF 2012).



**Figure 2-1: Location Map of Sultanate of Oman**

Due to an average rainfall of 100 mm, the sultanate is categorized as an arid nation. The main source of fresh water in the upper catchments is rainfall, leading in the subsequent replenishment of the aquifers. The groundwater from here moves slowly toward the ocean through the aquifers. Rain falling straight on the gravel plains between the shoreline and the hills does not seem to be the main cause of the recharge as the quantity is comparatively low and most of it is absorbed by the ground and then lost to evaporation. The quality of the groundwater is highly diverse along the Al Batinah region. The quality of groundwater is good in the mountain region which gradually falls owing to its contact with some salts during its course of journey towards the sea. In the last 20 years, due to nonstop deep and shallow well boring and constantly excessive pumping in the region, that further deteriorates groundwater quality (Sana et al. 2013; Sana & Shibli, 2003).

Some of the previous legislative measures taken to decrease the intrusion of seawater were: (1) the installation of fresh groundwater wells in Al Batinah were banned, and (2) the construction of recharge dams on the chosen wadis in the region. The salinity study conducted by MWR 2000 in the year 1999 showed that the water quality improved on the downstream side of the recharge dams owing to the recharging of groundwater with fresh dam water infiltration, though there was a rise of 54% in EC compared to the study of 1997. Some improvement has also been noticed in other areas as well. A deeper understanding of the SWI is imperative for any further action to improve the water quality in the area. In addition to achieving this goal, the use of a numerical model can also be used as a management tool for decisions regarding pumping schedules and the construction of new recharge facilities in the study area (Sana & Shibli, 2003). Reduction in the pumping rates is simple and most cost-effective but temporary method for preserving groundwater equilibrium in aquifers and managing SWI problems apart from establishing subsurface physical barriers in front of the intruding seawater body, Abstraction, Desalination & Recharge (ADR) and Aquifer Storage & Recovery (ASR) (Hussain et al., 2019). Groundwater quality varies as per the distance it will measure from the sea and its depth below the seawater level (Sherif et al., 2013). It has been observed modelling software proved to be very useful and cost efficient to simulate the behaviour of groundwater resources under given conditions of time and space. A rise in the water levels has been observed due to the construction of recharge dam in the region which also helped in reducing the salinity concentrations in some of the areas. But overdraft of groundwater draws saline water inland (Al Barwani and Hilmi 2006). Walther et al. (2012) were not agreed with the idea of recharge dams helping in increase of water heads and reported negligible effect on the groundwater volume. Shamma and Jack (2009) proclaimed that model developed for Salalah plain aquifer can be as a tool by the water and environmental authorities for management of the groundwater in that area. Use of desalinated water is energy-intensive, so a main requirement for commissioning new plants and upgrading old ones should be energy efficiency. Saudi Arabia uses 25% of its oil and gas output to generate electricity and produce water in cogeneration power-desalination plants with

35% of the desalination capacity of the Arab country. This share will top 50% by 2030 if water demand continues to rise at the current pace (UN-ESCWA & BGR, 2013). For better water resource assessment and management, a regional knowledge and database is needed. The mechanisms for gathering data are always unsatisfactory. For rainfall, runoff, groundwater levels and water quality, fair comprehensive time series data is available only in a few countries (Khorri, 2003). Most of the researcher including Lathashri and Mahesha (2015) reported about the data scarcity to simulate the saline water intrusion. Table 2-1 shows the water deficit in all the regions of the Sultanate of Oman, among which Al Batinah has got the highest.

**Table 2-1 Water deficit in different regions of the Sultanate of Oman (MAF & ICBA 2012)**

<b>Region</b>	<b>Area (km<sup>2</sup>)</b>	<b>Population</b>	<b>Population Density (Person/km<sup>2</sup>)</b>	<b>Water Deficit (%)</b>
Al Batinah	12,500	7,72,590	61.8	47.6
Musandam	1,800	31,425	17.4	1.1
Ad Dhahirah	37,000	1,51,664	4.0	17.2
Al Wusta	79,700	42,111	0.5	0
Ad Dakhliya	31,900	3,26,651	10.2	17.2
Ash Sharqiyah	36,400	3,50,514	9.6	1.9
Dhofar	99,300	2,49,729	2.5	7.9
Muscat	3,900	14,75,795	378.4	7.1

Lakey et al. 1995 split the rain gauges in Eastern Al Batinah into coastal, valley, and highland areas and found the mean annual rainfalls for these areas to be 68 mm/year, 90 mm/year and 174 mm/year, respectively. The variation in the intensity occurs due to orographic impacts. Water deficit in the nation is more than 300 MCM/yr, according to projections by the Ministry of Regional Municipalities, Environment and Water Resources (MRMEWR). Because of which intrusion of seawater is imminent in the coastal aquifers where the

majority of the population is located. From 1983 to 1999, the ministry conducted detailed salinity measurements covering over 1,000 wells in the Al Batinah region (MWR, 2000). In the 1999 salinity study, it was found 35 % of the wells had an Electrical conductivity (EC) of more than 6000 micro-mhos / cm and 10 % of the complete study sites had an EC of more than 16,000 micro-mhos / cm. It can be observed that an EC exceeding 2250 micro-mhos falls into the category of ‘very high’ salinity hazard according to the USDA classification of irrigation water (Helweg, 1992). The main catchments located in the Al Batinah region are shown in Figure 2-2.

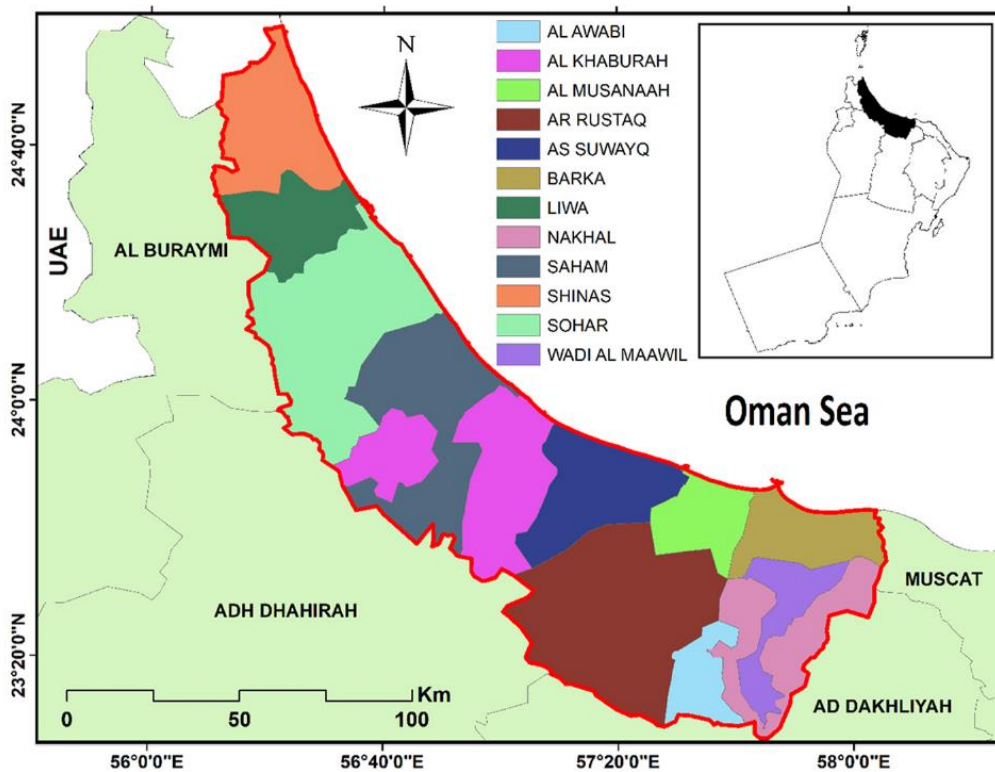


**Figure 2-2: The main catchment systems in Al Batinah region (Abulibdeh et al. 2021)**

### 2.3 National and International studies on Numerical modelling

The following studies were conducted in the Sultanate of Oman and in the other parts of the world in sighting the problem of depleting groundwater table and subsequent intrusion of saline water using various model codes:



Hani et al. (2023) studied the numerical simulation of saline water intrusion in a coastal confined aquifer (264 km<sup>2</sup>) in Seybouse basin, Algeria using MODFLOW & MT3DMS code. Calibrated model was used for the future prediction till 2045. Increment of 20% in the base pumping rates showed a reduction of 6.0 m in the piezometric heads with respect with mean sea level and saline intrusion showed up 10.0 km encroachment.

One-layer unconfined aquifer (125.6 km<sup>2</sup>) in the country Vanuatu of Pacific Island was studied. For calibrating and validating groundwater models, the Pacific Island Countries (PIC) lack sufficient groundwater and pumping well data. The region was used as an example study area, making use of the field data that was available to mimic the PIC's aquifer system. Using MODFLOW, the conceptual model was created and simulated in a steady state. The transient simulation in MT3DMS and SEAWAT was then performed using the simulated heads as beginning heads. The sea-level rise by 0.3 to 1.0 m did not substantially impact SWI inland (Sharan et al., 2023).

El – Hamidi et al. (2021) investigated the effect of climate change, Sea level rise and ground water abstraction rates on the Rmel-Oulad Ogbane coastal aquifer (ROOCA) in Morocco by using the finite difference method in Visual MODFLOW Flex. The numerical simulations were conducted for a period of approximately 76 years and dealt with saline intrusion relating to groundwater abstraction, climatic change, and sea level rise. The computed results under RCP4.5 show that the maximum extent (about 5.2 km) of SWI would increase in 2040 in the northwestern sector of the study area.

Dibaj et al. (2020) used FEFLOW to be modelled saltwater invasion in a multi-layer aquifer system in the Pingtung plain, Taiwan. Model results revealed all the layers were impacted by the intrusion, but top and bottom layers are affected more than the middle one.

Al-Muhayalan et al. (2020) applied 3D MODFLOW to define the boundary condition and other aquifer parameters of the Saq aquifer, Saudi Arabia. In addition, Artificial neural networks (ANN) and Adaptive neuro fuzzy inference systems (ANFIS) were employed to forecast groundwater level depletion over the long term. For analysing the effects of different groundwater pumping scenarios on aquifer depletion, a framework was created and used.

Baalousha et al. (2019) used MODFLOW-2000 to study the northern Karst non-homogeneous aquifer in Qatar which is the sole natural source of fresh groundwater in the country. It is formed of limestone with lots of ducts and cavities which get recharged with local precipitation. The pilot-point method and PEST tools were used to calibrate the model. Impact of number, position, and the distribution of pilot-points on the results of model calibration were examined including optimization of pilot point positions for a steady state flow. The findings showed for the given same number of points, uniformly placed pilot points perform better than points which are chosen randomly.

Razak et al. (2019) studied coastal aquifer of Tadjourah (Republic of Djibouti) in the Horn of Africa. This region suffered with high daytime temperatures and low erratic rainfall, causing continuous cycles of drought. Three RCPs (Representative Concentration Pathway) were used to simulate different climate scenarios up to 2100. The recharge information gleaned from the climate scenarios was used to simulate seawater intrusion into the aquifer using the SEWAT code. The findings show that there is a substantial probability of seawater intrusion contaminating the Tadjourah coastal aquifer. The findings of this study show how important it is for water resources management to comprehend how climate change may affect groundwater resources, particularly in coastal aquifers.

Sowe et al. (2019) used FEFLOW in Wadi Ham, UAE to simulate abstraction of saline water from the affected aquifer. They studied different simulation scenarios to achieve optimal pumping locations and rates. A distinction was made between situations of non-pumping and brackish water pumping. Rise in the groundwater salinity concentration (isoline 30,000 mg/l) was observed when there was no pumping, whereas salinity concentration (isoline 20,000 mg/l) reduced during the simulation of pumping saline water. This demonstrated an overall increase in groundwater quality and gradually stopped the infiltration of seawater into the aquifer. Maximum productivity was observed in controlling the intrusion by using sixteen abstraction wells ( $500 \text{ m}^3$  /day / well) at a distance of 1.5 km from the shoreline.

Chun et al. (2018) used SUTRA to study the salinity intrusion in the coastal groundwater system in South Korea considering SLR due to the climate change.

Their findings emphasize, both freshwater recharge rates and SLR should be taken into account for modelling an accurate assessment of climate change on saline water intrusion in a coastal aquifer.

A regional model (MODFLOW) was developed for the Qatar (entire country area of more than 11,500 km<sup>2</sup>) to improve the storage and recovery scheme for the aquifer in distress. Value of hydraulic conductivity used during the calibration varies from 0.1 m/day to more than 200 m/day. An agreement was found by the result produced during the simulation with the results available in the relevant literature. An urgent need of artificial recharge was intimated since the groundwater abstraction rate was found 250 MCM (Baalousha, 2016).

Al-Weshah and Yihdego (2016) used 3D numerical model MODFLOW-SURFACT to simulate northern Kuwait's Raudhatain and Umm Al-Aish freshwater aquifers performance which got polluted during the 1991 Gulf war due to extinguishment of fire in oil fields by using seawater. The developed model was used to assess the impact of seasonal recharge on groundwater and its flow pattern.

In Waqrah Economic Port Zone 3 (QEP3) located in Qatar, Visual MODFLOW was used to study the groundwater fluctuations due to dredging and dewatering water stored in two automated reservoirs. Results of the study intimated the groundwater flow direction towards the sea, wherein an artificial groundwater discharge field will be created by the groundwater basin surrounding the sediment basin (Lachaal and Gana, 2016).

In the Fujairah Emirate in the United Arab Emirates, Hussain et al. (2015) SUTRA to study the SWI in the lower alluvial plain of the Wadi Ham watershed. To mimic the efficiency of the control method employed, artificial recharge with treated wastewater, was used with three different stress conditions for ten years duration. In the first case, it was assumed that the current pumping and rainfall rates would continue through 2025. Keeping the base rates for pumping and recharge, salinity was studied as an initial scenario. Whereas the effects of recharge through one and three surface ponds were considered in second scenarios as next two scenarios. It was demonstrated that the aquifer's salinity concentrations significantly decreased by using the artificial recharge methods.

Lathashri and Mahesha (2015) used SEWAT to study the coastal aquifer in Karnataka, India. The model was calibrated by trial and error against the hydrogeological parameters until an agreement was reached between observed and computed values. The calibrated model was used for the transient state (two years) considering the steady state head as the initial head. The findings of the transient simulation showed that the model replicates the field conditions within acceptable limits and can be used to predict the SWI in the aquifer under various abstraction and climate change scenarios.

Nofal et al. (2015) utilized a newly developed multi-layered system configuration to model saltwater intrusion (SWI) in the Nile Delta aquifer, incorporating up-to-date information on the aquifer's heterogeneity and hydrochemistry with the SEWAT software. In past, in most of the Nile Delta aquifer research, due to data scarcity, the geological stratification of the aquifer was neglected, and aquifer was only considered a single layer of sand and gravel. The model was fully calibrated against the field data which further simulated in transient conditions for two years to study the water levels and SWI. The calculated water balance revealed that there was saltwater intrusion (SWI) into the aquifer at depths ranging from shallow to medium (up to 400 m). The deeper layers' groundwater flow towards the sea which help in pushing was the seawater from these aquifer layers thus preventing intrusion.

Pramada and Mohan (2015) used SEWAT code to study Chennai aquifer system in India. Aquifer is responsible to meet 20% of the total water supply requirement of the city. Discrepancy in the values of hydraulic conductivity may influence the length of SWI. The model run revealed even for an insignificant variation in hydraulic conductivity, the error in the intrusion length was discovered to be 14 m inland.

Ghazaw et al. (2014) used Visual MODFLOW to study the depleting level of groundwater of Saq aquifer located in Qasim area in Saudi Arabia in which recharge and inflow is negligible. Artificial recharge method to defy the depleting water level of the aquifer due to pumping. As per the results of his model run, he emphasizes that the runoff which was wasted previously can be stored in the existing pond due to artificial recharge which also help in boosting the aquifer life by 3%. The modelling results also revealed if no preventive

measure has been taken and pumping would continue, the water head in the region will drop in the next 30 years more than 65.0 m

Sana and Bawaain (2014) employed MODFLOW and MT3DMS to investigate groundwater levels and seawater intrusion (SWI) in the coastal aquifer of Salalah, which is situated in the southern region of Oman. The behaviour of the aquifer was simulated by injecting volumes of treated wastewater as a recharge source which showed a promising increase in the groundwater levels and reduced SWI in the study area.

Ghoraba et al., (2013) performed lab studies and numerical modelling (MODFLOW & MT3DMS) to examine the quality of sub surface water in the central part of Nile Delta which was a fertile agricultural land and densely populated. MODFLOW has been used to handle sub surface flow hydrodynamics through porous media, whereas the latter has been used to study the concentration of pollution in it. Model was calibrated by using the hydraulic conductivity values from the earlier research conducted in the study region. MT3DMS was used in the study region to simulate variations in ammonium contaminants. They proposed to clean up the impacted area by dewatering the polluted groundwater from aquifer for the treatment through eight extraction wells, located in contaminant's flow direction.

Al Taani et al. (2013) researched in Gulf of Aqaba, Saudi Arabia, a groundwater system situated in extremely dry climatic condition. With the exception of one, they collected groundwater samples from 23 different wells, the majority of which were privately held, shallow aquifer-drilled, and located relatively close to the east coast. Salinity was the main concern found about groundwater usability for drinking or agricultural uses. Out of 23 water samples, water from only one well had found to had a reasonable TDS value and fit to use, whereas rest groundwater wells displayed brackish water which may not even suitable for irrigation purpose.

An increase in the water supply requirement had been noticed in the Burdayah Al Qasim area getting supply from Saq Aquifer in Saudi Arabia. Pumping of water escalated from the aquifer resulted in the depletion of water head by 1.10 m per year. The results of the MODFLOW showed if the base rates of

abstraction increased by 10% per 10 years period, then there will be a depletion of water table of about 33.5 m only in 27 years. (Al Salamah et al., 2013).

Sindhu et al., (2012) studied the SWI in Trivandrum's coastal aquifers, India by using Visual MODFLOW and SEWAT code for the subsurface water flow and contamination transport respectively. Hydraulic heads in the observation wells were predicted for ten-year period based on the available data. SWI was computed by 1% increase in pumping rates. Most of the observation wells showed reduction in the water level except for three specific wells those are having reduced altitude or having proximity with the neighbouring flowing river. At this place, high groundwater recharge rates also reduce the adverse pumping impacts. In contrast, reduced heads attract the SWI inland polluting the aquifer. Heavy SWI was observed at Karikkakom pumping well area in comparison to other place, owing to 1% rise in pumping.

For efficient groundwater administration of Sana'a basin, Yemen, modelling was carried out by using FEFLOW. The model was optimized in transient state for the period through 1972-2006. Model calibration done until a fair agreement between measured and estimated water levels was achieved. Calibrated model was used for three separate scenarios, to estimate the drawdown for the period from 2006 to 2020. The results of the model run showed the basin is suffering from acute water shortage due to its overexploitation (Al-Wathaf & El-Mansouri, 2012).

A total of 313 passive recharge wells were installed across Qatar to enhance the natural recharge. These recharge wells allowed the rainwater to infiltrate in the aquifer with gravitational force. SWAT2005 code was used to simulate this recharge effect. The ideal number of recharge wells were estimated by using the model which needs to accumulate and infiltrate the surface water within 5 days following the most intense rainfall event in a representative year. Recharge of 10.7 MCM was contributed to the aquifer through the existing 161 recharge wells out of the total recharge (75 MCM) estimated by the model (Shamrukh et al., 2012).

In alluvial aquifer of Wadi Hada Al Sham, Makkah, MODFLOW was used to study the fluctuations of water head. Before using for the water heads prediction for the next five years, model was calibrated. A hope of drilling more wells

without having any impact on the groundwater volume and quality was studied. A difference within the range of 0-6.0 m was reported observed and computed values of the water level (Al-Hassoun and Mohmed, 2011)

A 3D mathematical model of varying soil density and miscible solvent transport was created to explore coastal aquifer contamination in western Japan. The study area chosen was an agricultural land situated on a coastal aquifer from which groundwater is continually abstracted as a primary source. Due to excessive pumping, the groundwater got contaminated due to SWI. using the finite difference framework, a numerical model was constructed, taking into account transition zone development and the fluid density variation within it. The model was able to simulate both saturated and unsaturated groundwater flow areas in the coastal aquifer under the influence of variable density conditions (Parera et al., 2010).

Kacimov et al. (2009) chosen the Eastern Al Batinah catchments and their unconfined aquifers in the Sultanate for their research. They studied intrusion of seawater which spreads several kilometres inland in the coastal region experimentally, analytically, and numerically. The numerical and analytical modelling of SUTRA and Dupuit-Forchheimer (DF) respectively was used. It was noted that intrusion got mitigated by pumping the saline water from the aquifer.

Abderrahman & Rasheeduddin (2001) studied a multi-aquifer system in Saudi Arabia by using MODFLOW code. The model was calibrated before using for prediction of aquifer behaviour under different volume drafts for a period of 22 years. Computed results intimated a continues fall in the water levels if the base rate of pumping would maintain.

After reviewing the available literature, some of the key hydrogeological parameters used by the researchers in their modelling practices were summarized (see Table 2-2). The information was categorized based on significant variables that are affecting the flow of groundwater at various locations in the prominent studies carried out in the Gulf region along with the average annual rainfall.

### **2.3.1 Summary of Literature review**

Few studies on groundwater flow and solute transport were conducted using the numerical models in the Arabian Peninsula which is suffering from arid and semi-arid climatic conditions with scanty rainfall. Due to lack of research, the concerned authorities, to sustain this fast-depleting natural water resource cannot suitably adopt groundwater management strategies. The groundwater scenario become more severe considering the salinity intrusion due to climate change, sea level rise and overdraft. Limited modelling has been attempted to simulate the effects of sea level rise due to climate change.

In the present research, several scenarios of pumping rates increment and reduction, sea level rise and fall due to climate changes will be considered to simulate the transient condition of the aquifer by using MODFLOW and MT3DMS codes. The model domain will be divided in a fine grid at pumping well stations to get a better result of groundwater and salinity intrusion. The model will be calibrated in the steady state (2000) and the transient state (2000 -2017) before subjecting it to the predictive scenarios from 2018 till 2040 by input of latest available hydrogeological data, rainfall and observation well/monitoring well data. These models are crucial for developing curative solutions to reduce seawater intrusion.



**Table 2-2 Hydrogeological parameters used for various studies in the Arabian Peninsula**

S. No.	Description of Study Area /Aquifer Description	Hydro-geological parameters					References
		Rainfall (mm/year)	Hydraulic conductivity (m/day)	Storage Coefficient	Specific yield	Transmissivity (m <sup>2</sup> /day/m width)	
	<b>United Arab Amirates</b>						
1.	<p align="center"><b><u>Wadi Ham Aquifer</u></b></p> <p><u>Quaternary</u> upper layer composed of wadi sand &amp; gravel.</p> <p>Lower layer of fractured ophiolite composed of sand and gravels with many cobbles and boulders which are weathered and cemented.</p>	150	2 - 250	0.1 - 0.3	-	100 - 200 (Wadi bed) 1000 -10,000 (Near Coast)	30  <a href="#">Sowe et al. 2019</a> <a href="#">Sherif et al. 2014</a> <a href="#">Sherif et al. 2013</a>
	<b>Sultanate of Oman</b>						
2.	<p align="center"><b><u>Southern coast of Oman, Salalah Aquifer</u></b></p> <p>Upper Layer of Wadi alluvium (Quaternary deposit) comprises of conglomerates, gravely clays and coastal calcarenite deposits.</p> <p>Lower Layer of Wadi alluvium (Quaternary deposit) comprises of conglomerates, gravely clays and coastal calcarenite deposits.</p>	110 - 450	50 – 60 (Upper Layer) 500 -1000 (Lower layer)	0.006 – 0.1	0.05-0.2	19800	35  <a href="#">Sana &amp; Bawain 2014</a> <a href="#">Shammas &amp; Thunvik 2009</a> <a href="#">Shammas &amp; Jacks 2007</a>

3.	<b><u>Northern Coast of Oman, Al – Batinah</u></b>	100	5 - 30	0.0001-0.001	0.2 - 0.01	-	-	Chitrakar & Sana 2016, Sana et al. 2013 and Lakey et al. 1995
	Older Layer 2 (Ancient alluvium) is relatively clayey, cemented alluvium & bedrock		0.2 - 5	0.0001-0.0009	< 0.07	-	-	
4.	<b><u>Jamma Aquifer, South-East Al Batinah</u></b>	60 -140	8 -35 (Layer-1)	-	-	-	-	Al Makhtoumi et al. 2018
	Layer-1 Quaternary Alluvium with low clay content Layer-2 Tertiary alluvium, more compacted and is characterized by lower hydraulic conductivity and porosity values.		0.3 (Layer-2)	-	-	-	-	
5.	<b><u>Samail Lower Catchment aquifer</u></b>	-	0.79 -7.76	-	0.2	-	-	
<b>Kingdom of Saudi Arabia</b>								
6.	<b><u>Gulf of Aqaba</u></b>	20	-	-	-	-	-	Al Taani et al. 2013
7.	<b><u>Jizan Aquifer</u></b>	<200 (Eastern side)	2.16 (Avg.)	0.01 - 0.25	-	540 – 5400 (173 Avg.)	-	Abdalla, 2016 Mogran, 2015

	unconsolidated cobbles, gravels, sand, and silt). The deep rock aquifers are usually confined, comprising of sandstone and limestone are usually confined, comprising of sandstone and limestone.	>500 (Western Side)						
8.	<u>Saq Aquifer</u> Medium to coarse sandstone, with local areas of fine sandstone	125	3.6	-	-	4500	-	Almuhaylan et al. 2020, Gazaw et al. 2014; Al-Salamah et al. 2013
9.	<u>Wadi Hada Al Sham</u> Composed of sandstone, siltstone, and alluvial deposits.	100 - 300	0.56	-	0.15	212	0.18	Al-Hassoun et al. 2011
<b>Qatar</b>								
10.	<u>Qatar Aquifer</u> <u>Upper</u> layer composed of limestone with dolomite. <u>Middle</u> layer is composed of chalky limestone and contains a layer of shale in the southern part of the country. Lower layer comprises chalky and dolomitic limestone.	50 -100	0.0 - >237		-	20 - 1000 (North) 2.6 (South)	-	Baalousha, 2016
11.	<u>Al Wakrah Aquifer</u> <u>Shallow</u> upper aquifer is formed within the limestone and overlying sediments. <u>Deep</u> lower aquifer is formed by Rus formation. The two aquifers are separated by the relatively impermeable and continuous Midra shale.	82	0.00864 – 17.28	-	-	-	-	Lachal & Gana 2016

		<b>Yemen</b>						
12.	<p style="text-align: center;"><u><b>Sana'a Basin</b></u></p> <p>Two-layered aquifer in which upper layer represents the Quaternary alluvium, Quaternary and Tertiary volcanic, with a thickness of alluvium varying from 100 to 300 m and thickness of volcanic varying from 300 to 800 m.</p> <p>Lower layer consists of sandstone with a thickness varying from 400 to 700 m.</p>	150 - 250	0.044 - 7.80	$3.74 \times 10^{-7}$	0.05 - 0.28	-	-	Al-Wathaf & El Mansouri 2012
			0.07 - 3.97	$0.90 \times 10^{-4}$		-	-	
13.	<p style="text-align: center;"><u><b>Wadi Siham, Tihama Basin</b></u></p> <p>Aeolin-Alluvial aquifer - 300m thick comprises of clay, silt, sand, gravel &amp; boulders.</p> <p>Tawilah aquifer – formed of sandstone.</p> <p>Amran aquifer – formed of limestone.</p> <p>Kuhlun aquifer - lies at a greater depth &amp; comprises of limestone stone</p>	0 - 100 (Coastal area)	-	0.0358	-	2677	-	Nasher et al. 2013
		300 – 400 (Close to cliff)						
		<b>Kuwait</b>						
14.	<p style="text-align: center;"><u><b>Al-Raudhatain and Umm Al-Aish</b></u></p> <p>Layer 1 - Poorly sorted gravelly sand</p> <p>Layer 2 - Calcareous siltstone / Shale</p>	110 -120	0.08 - 70	0.00006-0.00028	0.12 - 0.14	10 -1500	0.15 - 0.25	<p>Bhandary et al.2018</p> <p>Al Weshah &amp; Yehdigo 2016</p>

	<p>Layer 3 - Fine-grained conglomeratic sandstone</p> <p>Layer 4 - Calcareous siltstone/shale</p> <p>Layer 5 - Argillaceous and conglomeratic sandstone.</p>							
	<b>Bahrain</b>							
15.	<p style="text-align: center;"><u><i>Dammam Aquifer</i></u></p> <p>Zone A - Alat member consist of limestone (15 - 25 m thickness)</p> <p>Zone B – Khobar member consist of limestone (40 – 49m thickness)</p> <p>Zone C - Rus-Umm Er Radhuma aquifer</p>	< 80	-	-	-	350 - 10,000	-	Zubari, 2005 & 1999

## **CHAPTER 3    METHODOLOGY**

### **3.1    Introduction**

The Al Batinah coastal plain stretches for nearly 300 km along the west side of the Oman Sea, extending from northwest of Muscat, the country's capital, to the foothills of the Northern Oman Mountain. It has a varying width of 10 to 30 km. In the coastal region, in view of growing population, development-related activities as well as environmental degradation, water resources are increasingly under pressure due to over-exploitation. World Bank (1996) stated that policymakers and planners faced significant obstacles as a result of the development activities, making them especially vulnerable to overexploitation and result in SWI (Choudri et al. 2015). The Batinah's coastal alluvial aquifer has enabled the country's largest agricultural region to develop. Due to availability of fertile soil in this region major portion of water (86%) was used for the agriculture purpose and remaining 12% and 2% was used as potable water and industries respectively (Wehenmeyer et al., 2002).

This chapter describes the modelling approach adopted and data acquired and used in the present study. A detailed surface and subsurface characterisation of the study area has been made through hydrological and hydrogeological investigations. This also includes the data related to geomorphology, slope, landuse/landcover. The hydrogeological data was acquired from the previous literature and fieldwork. A detailed well inventory survey was carried out for the identification of observation wells, geological protrusion, type of wells and their dimensions. The electrical conductivity (EC) and groundwater head data from dug and tube wells were used.

### **3.2    Geographical location**

The topographic map shows that the Wadi Al-Jizi catchment is situated between Latitudes 2685288.72m N to 2702809.30m N and Longitudes 445120.53m E to 474236.85m E. (Figure 3-1). The coastal plain groundwater aquifer is situated

in the Al Batinah region, which is located in the northwestern part of the Sultanate of Oman. The study area is naturally bounded to the north by the Sea of Oman and to the south by the Al Hajer Al Gharbi Mountain range. The Wadi Al-Jizi catchment area encompasses approximately 1,154 km<sup>2</sup>, with the eastern part comprising about 519 km<sup>2</sup>. The study focuses on the aquifer system located in the eastern part of the Wadi Al-Jizi catchment area, which covers an area of approximately 123.6 km<sup>2</sup>. This aquifer system extends from the sea towards the Wadi Al-Jizi dam, which has a capacity of 5.4 MCM.

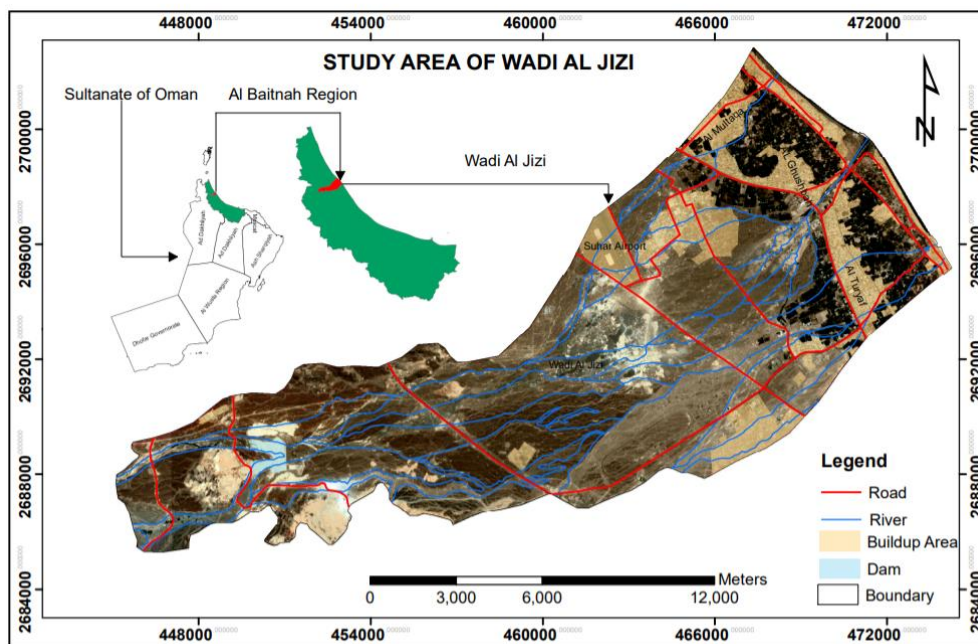


**Figure 3-1: Location map of Wadi Al Jizi Catchment**

### 3.3 Climate of the region

The Al Batinah region's climate is categorized as semi-arid. The 'normal' weather characteristics are clear, bright skies and light wind over 90 % of the year. The winter is pleasantly warm and dry, and it's hot and dry in the summer. Very hot and dry climatic condition and high evapotranspiration rates prevails in the region (Lakey et al. 1995). It is characterized by a mild, low-humidity winter, a hot, occasionally humid summer, and low, erratic amounts of precipitation. In the coastal area, the average annual air temperature is 28.5 °C and, in the mountains, temperature goes down to 17.8 °C. The annual evaporation in the Batinah plain ranges between 1660 -2200 mm year<sup>-1</sup> indoors

while the per capita renewable water supplies are estimated to be 550 m<sup>3</sup> / person (Al Barwani, 2012).

### **3.4 Topography of Al Batinah region**

Al Batinah region topography varies from 1700 m close the southern mountain front to the coastal sea level. Near the Jabal there is a steeper gradient of the ground and a flatter gradient of the ground close to the plain. The upstream catchments extend beyond the Al Batinah region, where the elevation reaches up to 3000 m near the Jabal Al Akhdar mountains on the Al Batinah region's southern boundaries. While the coastal plain elevation ranges from 100 m to 0 m (MSL) near the shore (MAF & ICBA 2012). The total wadi inflow from mountain area to the coastal plain of Al Batinah was estimated as a percentage of mean annual rainfall (MAR). The percentage ranged from 4.2 % in Upper Al Hawasnih wadi to 18.45 % in Upper Hatta catchment. Total wadi outflow to the sea was estimated to be 0.7% of MAR. Based on the rainfall distribution and stream flow tributaries, the catchment regions were defined as upper and lower catchments by the MRMWR (MAF & ICBA 2012).

### **3.5 Rainfall in the region**

Rain falling directly on the gravel plains between the coast and the mountains is not a key resource of recharging the aquifer, as the amount is relatively limited and much of it is absorbed by the soil and then lost by evaporation. Mountain precipitation is the main source of fresh water which recharges the aquifers in Al Batinah. It is generally agreed that most recharges are in the upper portion of alluvial fans near the mountain gorges along the wadis (MWR, 1996). Starting from there, the groundwater is flowing gradually into the sea through the aquifers. The locations of wadis flowing through the Al Batinah plain have changed several times over millions of years and have dispersed sediments transported from the mountain flow to build up the plain.

According to MAF & ICBA (2012), rainfall occurs in the coastal belt of the Al Batinah region between October and April. Additionally, there may be some rainfall as a result of thunderstorms in the foothills and hills in July. The average annual rainfall at higher altitudes in the catchment area, which are adjacent to



mountains and located at 1000 meters or higher, is approximately 350 mm (Young et al. 1998). This rainfall contributes to the recharge of the coastal aquifer. The Wadi Al-Jizi catchment is categorized as arid due to its average annual rainfall of approximately 100 mm.

In the southern mountain region, high rainfall is reported relative to the coastal region (Weyhenmeyer et al. 2002). The rainfall as high as 350mm was recorded in the Hajar mountain region which was dropped to 50 mm along the coastline area. Rainfall exhibits a significant amount of variability in both time and space. Wet periods are typically followed by prolonged dry spells, especially during years with high rainfall (Grundmann et al., 2012). The Oman Salinity Strategy (MAF and ICBA, 2012) states that the highest average rainfall record of 608 mm was observed in 1997, but this was followed by a long period of drought in southern Al Batinah until 2010, with the exception of 2007. The average rainy-day figures per year are 9.1 in coastal plain of Al Batinah and 13 rainy days per year for the mountains in Northern Oman. The rainfall in the region of Batinah occurs mostly during the winter season. In northern Oman, the main rainy season lasts from December to April and accounts for 58 to 83% of the country's yearly precipitation. Whereas 35 to 42% of the yearly rainfall happens in February and March. In the rainfall analysis for the Sultanate (1977 - 2003), 1997 saw the greatest average and 2010 saw the lowest average (Kwarteng et al., 2009).

The pattern of rainfall over the entire region exhibits significant changes over time. (Figure 3-2) A steep rise occurred in between 1985-1987, followed by a fall from 1989 - 1993. A similar pattern was also observed in the other regions with less precipitation up until 1994. In 1985 and 2001, the lowest rainfall was observed with a total of 13.5- and 35.6mm year<sup>-1</sup> respectively, whereas peak events happened in the year 1995, 1997 (626.1 mm year<sup>-1</sup>) and 2007 (Chitrakar & Sana, 2016).

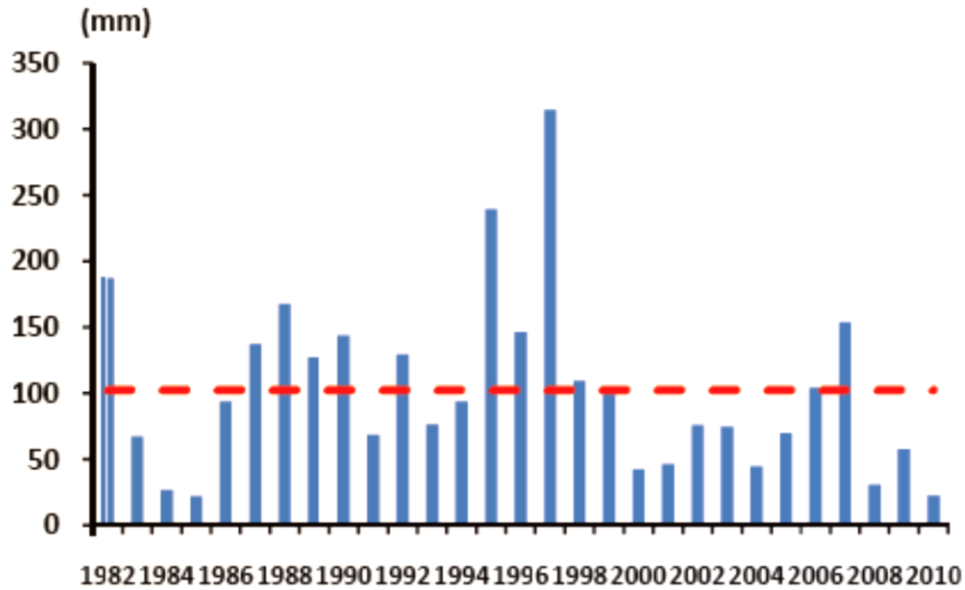


**Figure 3-2 Rainfall hydrograph (1982-2010) (Chitrakar & Sana, 2016)**

### **3.6 Hydrogeology of the Al Batinah region**

Al Batinah region hydrogeology is regarded to be a significant parameter supporting the existence of groundwater resource in the region. Most of the hydrogeological settings along the coastal plain of Al Batinah are generally similar. Al Batinah region could generally be split into two primary areas, distinguished by its rock type and geological environments, namely: mountainous region, consisting primarily of hard rocks, mainly ophiolite and calcareous. With a few sporadic cemented beds, the lowland and coastal plain areas are mainly composed of coarse gravel and boulders. The main aquifer having a depth of more than 300 m and 600 m in north and the south respectively located in the coastal plain. The plain was formed by rainfall because of the natural weathering process.

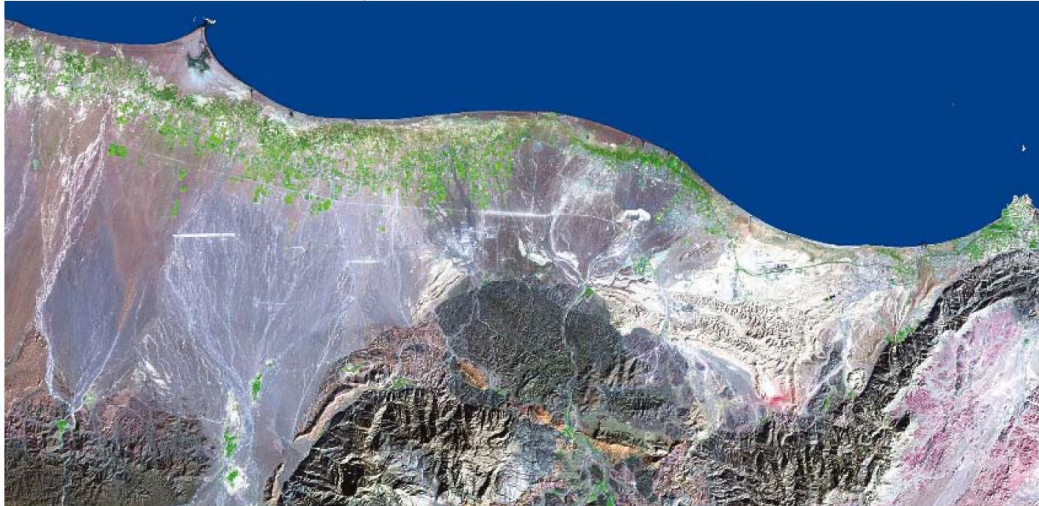


**Figure 3-3 A satellite image of Al Batinah region displays the mountains and alluvial plain, which creates a suitable environment for water retention. (MRMWR, 2008)**

The Al Batinah aquifers' primary source of freshwater replenishment is mountain rainwater. Out of a 100 mm rainfall, 80% is lost to evaporation, 5% flows to the sea, and 15% seeps into the earth to replenish aquifers. It is generally accepted that most recharges occur along the wadis (seasonal watercourses) in the upper portion of the alluvial fans near the mountain gorges (MWR, 1996). A satellite image of a part of the Al Batinah region is shown in Figure 3-3.

### **3.7 Description of the study area**

The study area within the Wadi Al-Jizi catchment is depicted in Figure 3-4, covering the region between Latitudes 26°52'88.72" N to 27°02'809.30" N and Longitudes 45°59'200" E to 47°42'36" E. The agricultural economy of the Sultanate of Oman relies heavily on this area, as it represents a significant portion of the country's agricultural production. The entire Wadi Al-Jizi catchment area covers approximately 1,154 km<sup>2</sup>, with the eastern part alone covering about 519 km<sup>2</sup>. The study focuses on the aquifer system in the eastern part of Wadi Al-Jizi, which covers an area of approximately 123.6 km<sup>2</sup> and extends from the sea towards the Wadi Al-Jizi dam.

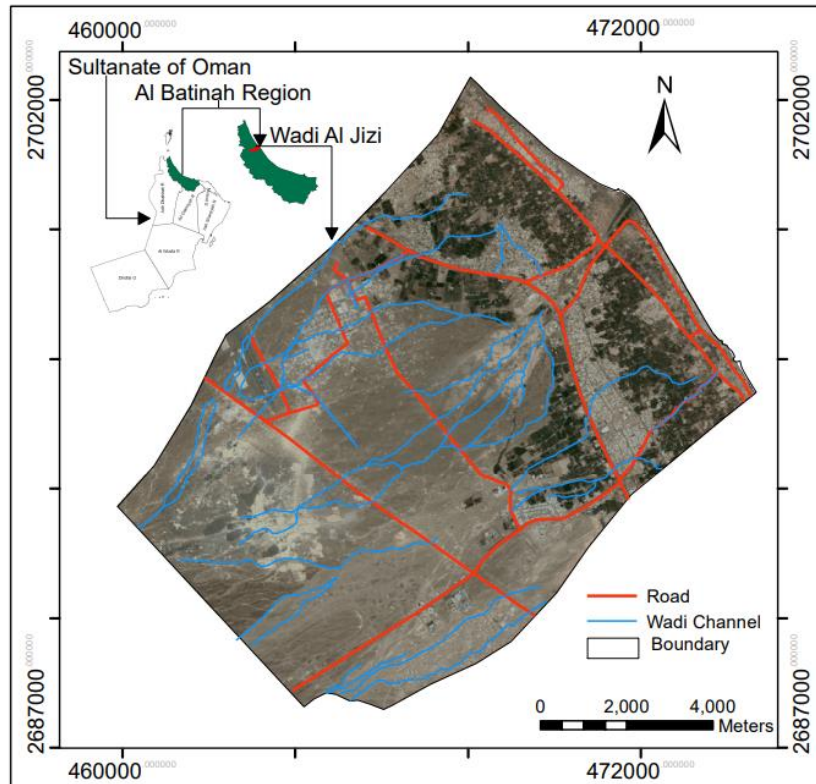


**Figure 3-4 Wadi Jizi Catchment area selected for the study**

### **3.8 Water Balance**

In comparison to groundwater, which is the main resource accounts for a greater portion (65% of the total water assets), whereas surface water sources makes up the rest (35% of the total water assets). The estimated water shortage was 378 MCM per year. As an estimate, Sultanate uses 25% more water than what naturally recharges its aquifer reserves. The continuous surge in population, development of agriculture facilities, rapid urbanization, industrial activities, in addition to the use of modern technology for borehole drilling and water pumping, exert substantial pressure on the water balance. In some fields, groundwater resources are utilized almost to the maximum, practically in the Al Batinah region where water abstraction has mainly exceeded groundwater recharge rates, resulting in continuous water table depletion and intrusion of salt water.

**Table 3-1 Water balance in Million cubic meter (Mm<sup>3</sup>) per year (Sana et al., 2013)**

Year	Water Demand			Available water resources			Deficit
	Agriculture	Drinking	Total	Underground water	Desalinated water	Total	
1990	1152	73	1225	899	41	940	285
1995	1152	156	1308	949	50	999	309
2000	1250	185	1435	1004	100	1104	331
2020	1250	460	1710	1004	100	1104	606

About 33% of the total country's population depends on the groundwater pumped from Al Batinah resources (Young et al.1998). Farmlands are close to the coastline due to easy accessibility of groundwater which is extracted through shallow dug wells (Sana et al., 2013). Lakey et al 1995 reported water balance for Eastern Al Batinah. All of the aquifers experienced a significant water deficit that year. Evidently, the region's aquifers began to absorb more saline water after 1995, indicating a rise in the water deficit. The water deficit data in Barka-As-Suwaiq and As-Seeb fields is shown in Table 3-1 (Sana et al., 2013).

### **3.9 Groundwater level**

Observation wells were used to measure the groundwater head in the study area. Electrical conductivity and some other water quality parameters were measured at different depths of the aquifer by using groundwater monitoring wells with different screen intervals (MRMWR,2000).

Figures 3-5, shows the water head fluctuations of few selected observation well (NJ-1, JA-2 & EA-1) due to water abstraction resulted owing to continuous pumping and recharge from the rainfall in the study area. The water level for the observation well is comparatively higher in the upper catchment in comparison with those located in the lower catchment or located in the vicinity

of heavy pumping. As the ground surface elevation increases towards the upstream near the mountain region, the groundwater elevation increases.

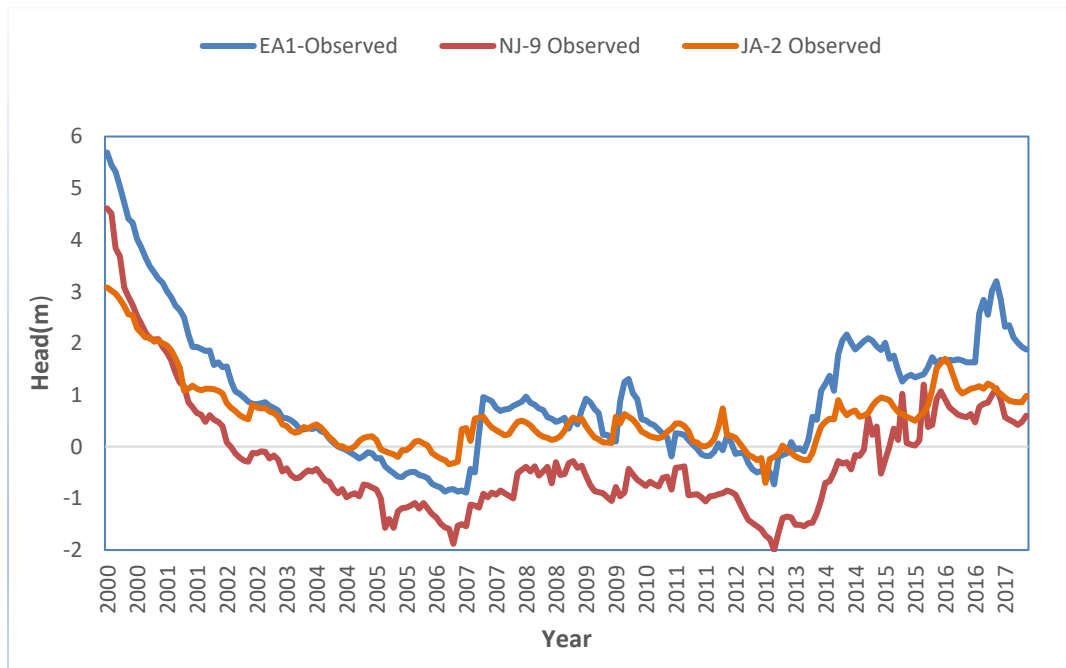


**Figure 3-5 Hydrograph of some selected observation wells**

Observation well EA-1 which is located mid-way between coastal area and mountain region shows a maximum water level of nearly 6.0 m, while the observation wells JA-2 in the lower catchment have less groundwater head nearly 3.0 m due to reduce ground elevation and its proximity to the existing pumping wells. It was observed that the water level in well EA-1 dropped to -1.0 m in the year 2005 and raised again to 1.0 m and 3.0 m respectively in the year 2007 due to cyclone event ‘Gonu’ and good rainfall events in the year 2015-2016 which resulted in large amount of surface and groundwater flowing from the upstream area and narrowly cumulate near to the gorge thereby infiltrating and resulting in high water level.

### **3.10 Saline intrusion in Sultanate’s Coastal Aquifers**

Electrical conductivity (EC) and total dissolved solids (TDS) are the usual parameters for measuring and expressing water salinity. EC refers to a substance's capacity to conduct an electrical current. It is expressed at a standard temperature of 25°C to ensure comparability of readings taken in different

climatic conditions. Water becomes a better conductor of electricity, as its TDS increases. The TDS can be measured rapidly from EC and therefore the saltiness of the water.

The density of freshwater is about  $1.0 \text{ gm/cm}^3$  which is lighter than salt water, and, when they meet, tends to form a wedge beneath the fresh water. Salt water and freshwater mix in a transition zone in which the water becomes progressively saltier downwards and towards the sea. A continuous movement of fresh water through the zone mixes with the salt water and prevent it from moving further inland or vice-versa (Figure 3-6).

If the water extracted by pumping from the aquifer is limited, the transition zone is maintained in constant position by recharging the upper parts of the aquifers. In case of excessive pumping, particularly near the coastal areas, the natural balance is disturbed, groundwater levels decline. The transition zone moves inland and upwards as the underground flow of freshwater decreases, and over time, the water drawn from wells close to the shore becomes saltier.

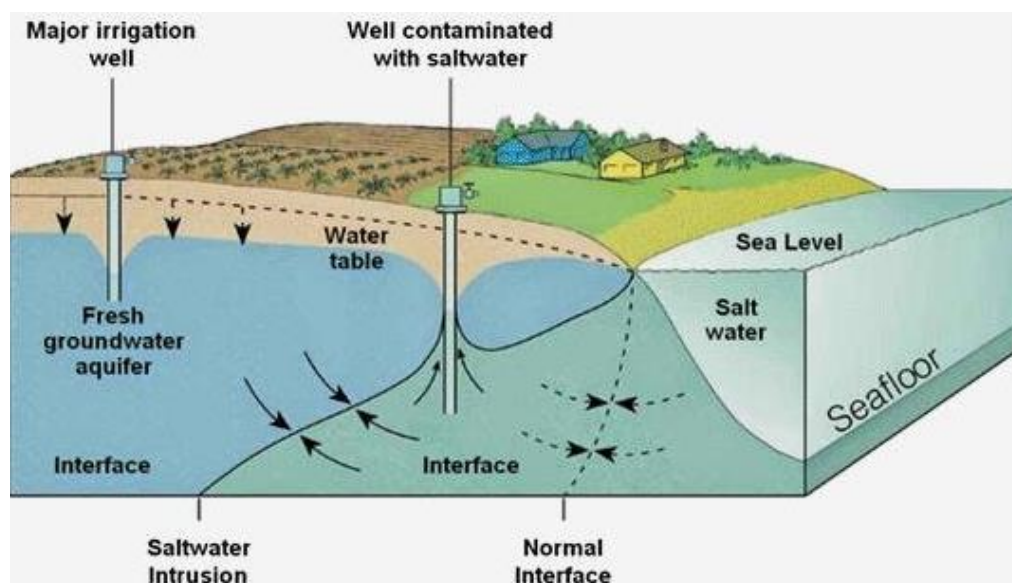


**Figure 3-6 Saltwater intrusion near the coast (Tabinas, 2014 – Accessed 2020, Dec. 5)**

In Oman, the issue of SWI is most severe along the Al Batinah coast, in Sur, and Salalah because of extensive pumping resulted in SWI, for more than two

decades, the precious agricultural land has either deserted or becomes unfit for cultivation (Shammas & Jack 2007, Sana et al., 2013; Sana & Shibli, 2003).

In Al Batinah coastal area, SWI was reported at places where the high extraction rate of groundwater exceeds the natural recharge. Saltwater intrudes aquifer through several other ways apart from SWI which take place when freshwater is over drafted, allowing the adjoining seawater to intrude inland to match with the declining head and to replenish the deficit volume. The evaporation of irrigation water, brackish upstream sources, wells that collect irrigation water and keep it from flowing back into the aquifer are possible additional sources of salt. In addition, as the irrigation water for the crops evaporates into the air, it leaves salt behind. The irrigation water then transports this salt back into the aquifer, increasing its salinity with each iteration.

The majority of agricultural wells are located in a narrow strip of territory along the coast. Both agricultural wells and boreholes are shallow dug, typically only reaching the upper 50 meters of the alluvial aquifer. About 58,400 number of wells were drilled in the governorates of Al Batinah for tapping groundwater. Importantly, 205 of them were largely abandoned due to intrusion of salinity along the coast resulted in the loss of investment of approximately OMR 12 million (MAF & ICBA 2012).

### **3.10.1 Adverse effects of saltwater intrusion in Al Batinah**

In Al Batinah region quality of groundwater is diverse since the quality found to be excellent in the mountain area at the source of bed rock seepage. As the water moves towards the sea, during its course of travel it dissolve salts like calcium carbonate which reduce its quality in plain and lowland areas. Withdrawals of groundwater in arid locations almost always exceed the rate of natural recharge and the piezometric surface (the aquifer's upper limit) gets lowered, resulting SWI in the groundwater system (Bear et al., 1999). A TDS value less than 1500 mg L<sup>-1</sup> was observed in the groundwater tapped in mountain area close to the recharge source and TDS value in the range of 1,500 – 6500 mg L<sup>-1</sup> founds in the coastal plain. The groundwater salinity classes are shown in Table 3.2.



The salinity and pollution levels of the surface water bodies influence groundwater quality (Hussain et al. 2019). In Sultanate of Oman, approximately 6000 hectares of agricultural property have been deserted owing to saline intrusion and another 5,000 hectares have moderate salinity effects. This has adversely affected livelihoods in rural areas. Aggressive abstraction of water and the subsequent intrusion of seawater depleted these important coastal aquifers. Saline intrusion results in an estimated net present value of loss of US\$ 288 million over 25 years using a discount rate of 8%. This is broken down into the multiple losses resulting from crop production; *aflaj* (historical irrigation channels in Arabian Peninsula) drying up, losses to domestic customers, increased energy demand, and irreversible aquifer loss (FAO, 2009).

**Table 3-2 Classification of groundwater salinity (MAF & ICBA 2012)**

Level of Salinity	Classification	Water Salinity	
		TDS (mg/l)	EC (µs/m)
Class 1	Fresh water	< 1500	2.14
Class 2	Low Salinity	1500 - 3000	2.14 – 4.30
Class 3	Moderate Salinity	3000 -5000	4.30 – 7.0
Class 4	Moderately High Salinity	5000 -7000	7.0 -10.0
Class 5	High Salinity	7000- 10000	10.0 -15.0
Class 6	Very High Salinity	>10000	>15.0

Japan International Cooperation Agency (JICA) in 1982 started a five-year project to establish a hydrologic observation network in Al Batinah area and carried out detailed hydrologic and hydro-geologic surveys (JICA, 1986). Increasing demand for irrigation water has been discovered to result in increased salinity in coastal aquifers. In that study, several mitigation measures have been suggested. During 1982 to 1984, the Public Authority for Water Resources (PAWR) conducted three extensive surveys using approximately 345 coastal wells scattered from As-Seeb to Shinas and demonstrated a serious problem with salinity intrusion (Dale, 1983).

During the period from 1983 to 1986, Davison (1986) showed deterioration in groundwater quality along the AL Batinah shore. Hydroconsult (1985) in collaboration with the Ministry of Agriculture and Fisheries (MAF) carried out a preliminary soil and groundwater study in the coastal region of Al Batinah. Al Batinah coastal plain was estimated to have suffered from an annual water deficit of approximately 47 MCM. From the year 1992-1995 a report on salinity surveys prepared by the Ministry of Water Resources (MWR, 1996) recognized the need for detailed technical studies at numerous locations before appropriate corrective action could be taken. Approximately 1100 wells have been used in the area for a large monitoring network.

A later report by the Ministry of Water Resources (MWR, 2000), covering the period from 1997 to 1999 in which 1033 monitoring wells were tested, showed a large-scale groundwater scarcity in the Al Batinah coastal plain aquifer. Most affected areas identified in this report were from Barka to As-Suwayq and salinity generally increased when compared with the results of the 1997 survey. The wells located on the downstream side of the dams like in Wadi Ahin (Saham) and Wadi Al Jizi (Sohar) indicated retrieval in the groundwater.

Barwani and Helmi (2006) in their study mentioned a significant decline in the quality of water in the Al Batinah region. This was depicted by a decrease of 7% in the regions of appropriate agricultural water (2,000 - 6,000  $\mu\text{S} / \text{cm}$ ) reflecting a loss of 2,714 hectare of irrigated land. Also, in the Wadi Al Taww Barka region, the saline interface was recorded 12 km inland affecting the date palm. A saltwater wedge, stretched over several kilometers inland, lies beneath the freshwater aquifer in the coastal area. The interface between the seawater and the freshwater is progressing in all areas of Al Batinah, indicating over-exploitation of the aquifer. Despite unusually high rainfall from 1995 to 1997, SWI in the Wadi Al Taww and the Wadi Al Maawil was not reduced (MRMWR, 2008).

During 1998 to 2004, low average rainfall and wadi flows resulted further deterioration in groundwater quality (Chitrakar & Sana, 2016). In the 1999 salinity study, 35% of the wells had an Electrical Conductivity (EC) of more than 6000  $\mu\text{S} / \text{cm}$  and 10% of the complete study sites had an EC of more than 16,000  $\mu\text{S} / \text{cm}$ . The study of 1999 showed an EC rise of 54% compared to the

study of 1997. It can be observed that an EC exceeding 2250  $\mu\text{S}/\text{cm}$  falls into the category of 'Very high' salinity hazard according to the USDA classification of irrigation water (Helweg, 1992).

### **3.11 Secondary Data**

The preparation of the base map was based on the Ministry of Defense topographic map NG40-14F1, which has a scale of 1:50,000. The basins' boundaries, natural features, and Geo-referencing were delineated using this base map. Using ArcGIS 9.0 software, a groundwater prospects map was created by visually analysing a satellite image to delineate soil lithological units and geomorphological units.

#### **3.11.1 Soil**

Soil is the most vital natural resource available through nature for cultivation and human habitation. The point of origin, process of weathering, climatic conditions, pressure and temperature, all play a significant role in its formation and control (Nag and Kundu 2018). The amount of the water which seeps and retains in the subsoil depends upon the type of soil whether fine or coarse grained and its ability to flow the water through it (Bahgwat et al. 2018). The unconsolidated topsoil in the study area is a result of geological weathering of rocks.

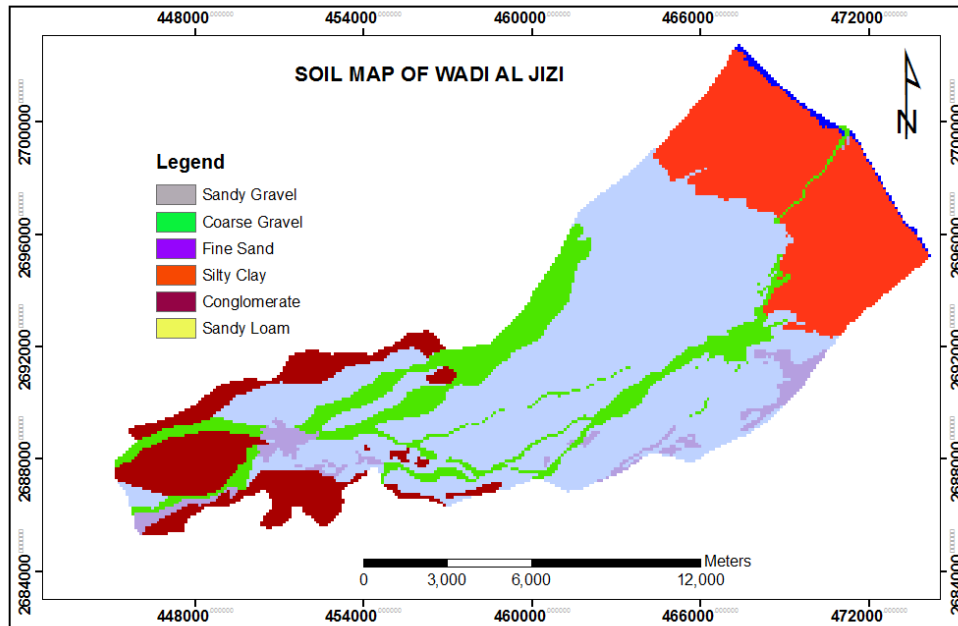


**Figure 3-7 Soil map**

The study area has six types of soils, including sandy gravel, coarse gravel, fine sand, silty clay, conglomerates, and sandy loam (Figure 3-7). Sandy gravel is the most common soil type, covering about 50.4% of the study area. Coastal areas are mainly covered by silty clay, while fine sand is only present along the coastline. Sand and gravel have high porosity and permeability, whereas clayey soils have lower infiltration rates (El Hatim 1977, Rabu et al. 1993).

### **3.11.2 Land Surface characteristics**

The characteristics of land surface, such as land-cover and land-use, have an impact on both groundwater recharge and microclimate. The distribution and occurrence of groundwater are significantly impacted by various factors such as geomorphology, ecology, climatic conditions, and anthropogenic activities, which in turn determine the land-use and land-cover characteristics (Chowdhary et al. 2019). Water bodies, cultivated land, and saturated surfaces are highly effective in recharging groundwater, whereas areas affected by urban development are considered less effective in this regard. The study area's land-use and land-cover data were mapped by using Google Earth (Digital Globe)

and topographic map. The images were processed through ENVI 4.0 image processing software.

Figure 3-8 shows that the predominant land-use types in the study area are open spaces (71.9%), plantations (12.7%), and built-up areas (14.8%). A small part of the study area is occupied by the reservoir dam. The infiltration of water is not contributed by constructed zones such as concrete surfaces, roads, and buildings, but rather by the plantation area which significantly contributes to recharge.

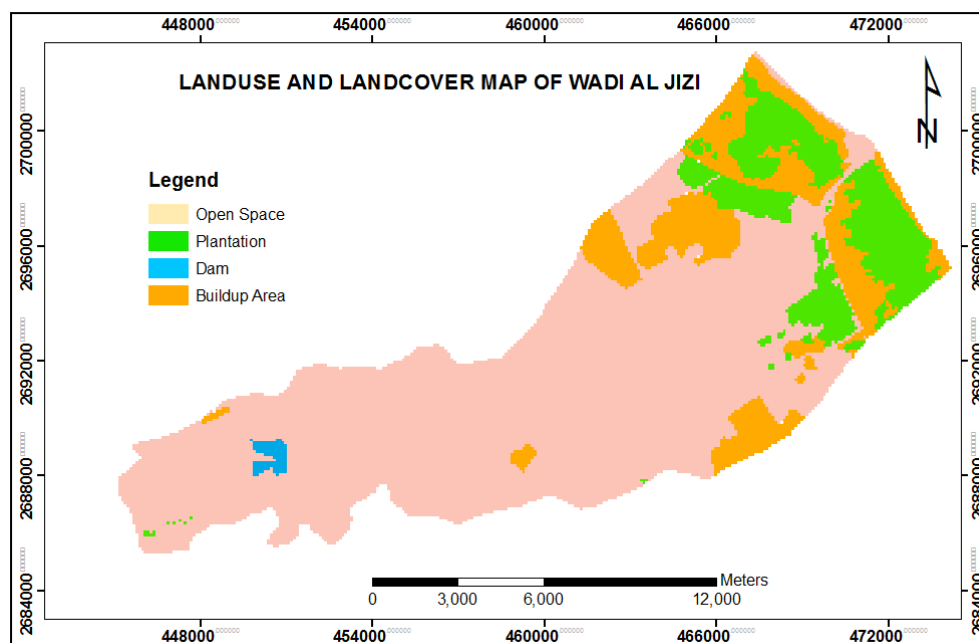


**Figure 3-8 Land use and Land cover map**

### 3.11.3 Geology

Figure 3-9 displays the geology map of the study area, prepared using the report published by MRMWR. At the foothills of the mountains, the alluvial plain of Al Batinah is situated at the base of alluvial fans. The terraces in the alluvial plain of Al Batinah are remnants of older alluvial fans and are composed of cemented rock beds, gravel, and sand of fluvial origin. These terraces contain high permeability wadi gravels and have storativity up to 50 meters thick. These aquifers are presently the main source of groundwater in the area and are entrenched into the terraces. Water from the mountains is supplied to the coastal

plain alluvium through alluvial channels. The wadi fans are distributed over the northern margin terraces and blend with the alluvium of the coastal plain. The study area is predominantly covered by alluvium, which comprises over 97% of the land surface. This alluvial cover has a high capacity for groundwater recharge.

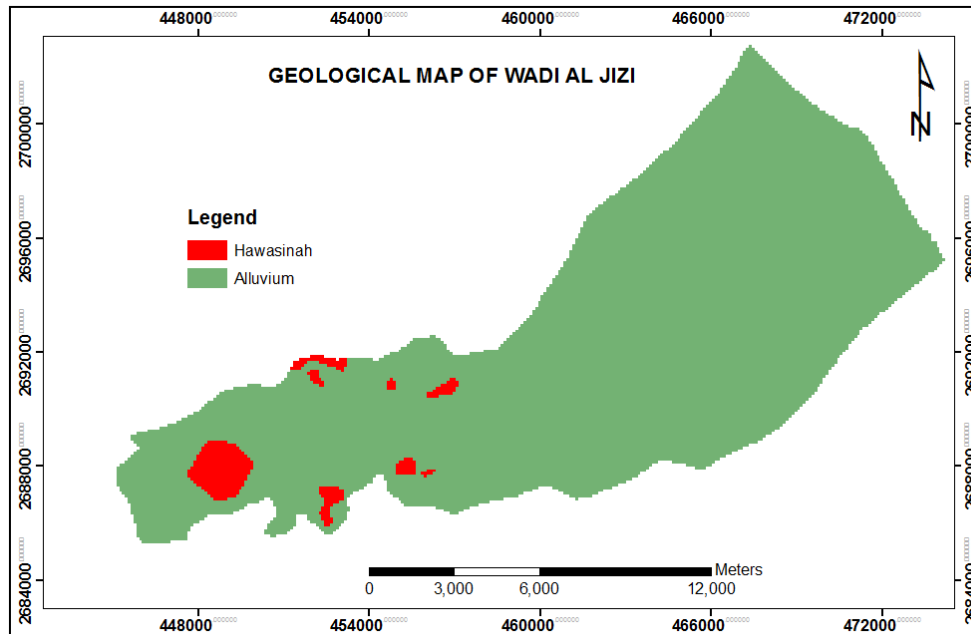


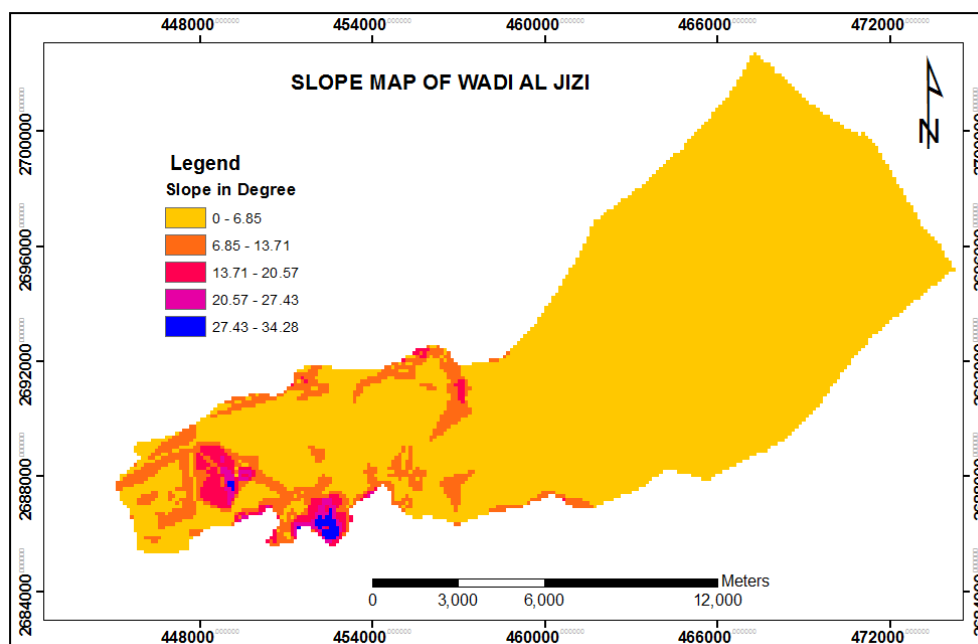
**Figure 3-9 Geological map**

The area in the valley bottom of the Hajar Mountain range and wadis contains ‘high’ and ‘very high’ groundwater capabilities. On the other hand, ‘low’ to ‘very low’ groundwater contained in the majority of the mountain area (Abrams et al. 2018).

The coastal alluvium plains are composed of three main divisions, namely upper gravels, clayey gravels, and cemented gravel beds. These divisions differ in their ability to store water and their permeability, with the upper layer being the most productive. This layer is primarily composed of flood-flow deposited sands, uncemented clean gravel, and boulder beds. The lower gravel beds, on the other hand, have low permeability and are sometimes cemented with clay. There is potential for fields with uncemented gravel in this region (Young et al, 1998).

### 3.11.4 Slope

The rate of rainfall infiltration is directly affected by the surface gradient of the watershed. Areas with steeper slopes tend to allow less infiltration, resulting in reduced recharge to the aquifer. To put it differently, when the surface gradient of the watershed is steep, there is less chance for rainwater to infiltrate into the ground due to rapid runoff (Mangesh et al. 2012, Yeh et al. 2016). The topographic map was used to generate a slope map with the help of Arc GIS software.



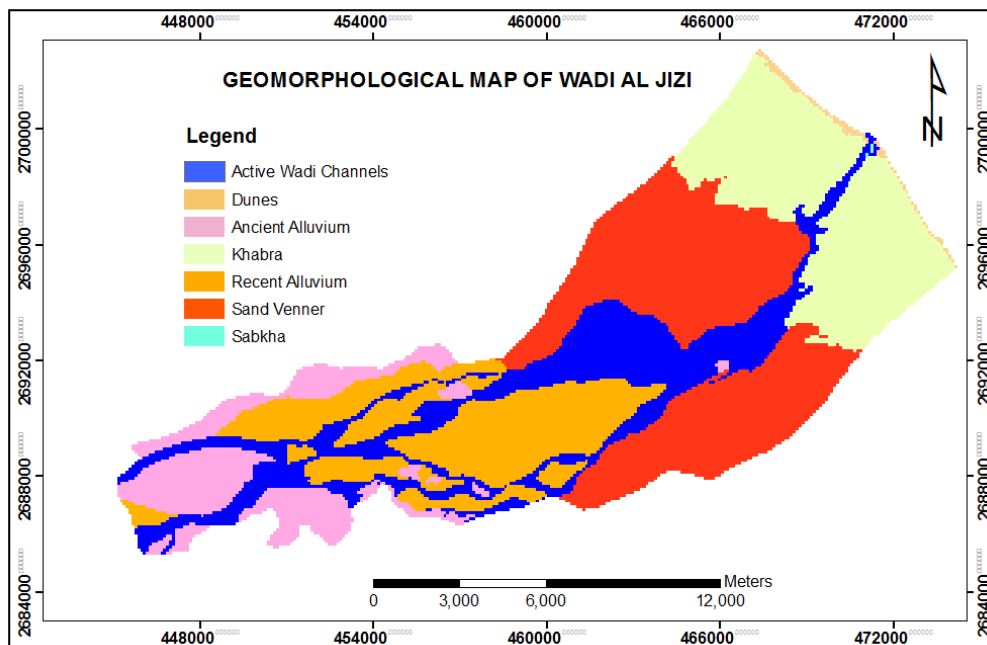
**Figure 3-10 Slope map**

Figure 3-10 displays the variation of slope from  $0.0^{\circ}$  to over  $34.0^{\circ}$ . 97.75% of the study area has a slope range of 0 to 6 degrees, while the class with the highest slope range of 28 to 32 degrees covers an area of approximately 0.11%, indicating a lower likelihood of groundwater occurrence (Agrawal & Garg 2016).

### 3.11.5 Geomorphology

The morphology of a geographical area is influenced by the geological structure's development and represents unique landforms and structural characteristics. Geomorphological maps are used to identify and characterize

both structural features and landforms. The geomorphology of a region is a crucial factor that influences the storage and flow of groundwater (Chowdhury et al. 2019, Waikar & Nilawar 2014). The Al Batinah coastal plain is a significant area for agriculture, industry, and settlement, and it consists of two distinct geomorphological units. The northern front of Al-Jabal Al-Akhdar is drained by a series of deeply incised wadis, leading to the conversion of coastal terraces into gravel terraces and finally into a coastal plain. This plain is characterized by scattered sabkhas, coastal sand dunes, fertile soil strips, and alluvial deposits, and serves as a hub for agriculture, industry, and settlements (MRMWR, 2008).



**Figure 3-11 Geomorphological map**

A geomorphology map of the study area was obtained using ArcGIS from the Ministry of Petroleum and Minerals, Oman map, which is presented in Figure 3-11. The region with the greatest potential for groundwater recharge is predominantly composed of wadi terraces and is primarily used for agriculture. A considerable portion of the precipitation can infiltrate the ground and reach the subsurface layers. The area's geomorphological features can be classified into seven units, namely active wadi channels, ancient alluvium, recent alluvium, sand dunes, khabra, and sand veneers. The sand veneers unit covers



the largest proportion of the study area's geomorphology, accounting for 29% of the total area. Khabra occupies 20.9% of the area, while the active wadi channels and recent alluvium cover 19.4% and 18.7%, respectively. These units have a high potential for water and thus have been given higher weights.

### **3.12 Groundwater modelling**

With the advent of technologies, many latest groundwater modelling codes helps in providing real-time simulation through visualization and analysis both in case of 2D and 3D conditions. A user-friendly graphical interface makes the model's application much easier (Praveena & Aris 2010). A numerical model can also be used as a management tool for making choices about pumping patterns and building the fresh recharge facilities in the study region (Sana & Shibli, 2003).

Groundwater Modelling System (GMS) used by thousands of people in more than 90 countries proved to be a comprehensive, efficient and exciting groundwater modelling code. Every stage of a groundwater simulation can be incorporated using the tools provided by GMS, including site description, model development, calibration, post-processing, and results visualization at each model run. Data scarcity may hold some of its advantages and resulted in its limitations such as insufficient observation data about a particular area may not simulate the results with high accuracy, still the macro dynamic features of groundwater and the hydrogeological conditions can be obtained through inverse simulations. In all, a 3D numerical modelling code is an efficient method to understand the groundwater flow for proper development, utilization and management of existing resources.

### **3.13 Model Development**

The Groundwater Modelling System (GMS), comprising MODFLOW and MT3DMS, is employed to investigate subsurface water flow in Wadi Al Jizi. A 3D representation of the groundwater flow and contaminant transport systems is developed through a conceptual model. This model utilizes all the necessary geological and hydrogeological data for the study area, including geological and topographical maps, bore logs describing the physical and chemical parameters

of the aquifers, and observed salinity data. Conversion of the conceptual model into the numerical model input files is next stage followed by the calibration to demonstrate that the model is capable of generating the same scenarios as it is contained on the study site in terms of observation values or targets. Predictive scenarios will be considered for studying water head fluctuations or SWI once the calibration is satisfactory and within the limits.

### **3.14 Three-Dimensional Mass Transport Multi species (MT3DMS)**

For simulating solute transport (SWI), a 3D Mass Transport Multi Species (MT3DMS) was utilized. This software offers a wide range of capabilities and options for modeling the advection, dispersion/diffusion, and chemical reactions of contaminants in groundwater flow networks, which are tailored to specific hydrogeological conditions. (Zheng and Wang, 1999). MT3DMS is designed to work seamlessly with any block-centred finite-difference flow model, such as MODFLOW. It operates based on the assumption that variations in concentration field do not have a significant effect on the flow domain. Once the flow model is created and configured, the transport model can save its information in disk files, which can later be accessed by the transport model.

MT3DMS has the benefit of enabling users to model the transport of pollutants without the need to acquire a new flow model or adjust an existing one to match the transport model. Moreover, conducting independent flow simulations and calibrations separate from the transport model can lead to considerable memory savings. The structure of the model also allows for faster execution times in cases where multiple transport runs are necessary, while maintaining the same flow solution. MT3DMS is capable of simulating variations in the concentration of dissolved pollutants in groundwater, considering processes such as advection, dispersion, diffusion, chemical reactions, and accounting for different types of boundary conditions and external sources or sinks.

To resolve the governing equations of a numerical model, a grid is superimposed on the study area. The model proceeds by formulating a water balance equation for every cell in the grid, producing a set of equations that are solved numerically for each cell. Inflows and outflows

are depicted for each cell, and the solution yields a hydraulic head value. There are two grid designs available: finite difference grids and finite element grids. The finite difference grid, utilized by MODFLOW, features rectangular cells.

### 3.15 Governing Equations

MODFLOW is a computer program that uses the finite-difference technique to numerically solve the 3D groundwater flow equation for a porous medium (McDonald and Harbaugh 1988; Harbaugh et al., 2000). It has a successful track record of application in various regions around the world. The code and information about studies that have utilized MODFLOW can be found in McDonald and Harbaugh (1988).

Although MODFLOW was made to be readily improved, the design was focused on changes to the equation for groundwater movement. It is often found a requirement to solve additional equations dealing with contaminant transport or for calculating parameter values which may bring an agreement between the computed and the observed heads of groundwater. The partial-differential equation of groundwater flow used in MODFLOW is as shown in Eq. (3.1).

$$\frac{\partial}{\partial x} \left( K_{xx} \frac{\partial h}{\partial x} \right) + \frac{\partial}{\partial y} \left( K_{yy} \frac{\partial h}{\partial y} \right) + \frac{\partial}{\partial z} \left( K_{zz} \frac{\partial h}{\partial z} \right) - W = S_s \frac{\partial h}{\partial t} \quad (3.1)$$

where,  $K_{xx}$ ,  $K_{yy}$  and  $K_{zz}$  represent the values of hydraulic conductivity in the x, y, and z directions, respectively, assuming they are parallel to the primary axes of hydraulic conductivity (L/T); The variable h corresponds to the potentiometric head (L), while W represents the volumetric flux per unit volume that accounts for the sources and/or sinks of water. A negative W value indicates water flowing out of the groundwater system, while a positive value denotes water flowing in (T-1).  $S_s$  denotes the specific storage of the porous material (L-1), and t represents time (T).

If the main axes of hydraulic conductivity are parallel to the coordinate directions, Equation 4.1, along with the input of appropriate initial and boundary, may represent a transient 3D groundwater flow in a non-homogeneous and anisotropic medium.

The outcomes derived from utilizing MODFLOW to simulate groundwater flow can be utilized to operate MT3DMS, an enhanced edition of the 3D Mass Transport Model (MT3D) created by Zheng (1990). The model can simulate advection under steady and unsteady flow conditions, anisotropic dispersion, first-order decay and production reactions, and both linear and nonlinear sorption (Zheng, 1990). This model is based on the general Equation 3.2 of mass transport as follows:

$$R \frac{\partial C}{\partial t} = D_{xx} \frac{\partial^2 C}{\partial x^2} + D_{yy} \frac{\partial^2 C}{\partial y^2} + D_{zz} \frac{\partial^2 C}{\partial z^2} - V \frac{\partial C}{\partial x} - \mu RC \quad (3.2)$$

where, concentration of solute is represented by C, while  $D_{xx}$ ,  $D_{yy}$  and  $D_{zz}$  represent the dispersion coefficients in the x, y, and z directions, respectively. V denotes the average velocity of the pore water, R is the retardation factor, and  $\mu$  is the decay coefficient. In the case of simulating seawater using MT3DMS, the decay constant is assumed to be zero, resulting in  $\mu RC = 0$ .

### 3.16 Simulation Hypothesis

The simulation hypothesis is started with the conceptual model being developed and then the recharge and pumping levels are prepared, as necessary. For the year 2000 pumping and recharge rates data, the model was then tuned to the steady state. The transient calibration period was set from 2000 to 2016. After transient simulation, the model was further used for the predictive scenarios through 2018 – 2040. The rates of recharge were used according to the wet and dry cycles recorded for the area at the Al Khan rainfall station by taking the average of rainfall for the wet years to calculate the expected amount of rainfall of wet years and the average of rainfall of the dry years for calculating the expected amount of rainfall of the dry years. The pumping rates was divided on 22 pumping wells used in the model, two of them located at the city well field (also known as Sohar Development Office) and responsible to provide portable

water to the Sohar city and remaining 20 wells for the extraction in the other areas of study.

To study the seawater intrusion the MT3DMS software was coupled to the transient MODFLOW and calibrated to the salt concentration with a group of electrical conductivity monitoring wells near the coast till 2016 readings. The model was then allowed to predict the SWI for the period of 2016 to 2040 for different scenarios of abstraction and SLR due to climate change.

### **3.17 Hydrogeological conceptual model**

The precision of a numerical flow model relies heavily on the accuracy of the conceptual model of the geological formation under study and the proper estimation of the water balance within the area of interest. Conceptual models play a critical role in the modelling of groundwater systems as they allow for a comprehensive understanding of their physical behavior. Furthermore, hydrogeological conceptualization is an essential tool in comprehending water-related mechanisms and contributes significantly to the management of water resources. The main components of the groundwater flow system are illustrated in Figure 3-12.

A typical pattern of sediment accumulation was identified in the Al Batinah plain which suggested a threefold classification of the alluvial aquifer system viz. upper unconsolidated gravels, middle clayey gravels and lower cemented gravels. As per the latest work carried out by the Ministry of Water Resources (MWR), bedrock aquifers can be an important source of seepage to the alluvium and must also be considered.

The alluvial aquifer receives recharge from direct infiltration of rainfall, Wadi flow infiltration and bedrock seepage derived from infiltration of rainfall in the upper catchment. Groundwater flows from the southwesterly mountains to the coast, both within the alluvium and underlying bedrock aquifers. A substantial amount of this flow must have evaporated or discharged to the sea in coastal depressions before 1970. Today, the bulk of this water is withdrawn through multiple irrigation wells (4000 nos.), with little to no flow to the sea (MWR, National well Inventory, 1996).

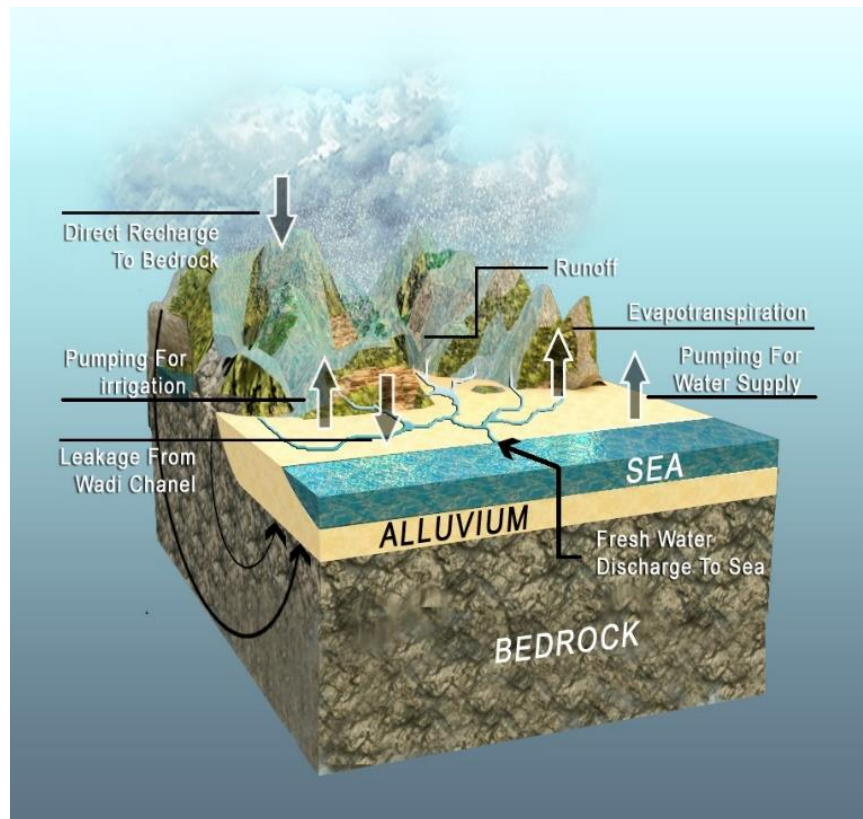


**Figure 3-12 Conceptual model of Wadi Al Jizi groundwater flow system**

The conceptual model consists of the following four coverages:

- Sources/Sinks which includes the boundary conditions encompassing the model and the extraction wells were considered. To observe the fluctuations in the groundwater heads due to the pumping activity in the study area, 22 extraction wells were taken into account.
- Recharge in the model domain which includes the applicable recharge rates.
- Monitoring wells includes a collection of the selected observation points for monitoring the groundwater head or the salt concentration in the area. To assist in the calibration of models, uniformly distributed monitoring wells in the study area were available.
- Layer 1 and Layer 2 of the model.

### 3.18 Model Domain, Grid and Zoning

The modeled domain of the current study is consisted of Wadi Jizi catchment between the downstream limit of the Jizi dam reservoir and the coastline near the sea. This accounts for about 135 km<sup>2</sup> (about 26% from the total eastern part area of the catchment). The finite difference grid used in the model has a length of 11903 m in the x-direction and 15285 m in the y-direction and consists of 356 columns and 357 rows. The average cell sizes are 33.4 m × 42.8 m. To account for potential significant changes in groundwater levels near pumping wells, a finer grid with cell sizes of 5m x 10m was utilized in those areas. The grid becomes coarser (40 x 80 m) in other regions. The model includes a total of 254184 grid cells, with 219916 of them being active and the rest being inactive. It is important to note that the actual depth of the aquifer is not yet known in the eastern part along the coastline since all the wells are up to 120 m deep in this area. Based on the available bore-logs, grid top elevation and bottom elevations were maintained at 61.0 and -33.0 m respectively. The bottom elevation of the layer 2 was fixed at -100.0 m. Both the layers completely cover the whole model domain

The model assigned specific head boundaries to the boundary representing the shoreline on the north-west side of the model domain and the south-west side boundary upstream of the catchment. The water levels of the upstream boundaries were estimated initially by utilizing the water level measurements obtained from observation wells situated at or near the upper boundary. Since the east and west sides of the model domain are parallel to the wadi flow direction, they were considered as no-flow boundaries. The model accounted for inflow from rainfall recharge, while outflow was represented by discharge to the sea and from pumping wells already present in the Wadi-Al Jizi area. Model domain was divided in five zones wherein zone 1 is 1.3 to 2.2 km from the coastline, and zone 2 is between 2.2 to 4.4 km, zone 3 is lying between 4.4 to 6.9 km, and zone 4 lying between 6.9 and 10.2 km whereas zone 5 is lying between 10.2 to 13.7 km distance. This coarse zoning pattern was used to simulate groundwater heads whereas finer zones will be considered to study the salinity intrusion in the study area.

### **3.19 Boundary Conditions**

Specific head boundaries were designated on the western upstream side and eastern side of the model domain. The eastern boundary is considered along the sea, wherein the ground elevations was assigned to zero (mean sea level), whereas no-flow boundaries along the northern and southern side were allotted forming the catchment limits and insist no in-flow or out-flow of water took place through these boundaries running along with the bottom of layer 2 in the model.

One of the main objectives of this study is to simulate the salinity intrusion, therefore it is imperative to calibrate the model to the actual fluctuation of the groundwater level near the coastline, rather than to adjust the water level near the upstream western boundary which, if so, will require a flux rate schedule during the entire simulation period. It is possible to achieve a more accurate simulation by applying the recharge on the appropriate zone starting from the upper reach of the eastern part of Wadi Jizi towards the dam reservoir containing about 95% of the total recharge. In the actual field, the head at the upper boundary fluctuates according to the wet and dry times, but for the model it is assumed that the recharge is obtained laterally directly from the surface in a small polygon starting at the upper specified boundary. Since such a boundary cannot be expected to maintain its level for prediction runs over simulation cycles, it is presumed to be a constant head boundary and the recharge is expected to be from the surface for simulation purposes only. While Jizi dam has significant effects on the recovery of the aquifer as seen in some monitoring wells, it is excluded from this model, and all recharge is presumed to be spread laterally over the entire polygon of recharge.

### **3.20 Recharge**

The rainfall data for the last 19 years (1999 - 2017) collected from the Al Khan rainfall station revealed that there were two wet periods of two years (2006 & 2007) and four years (2013 -2016) having an average rainfall of 135 mm and 129 mm respectively. In contrast to this, two dry periods having long duration of six years (2000-2005) and five years (2008-2012) got an average rainfall of 29 mm and 34 mm respectively as shown in Figure 3-13. The sequence of the



average rainfall for dry and wet periods assumed/expected to occur in same pattern for the next 23 years, considered for the predictive scenarios. About 43% of rainfall is considered to directly recharge aquifers; the remainder either evaporates or discharges into the sea as surface runoff. Precipitation infiltration makes up the majority of the recharge to the groundwater system for model simulation. Based on the rainfall in the year 2000, the average recharge rate for steady state was calculated to be 0.001358 m/day. Recharge rates calculated against the rainfall is shown in Appendix Table A-4-1.

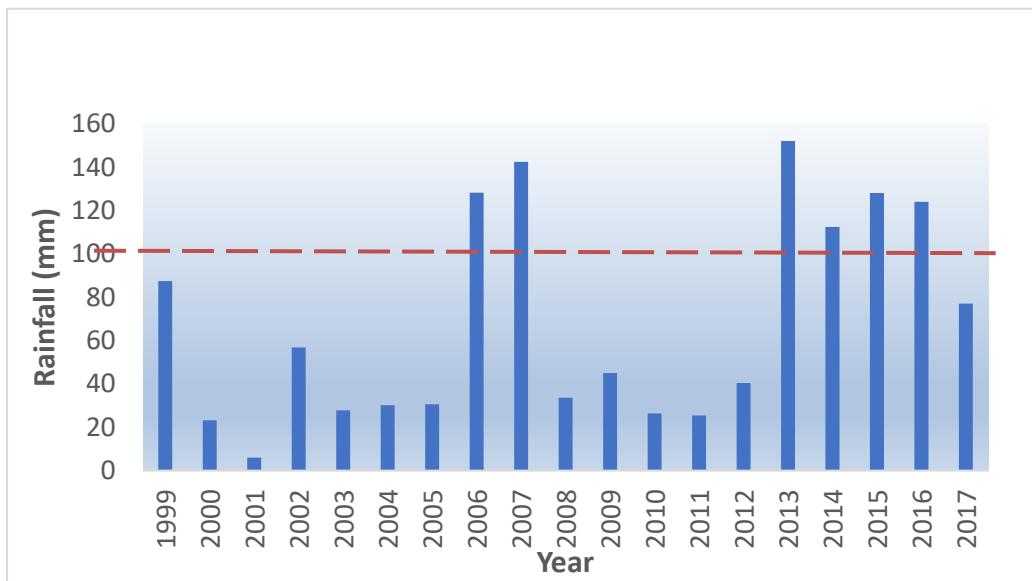


**Figure 3-13 Rainfall hydrograph of Al Khan rainfall station**

### 3.21 Groundwater abstraction

In all, 22 pumping wells were used to represent the total amount of water abstracted from the study area. The pumping wells were named and located in the study area as shown in Table 3-3, Table A-2, Table A-3 and Figure 3-14.

Two wells (Well\_1 & Well\_2) were lying in the Sohar Development Office (S.D.O.) well field managed currently by the DIEM company, remaining all twenty agricultural wells were considered as per the study conducted by Al-Shibli (2003). Except SDO well field, the factual abstraction data was

unavailable, therefore available data were lumped and distributed manually in the model area for the steady state. Further, it was adjusted during calibration and validation process in transient simulation.

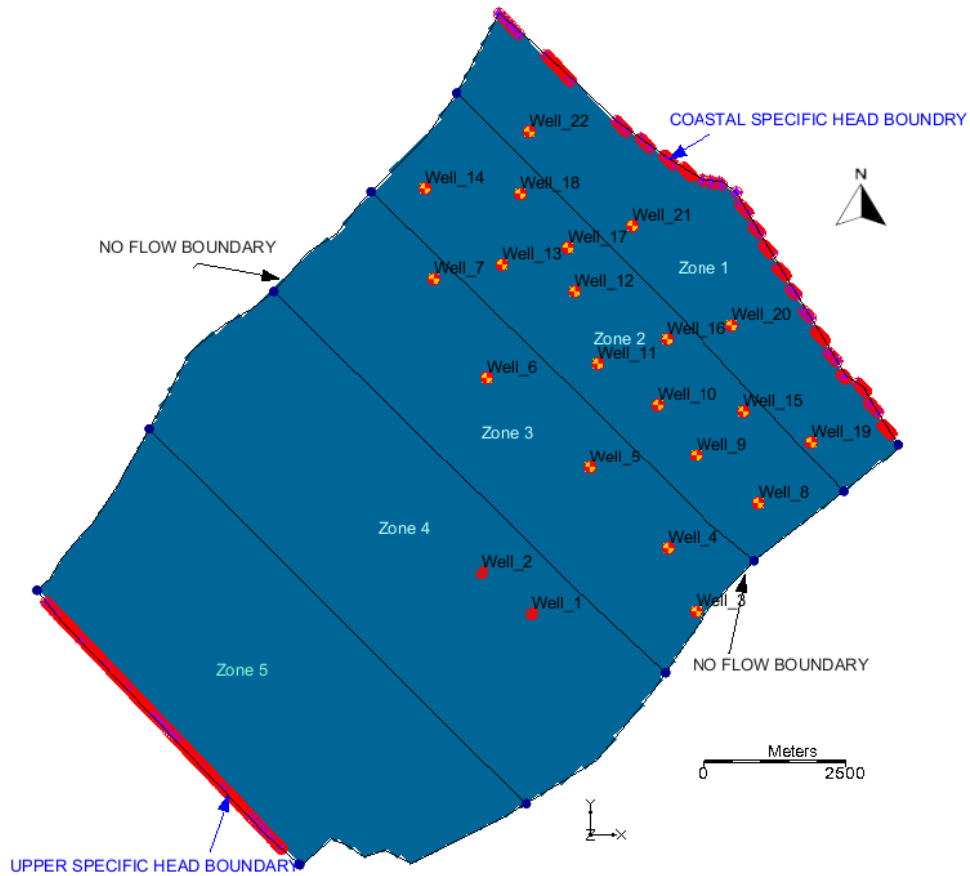


**Figure 3-14 Model domain showing different zones and pumping well location**

**Table 3-3 Spatial location of pumping wells in the study area**

<b>Pumping Well ID</b>	<b>Location</b>	
	<b>Easting</b>	<b>Northing</b>
Well_1	467767	2692277
Well_2	466891	2692999
Well_3	470667	2692310
Well_4	470180	2693430
Well_5	468797	2694860
Well_6	466973	2696455
Well_7	466038	2698192
Well_8	471779	2694223
Well_9	470671	2695084
Well_10	469991	2695972
Well_11	468938	2696707
Well_12	468529	2697976
Well_13	467240	2698448
Well_14	465889	2699792
Well_15	471524	2695862
Well_16	470164	2697135
Well_17	468400	2698746
Well_18	467567	2699694
Well_19	472711	2695316
Well_20	471308	2697375
Well_21	469543	2699136
Well_22	467724	2700794

### **3.22 Groundwater levels**

Pumping rates and the recharge rate in the wet and dry season will influence the groundwater head in the study area. Table 3-4 illustrates the spatial location and elevation of all groundwater observation wells selected in this study to observe the water level fluctuation. These wells were located in the four different zones

of the model domain and represent a reasonable selection of observation wells for the study in Wadi Al Jizi area as shown in Figure 3-15.

**Table 3-4 Observation wells detail**

Observation Well ID	Easting	Northing	Elevation(m) AMSL*	Drilled Depth (m)
NJ-1	471881	2698570	2.60	100.0
NJ-2	473939	2695347	4.53	100.0
NJ-10	467935	2701581	4.82	80.0
JA-2	468668	2696578	11.80	40
SARKM	469307	2694141	16.06	-
NJ-9	466549	2697105	16.02	80
DE-5	466905	2694224	23.96	58.0
EA-1	466729	2692859	29.23	200
JA-5	464358	2692925	45.40	55

AMSL\*= Above mean sea level

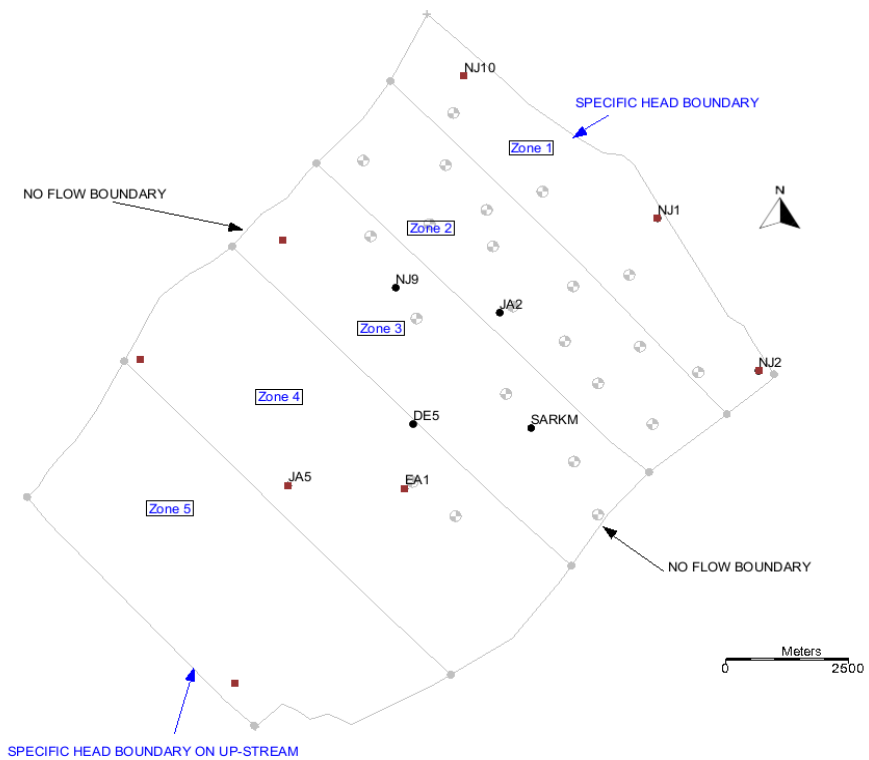


**Figure 3-15 Observation wells spatial distribution over the model domain**

### **3.23 Hydrogeological Parameters**

The essential hydrogeological parameters for numerical simulation of groundwater are hydraulic conductivity, specific yield, and storage coefficient. Initially, these parameters were estimated using field investigation data or literature review data. The literature reviewed so far highlighted hydraulic conductivity crucial and sensitive parameter in modelling for several studies. Any attempt to develop a model with practical hydraulic conductivity values obtained in the field should be made, ideally through pumping tests. By arbitrarily varying the spatial distribution of hydraulic conductivity, an experienced modeler can almost always produce a modelling result which closely resembles the collection of field data used for calibration. Another parameter, storage coefficient which is the product of layer thickness of a confined aquifer and its specific storage, is required for the transient simulations. Though for the same work of transient simulation in an unconfined aquifer, specific yield is used. Effective porosity is only needed if the model is used in conjunction with other programs that use MODFLOW produced results to measure the average linear groundwater flow velocity. This velocity is important to track particles from water as they pass through the porous medium. After assigning time parameters, and space and hydrogeologic parameters for each model cell, the next step is to accurately describe boundary conditions using the most appropriate MODFLOW packages. Since the choice is not straightforward, the package that will be used for a particular boundary will often be decided during model calibration.

### **3.24 Model Calibration and Validation**

Model calibration process is a major part of every groundwater simulation exercised in which the model is run in a systematic fashion repeatedly with certain input parameters such as recharge and hydraulic conductivity until the calculated values matches the observed values within an acceptable level of precision. Adjusting input data is not irrational, since such data are imperfectly understood, and a certain range of values that may be true. Trials and errors in between thirty to fifty numbers are usually common before achieving satisfactory calibration values. However, there is no surety that the combination

of parameters found through trial and error is unique. The aim of verification is to prove that the model can simulate any historic hydrological event for which field data are available. In general, some additional parameter refinement will be needed during the verification. GMS includes a suite of resources to help calibrate models. It provides a range of model tuning solutions including calibration targets and statistical plots. Observations both for point and flux are assisted.

## **CHAPTER 4 RESULTS AND DISCUSSIONS**

### **4.1 Introduction**

In undisturbed circumstances, freshwater usually flows from a coastal aquifer towards the sea. Nonetheless, excessive pumping from a coastal aquifer can cause a decline in the water table or piezometric surface, reaching a point where the piezometric head in the freshwater body is lower than that of the neighbouring seawater wedge. Consequently, the boundary between freshwater and seawater will proceed to move inland until a new balance is established. This process is referred to as salinity intrusion. When the freshwater-saltwater interface moves inland where a pumping well is extracting water makes its extracted water contaminated with salts. Without careful control of the pumping rate, seawater will inevitably reach in the vicinity of the pumping well and will be abandoned. Therefore, intrusion of seawater contributes to degradation of freshwater supplies making pumping wells and agricultural fields abandoned. Groundwater modelling system (GMS) MODFLOW and MT3DMS programs were applied in the Wadi Al-Jizi models which help us to understand the process of water flow subsurface and intrusion of saltwater in coastal aquifers simulating the infiltration of saltwater and to estimate the concentrations of solvents in coastal aquifers. The calibration of the model was conducted for both steady state and transient conditions and it was employed to project the salinity levels of the aquifer in the year 2040. The year 2040 is selected because six priority areas were identified as per “Oman Vision - 2040” to work upon and water sustainability is prioritized as one of them.

### **4.2 Steady-State Groundwater Flow simulation**

The model was initial calibrated in the steady state for the year 2000. During the calibration process, adjustment was made by using ‘trial & error’ method, with numerous trials in the value of hydraulic conductivity until the field values and computed value matched within a precise value of water level in nine observation wells distributed across the model domain. The water level confidence interval chosen within  $\pm 1.5$  m. For an aquifer, an unconfined layer

1 and a semi-confined layer 2, with an initial hydraulic conductivity value of 30 and 2 m / day respectively has been chosen based on the soil type and previous studies carried out in the region.

Lahey et. al (1995) carried out a study in the Northern Al Batinah to explore some of the main hydrogeological features of the underlying alluvium aquifer. The study revealed that the hydraulic conductivity exhibits a wide range, ranging from 0.3m/day to 449m/day. The hydraulic conductivity was found to be the lowest in cemented, clayey sands, whereas the highest values were detected in uncemented sands and gravels. The value of storage coefficient varies from  $1 \times 10^{-5}$  to  $1 \times 10^{-2}$ . The unconfined, uncemented sands and gravels were associated with the highest values. The value of transmissivity varies from 0.9m<sup>2</sup>/day to 16,900m<sup>2</sup>/day and the aquifer yield ranged from 1.0 L/sec to 515 L/sec.

**Table 4-1 Hydrogeological parameters used for steady state model simulation**

Location	Applicable Model Zone	Layer 1		Layer 2		Recharge rate (m/d)
		H. K.	Vani	H. K.	Vani	
Near Coast 1	1	163	20	180	20	0.001358
Near Coast 2	2	220	25	220	25	
Valley 1	3	195	20	198	20	
Valley 2	4	125	20	110	20	
Near Mountain	5	7.5	20	4	10	

\*H.K. = Hydraulic conductivity      Vani = Vertical anisotropy

Estimates of net water demand by the National Well Inventory (NWI) are based on assumed conditions. MWR and other studies have shown that NWI estimates (20%) are too high (Lahey et al. 1995). Well monitoring hydrographs clearly depicted that the rise and fall in the water levels is in response to the wet and the dry periods in Wadi Al- Jizi with no apparent overall long-term decline. This suggested that the long-term average recharge from all the sources must be equal to total groundwater abstraction, plus any outflows towards the sea, minus



the amount of saline intrusion that is taking place. Using water level data for coastal wells, MWR (1995) estimated that salinity intrusion into Wadi Al Jizi at that time was around 0.8 MCM per year. This estimate serves as a useful calibration guide for the model.

A pumping rate of 1474 m<sup>3</sup>/day for SDO wellfield supply wells and a agricultural well (3 nos.) and 1814m<sup>3</sup>/day for the remaining agricultural wells (19 nos.) in all total of 22 pumping wells with an average recharge rate of 0.001358 m/day is used for the year 2000. The overall recharge applied for the 519 km<sup>2</sup> area of Wadi Al Jizi was compressed to apply on the polygon recharge area (123.6 km<sup>2</sup>) of the model which is about 24% of the total area of Wadi Al-Jizi east.

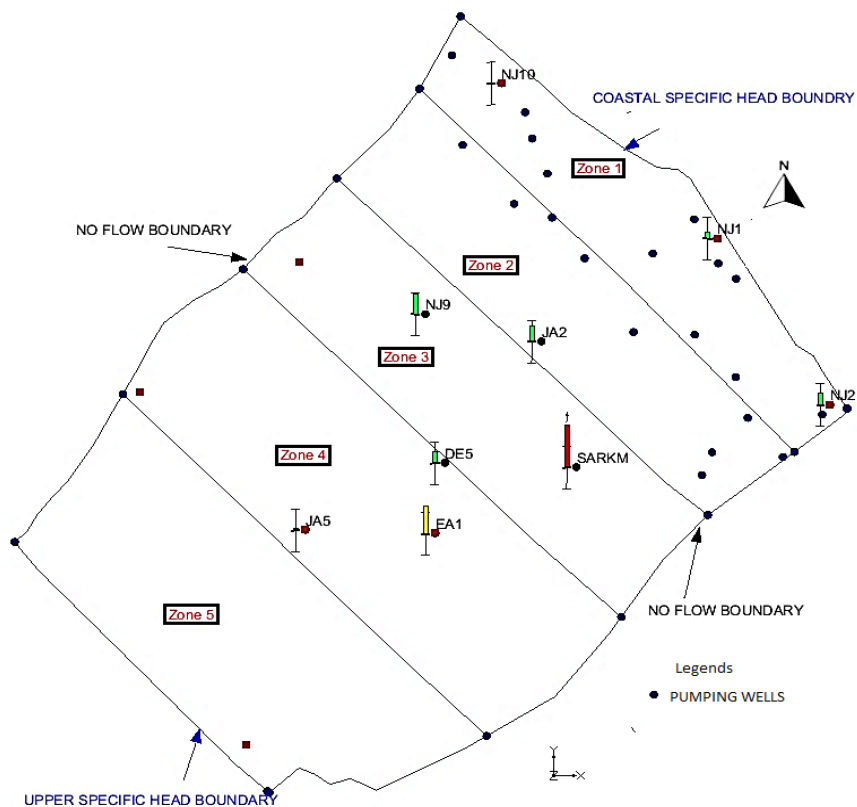


**Figure 4-1: Calibrated water heads in the steady state condition in the year 2000**

The observation target bar (green, red or yellow color) near the observation wells were used for calibration work to compare the computed results with the observed values in steady state in 2000. The colored bar represents the error. If the bar lies entirely within the target, the color bar is drawn in green. If the bar

is outside the target, but the error is less than 200%, the bar is drawn in yellow. If the error is greater than 200%, the bar is drawn in red. The top of the target corresponds to the observed value plus the interval and the bottom corresponds to the observed value minus the interval. The green color of the target bar monitoring bar indicates that the computed value fall within the monitoring confidence interval of  $\pm 1.5\text{m}$  (Figure 4-1). In an observation well, a confidence interval of  $\pm 1.5\text{ m}$  between observed and simulated values for the water level was deemed acceptable.

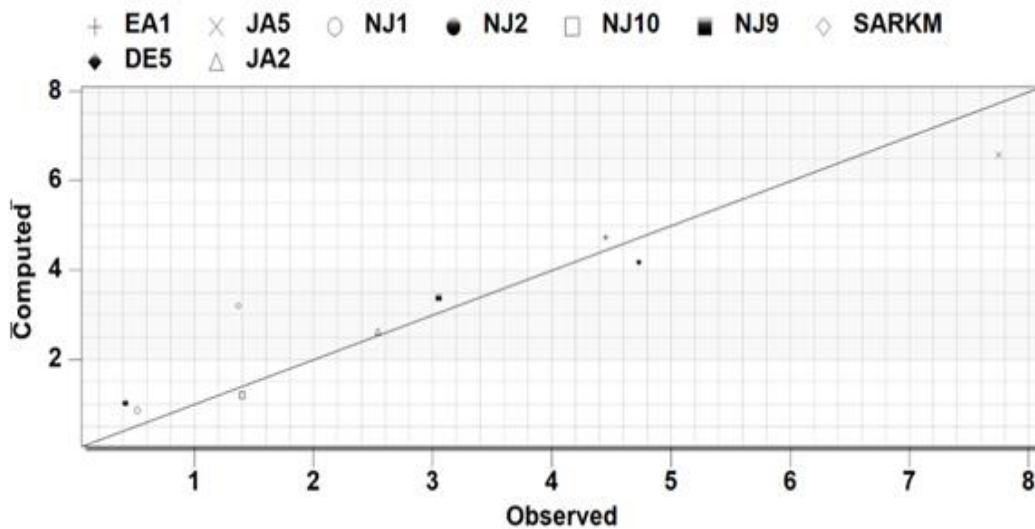


**Figure 4-2: Observed versus computed head (m) in steady state conditions in year 2000**

Table 4-1 shows the calibrated hydraulic conductivity values for Layer 1, which were determined to be 7.5 m/day for the upper zone (near the mountains) and 163 m/day for the lower zone (near the coast). For the Layer 2 of the model, the calibrated values of hydraulic conductivity were 4.0 m/day for the upper zone (near mountains) and 180 m/day for the lower zone (near the coast). The range of the hydraulic conductivity was 7.5 – 220 m/day and 4.0 – 220 m/day for the Layer 1 and Layer 2 respectively. The highest values of hydraulic conductivity (220 m/day) were found in the Zone 2 region in the middle part of the model not too far from the coastline whereas the lowest values (4.0 m /day) were shown in the upstream region of the model. Al-Shibli (2002) study for a comparable region highlighted that the steady state hydraulic conductivity

ranges from 6–80 m/day and 8–80 m/day respectively for the layer 1 and layer 2. The model domain grid resolution, however, was not the same as in the current research. In this research, the calibrated hydraulic conductivity is within the parameters published by Lakey et al. (1995). Table 4-2 shows the calibrated results in the steady state for the year 2000 with a Root-Mean-Square Error (RMSE) of 0.65.

**Table 4-2 Calibrated heads in the year 2000 in Steady state simulation**

<b>Observation Well ID</b>	<b>Observed Head amsl (m)</b>	<b>Computed Head amsl (m)</b>	<b>Difference(m)</b>
NJ-1	0.52	0.85	-0.33
NJ-2	0.42	1.00	-0.58
NJ-10	1.40	1.20	0.20
JA-2	2.54	2.63	-0.09
SARKM	1.37	3.19	-1.82
NJ-9	3.05	3.38	-0.33
DE-5	4.73	4.20	0.53
EA-1	4.45	4.70	-0.25
JA-5	7.75	6.50	1.25

### **4.3 Sensitivity to the Hydraulic conductivity value**

Hydraulic conductivity, one of the most important hydrogeological parameters of aquifer, was calibrated manually using trial and error procedure. This input parameter was varied to determine the model response by conducting sensitivity analysis and calculating and plotting the groundwater fluctuations. Out of nine, four observation wells one from each zone was selected to exhibit the response of groundwater head with respect to the variation for this parameter. Figure 4-3 shows the sensitivity of hydraulic conductivity ( $K$ ) in layer-1 and layer-2 when  $K$  values were varied by upto  $\pm 30\%$  from their calibrated values. Both layer 1 and layer-2 were found to be sensitive to the variation of hydraulic conductivity.

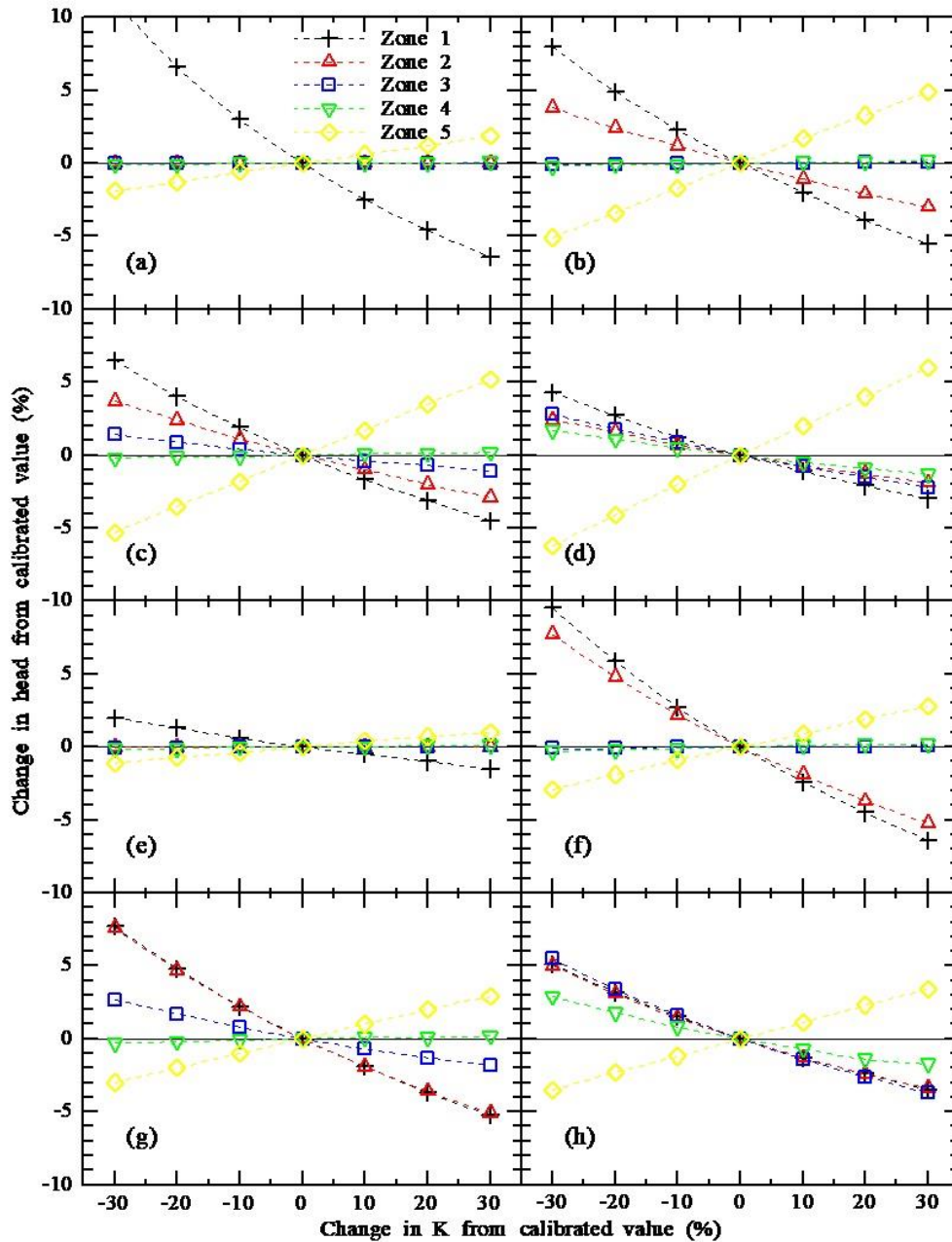


**Figure 4-3 Sensitivity of water table to variation of hydraulic conductivity in Layer 1: (a) NJ-1 (b) JA-2 (c) NJ-9 (d) EA-1 and Layer 2: (e) NJ-1 (f) JA-2 (g) NJ-9 (h) EA-1**

Out of nine observation wells, four wells NJ-1, JA-2, NJ-9 & EA-1 were selected from zone-1, zone 2, zone 3 and zone 4, respectively (one from each zone). For all zones in both the layers, except zone 5, it was observed that by reducing the hydraulic conductivity groundwater elevation increases with the most significant rise in zone 1. In zone 5 groundwater elevation falls because of

an increase in the hydraulic conductivity as shown in Figures. 4-3(a) to 4-3 (d) except for well NJ-1, which showed a slightly raised water table. Figures 4-3 (f) and 4-3 (g) showed fluctuation in the head of observation wells JA-2 and NJ-9 respectively due to variation of hydraulic conductivity in zone-2 in layer 2. This can be attributed to the reason that these wells might be in heavy pumping zones and high value of hydraulic conductivity assigned to the zone.

#### 4.4 Transient Model calibration and validation for Groundwater Flow

The word used for storage of unconfined aquifers is known as the specific yield ( $S_y$ ). Specific yield is the amount of water discharged by an unconfined aquifer from storage for each unit of aquifer surface area per unit of water table decline. Specific yields of unconfined aquifers are much greater than confined aquifers. No data relating to storage coefficient was available within the model area. A previous study in the area (BRGM, 2000) showed that the storage coefficient can vary from  $1 \times 10^{-7}$  to 0.3. JICA (1986) assumed that the storage coefficient ranges from 10 to 15%.

**Table 4-3 Calibrated hydrogeological parameters used for transient model simulation**

Applicable area	Applicable Model Zone	Layer 1			Layer 2		
		H.K.	Vani	Specific Yield	H.K.	Vani	Specific Yield
Near Coast 1	1	150	20	0.05	180	20	0.005
Near Coast 2	2	220	25	0.05	220	25	0.005
Valley 1	3	195	20	0.05	198	20	0.005
Valley 2	4	125	20	0.05	110	20	0.005
Near Mountain	5	6	20	0.05	4	10	0.008

\*H.K. = Horizontal Conductivity Vani. = Vertical Anisotropy

During the calibration, specific yield for both layer 1 and layer 2 of the aquifer is allotted. With numerous trials and fine tuning in the values of hydraulic conductivity and specific yield (Table 4-3), the model was able to give

acceptable computed values for the water levels concern. Monitoring data indicated that the water levels dropped during the period of droughts as groundwater level declined and the saline water intruded in the coastal aquifer areas where water levels fall below sea level. Likewise, water levels increase during wet period having sufficient ground recharge with which groundwater storage is replenished, and salinity intrusion is reduced, and may even be reversed in some areas. Nonetheless, the groundwater supply is now largely overdeveloped in the coastal region, pumping excessive amount of water for agricultural and domestic needs, therefore, even during wet periods having more than average rainfall, salinity intrusion can occur in the sectors where water levels are not rising above sea level.

The transient simulation through 2000 - 2017 was carried out considering the water heads resulted from the steady state simulation as an initial head. This will allow to simulate the fluctuations of water level impacted by wet and dry period for several years. Period from Jan. 2000 - Dec. 2009 was chosen to calibrate the model, whereas validation in transient condition was conducted through Jan. 2010 to Dec. 2017. Nine observation wells located across the model domain chosen for achieving transient results in water level. The model consisted of 18 stress periods, each comprising 12 monthly time steps, resulting in a total of 6574 days. To confirm the accuracy of the model, newly obtained pumping rates and recharge data spanning the period from 2010 to 2017 were used. The parameter hydraulic conductivity was used with a minor adjustment in the value in zone-1.

Figure 4-4 shows the comparison of the observed and the computed groundwater elevation in selected observation wells, namely, NJ-1, JA-2, NJ-9, EA-1, JA-5, and DE-5. Although the abstraction rates are not accurate as mentioned before, the qualitative agreement between the observed values and model prediction is quite good. The computed head demonstrates good agreement with the observed head. The groundwater elevations show higher values resulting from the recharge due higher values of rainfalls in years 2006, 2007 and years 2013 to 2017. The model could predict these changes in the water table quite satisfactorily.

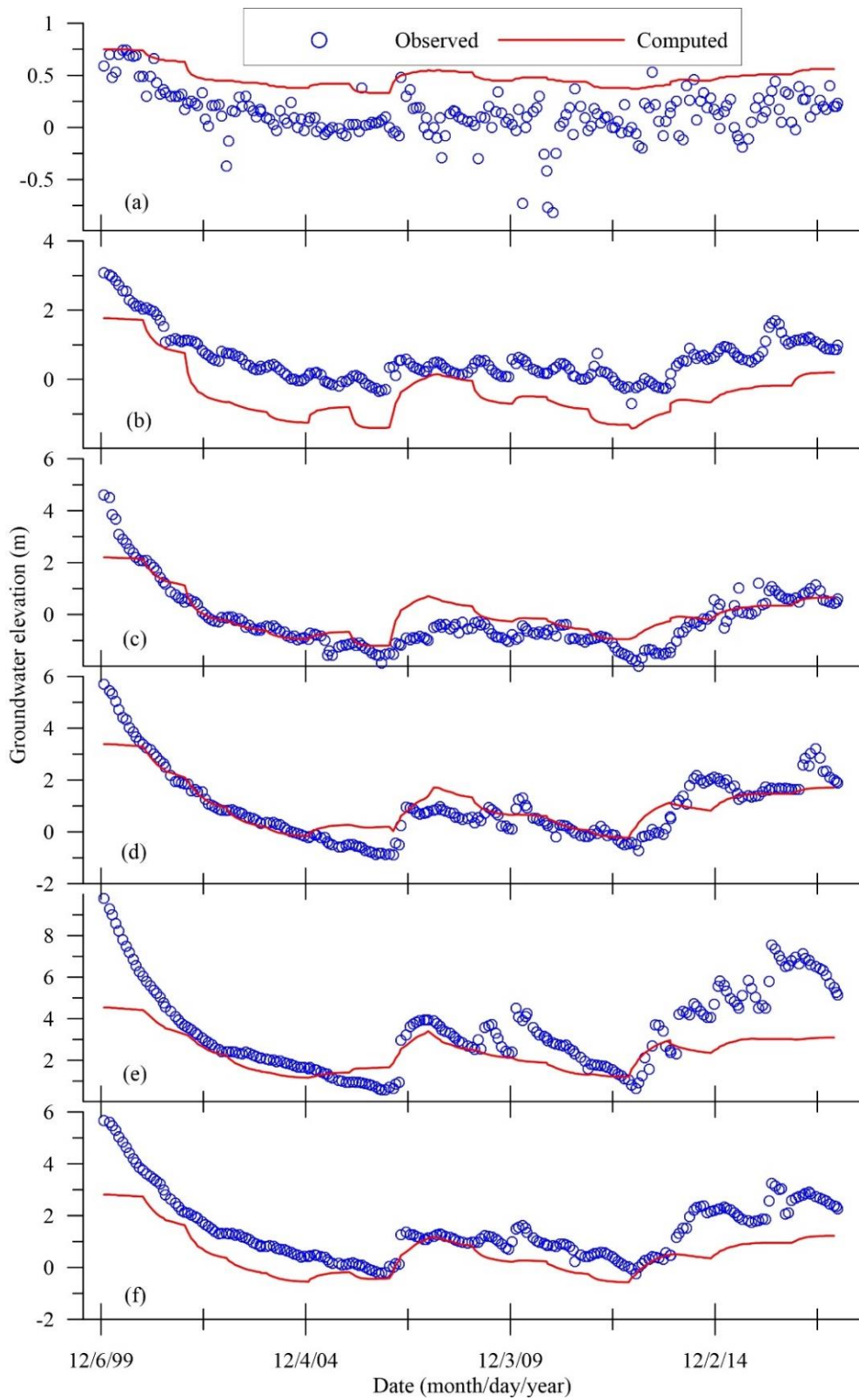


**Figure 4-4 Time series plot of selected observation wells (a) NJ-1, (b) JA-2, (c) NJ-9, (d) EA-1, (e) JA-5 and (f) DE-5.**

#### **4.5 Predictive simulation**

The primary goal of the predictions is to assess the aquifer performance under various pumping conditions to predict the management of groundwater supplies for the following 22 years' worth of demand. The anticipated abstraction increments, and reduction rates were used for from the year 2018 to the year 2040 to estimate the aquifer performance in terms of water level and SWI. At this stage, the model was used to forecast the aquifer's future behavior under transient conditions under proposed demand management/conservation and supply augmentation programs for the period 2018 –2040 (22 years). Following validation, the validated model was used to predict how the aquifer system would react to expected changes in hydrological stresses over the course of the following 22 years. (2018 - 2040). Forecast was carried out using base pumping rates of 2017. The recharge rates used in the predictive simulation followed the same trend of the past 17-year cycle from 2018 - 2040, but in the real situation, for several years, there is either no rainfall or very small amount of rainfall takes place, which causes the groundwater levels to drop steeply below the seawater level causing intrusion of seawater. In contrast for a few years, heavy intensity of rainfall recovers the water level of the aquifer, and the transition zone shifts towards the sea.

The simulated head in the year 2040 showed a maximum fall of head of 4.14 and 5.23 m in monitoring wells SARKM and JA-5, respectively, as compared to the observed head in year 2017 (Table 4-4).

Two different scenarios of pumping rate (increment and reduction) and Sea level (increase and fall) due to climatic change was considered in the study area to observe the fluctuations of water table and resulting salinity intrusion.



**Table 4-4 Observed and computed head of observation wells**

Well id	Observed head (m)	Computed head (m)		Fall of groundwater elevation (m) from year 2017 to 2040
	2017	2030	2040	
NJ-1	0.24	0.36	0.37	-0.13
NJ-2	0.18	0.11	0.12	0.06
NJ-10	0.96	-0.01	0.01	0.95
JA-2	1.02	0.78	0.96	0.06
SARKM	2.82	-1.40	-1.30	4.14
NJ-9	0.71	-1.16	-1.07	1.78
DE-5	2.62	-0.87	-0.74	3.36
EA-1	2.47	-0.59	-0.44	2.91
JA-5	6.19	0.78	0.96	5.23

#### **4.5.1 Scenario 1: Incremental Pumping rates**

In this scenario, pumping rates that were adopted from the year 2000 to 2017 are kept as they are but for the year 2018 to 2040, the pumping rates from year 2018 were increased by 10 %, 20 % and 30 %. This increment was considered, keeping in mind the possible increase in the population or increased agricultural use of water in the study area. Recharge pattern that occurred in period of the past 17 years was applied.

Figure 4-5 (a) shows the simulated water level lowered by more than 3.5 m when compared with the observed value in year 2017 for the observation well JA-2 which is lying adjacent to the pumping wells in zone-2. Figure 4-5 (b) shows the simulated water level lowered by more than 2.0 m for the observation well EA-1 which is lying adjacent to the pumping wells in zone-3 a pumping rate increment of 30%.

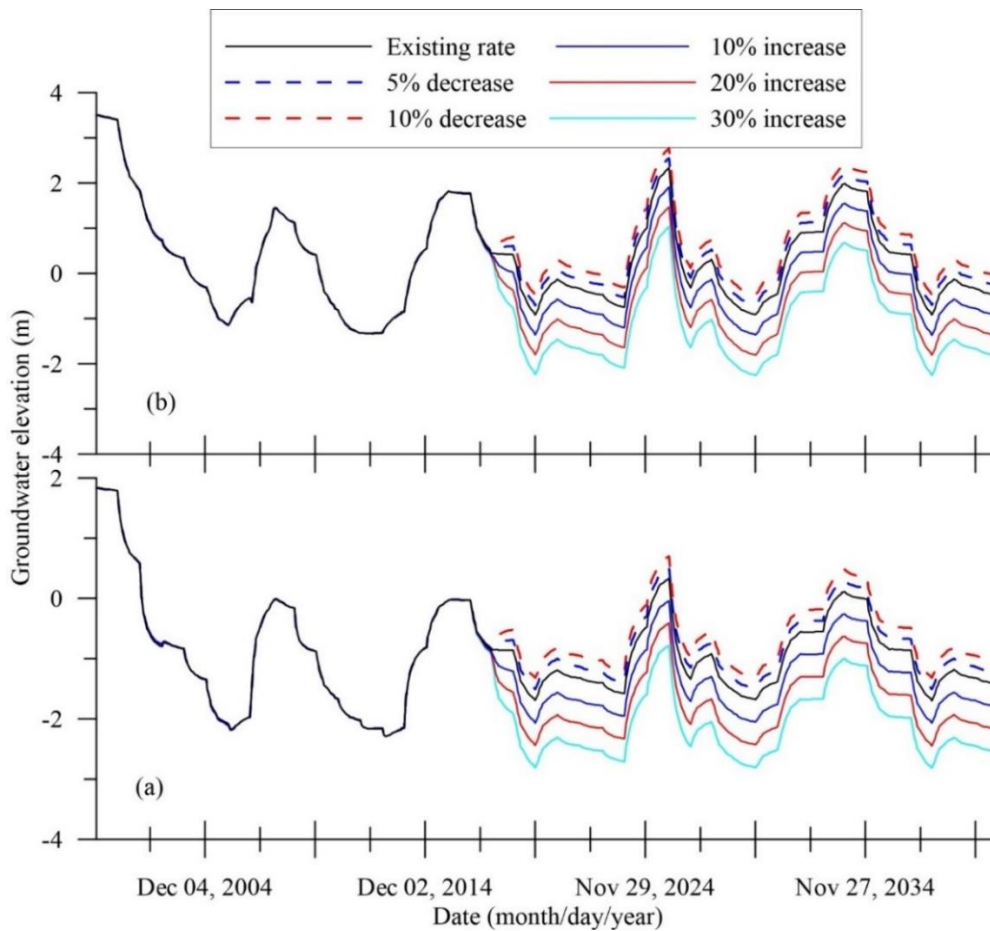


**Figure 4-5 Predictive simulation of groundwater elevation in (a) observation well JA-2 (b) observation well EA-1 for different pumping scenarios**

#### **4.5.2 Scenario 2: Reduced Pumping rates**

In this scenario, the pumping rates that were adopted from the year 2000 to 2017 are maintained, but for the year 2018 to 2040, the base year 2017 pumping rates were reduced by 5% and 10%. This reduction in the pumping rates was considered due to use of treated wastewater and enhancement of agricultural water conservation in the study area. Recharge pattern that occurred in period of the past 17 years was applied. Reduction in pumping rates will allow the aquifer to rest and allow natural recovery of water head. The groundwater elevation is raised by approximately 0.5m as a result of 10% decrease in pumping rates from year 2017 value at both the observation wells (JA-2 and EA-1). However, reducing pumping rates in this agricultural area would require

strong policies regarding water conservation and more efficient use of water for agriculture.

#### **4.5.3 Scenario 3: Effect of Sea level rise due to Climate change**

The model simulates the variation of the observed water heads in a reasonable manner for the purpose of the present study of salinity intrusion near the coast.

#### **4.6 Solute Transport Model**

Simulation of salinity intrusion along the coast was carried out using MT3DMS. MT3DMS is a contaminant transport model that simulates advection, dispersion, and chemical reactions of soluble pollutants in a three-dimensional groundwater flow system (Zheng & Wang, 1999). Advection, dispersion and source & sink mixing were used as main package to run transport model. Advection is the process that carries dissolved solid along groundwater from one point to another. Diffusion leads solute to move from high concentration to low concentration area. The coastal boundary conditions are based on a combination of a defined head for water head simulation and variable coastal salt concentration for the three-dimensional solute transport model. The boundary conditions for solute transport, whether steady-state or transient-state, are dependent on the boundary conditions specified in the groundwater flow model. This is to allow the model to measure the salt concentration when it moves from the sea due to a decrease in water level below seawater level, and to flow from land to sea during wet periods when the water level rises due to an increase in recharge. All the boundary conditions used are same as in the MODFLOW, therefore, if the aquifer water table is below seawater level, only the flow from the sea will be accounted for.

The model's east (coastline) boundary for both layer 1 and layer 2 were allotted constant inflow concentration of 34,000 mg/L and the west (mountain) boundaries was allotted 4375 mg/L as per the salinity concentration observed in the well NJ-3 close to this upstream boundary. Recharge was assigned with a concentration of 500 mg/L. MT3DMS was coupled to the transient Wadi Jizi groundwater MODFLOW simulation of 2000 - 2016. MRMWR salinity data for 2000, 2005, 2010 and 2016 were used as observational data for salinity

monitoring wells. Table 4-5 shows the location of twenty salinity monitoring well with the observed salinity concentration in the year 2000, 2005 2010 and 2016 used for the study purpose.

**Table 4-5 Location of salinity monitoring well with observed salinity in the year 2000, 2005, 2010 and 2016**

Salinity Monitoring Well ID	Location		Observed Salinity concentration (mg/L)			
	Easting	Northing	2000	2005	2010	2016
NCH-83	467229	2700384	704	480	672	479
NCH-88	468864	2698976	768	666	717	696
NCH-92	470352	2696757	538	506	672	763
NCH-98B	471786	2694426	1600	806	956	864
NCH-85	468169	2699244	704	1005	896	928
NCH-91	469459	2698187	499	800	736	966
NCH-99	471603	2693985	1984	1574	1056	1357
NCH-89B	468777	2699829	1965	704	845	1805
NS-8	470703	2698280	365	1350	2022	1984
NCH-96	472219	2695886	2688	2227	2144	2138
NS-1	473798	2695159	2880	5645	2822	2624
NCH-80	467032	2702124	934	1434	3430	2861
NCH-95	471469	2696707	877	1440	1830	4168
NS-12	468371	2701019	2432	4368	5216	5200
CHS-165B	472438	2695095	2048	1837	4096	6088
CHS-164	473080	2694336	1856	2432	5560	7256
NCH-84	468500	2700508	2240	1267	2778	9480
NS-4	472224	2697789	4080	9136	11680	11360
NS-5W	471900	2698089	3008	7944	9784	15688
NS-10B	469853	2699767	2112	4848	8440	6872

#### **4.6.1 Steady State Transport Calibration and Validation**

The rise and fall of groundwater salinity along the shore follows the same trend as the dry and wet period seasonal analysis. The head of the water began to diminish in dry years when the recharge was reduced due to low rainfall, and seawater with high salt concentrations drifted to land and mingled with fresh water. In wet years, freshwater level will surge above saltwater level, pushing the wedge contact closer to the sea. As the water head drops and the transition zone shifts onshore, salt migration from the high concentration of seawater often occurs by upconing from the transition zone during the events of heavy pumping.

The calibration and validation of the transport transient model were performed by comparing the simulated groundwater salinity with the observed values for 20 monitoring wells from the period of 2000 to 2016. Salinity data from the monitoring wells operated by the Ministry of Regional Municipality, Environment and Water Resources (MRMEWR) were used. The location of the salinity monitoring wells selected in the model domain is depicted in Figure 4-6.

The model domain which was divided into 5 zones (zone 1 to zone 5) for the groundwater modelling was further divided zones 1 & zone 2 into three parts each thus making a total of 9 zones for modelling the salinity intrusion. The zone 1 and the zone 2 which were close to the coastal area and more susceptible to the salinity intrusion were sub divided into three parts each to get clearer picture of salinity intrusion which was more prominent in the coastal zone, whereas zone 3, zone 4 and zone 5 were untouched. Further, zone 1 is sub-divided in three parts (1A, 1B, 1C), having an average width of 592 m, 678 m and 515 m respectively whereas zone 2 was divided in three more sub- divisions (2A, 2B, 2C), having an average width of 731 m, 653 m and 840 m respectively.

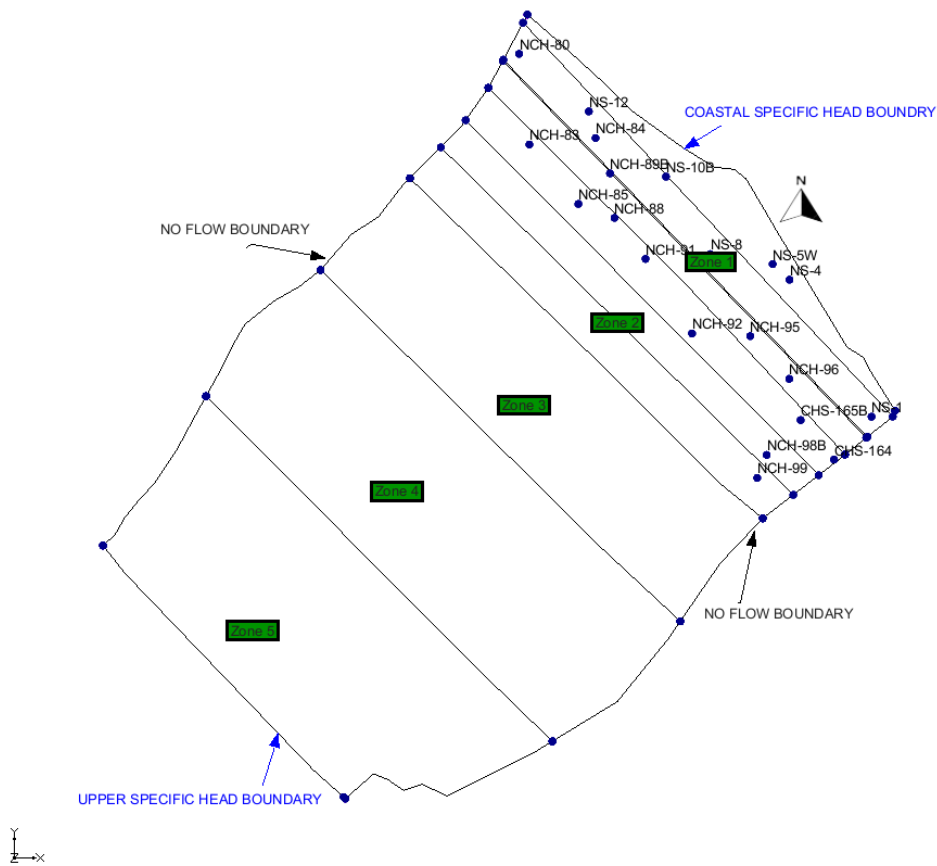


**Figure 4-6 Spatial distribution of salinity monitoring wells and zoning in model domain**

Calibration was performed to achieve the appropriate degree of correlation between the observed and the model's measured average concentration by changing the aquifer's initial concentration, porosity, and longitudinal dispersivity. The initial estimates of these values were derived from soil type and prior research. The hydrological parameters, including porosity, longitudinal dispersivity, the ratio of transverse dispersivity to longitudinal dispersivity, and the ratio of vertical dispersivity to longitudinal dispersivity, were adjusted through a process of trial and error. The calibration leads up to 0.6 for porosity and up to 14500 for longitudinal dispersivity near the coast and lower values moving to the upper reaches. Color coding of the computed salinity contour were chosen to match with the existing salinity maps with the authorities.

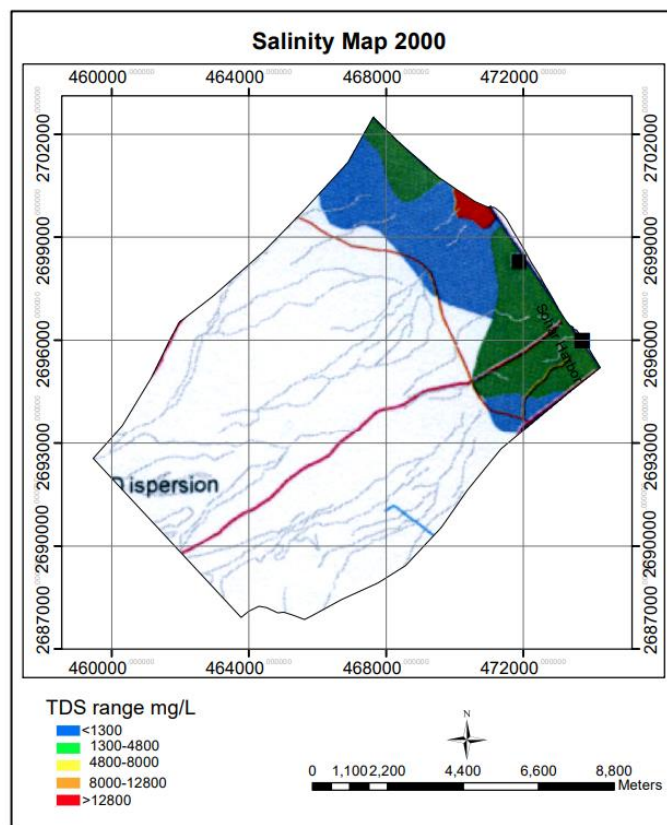
**Table 4-6 Transient state transport calibrated parameters**

Applicable Model Zone	Layer 1		Layer 2		Layer 1 / Layer 2	
	Porosity	Longitudinal Disp. (m/d)	Porosity	Longitudinal Disp. (m/d)	Hor. Disp. / Long. Disp.	Ver. T. Disp. / Long. Disp.
1A	0.5	14000	0.5	14000	0.1	0.01
1B		4000		4000		
1C		1250		1250		
2A	0.4	80	0.2	80		
2B		20		20		
2C		20		20		
3	0.2	20	0.6	20		
4	0.2	15	0.4	15		
5	0.2	15	0.2	15		

Table 4-6 presents the calibrated geo-hydrological parameters, which include porosity, longitudinal dispersivity, the ratio of horizontal dispersivity to longitudinal dispersivity, and the ratio of vertical transmissivity to longitudinal dispersivity. These parameters were used for the transient simulation, which consisted of a total of 17 stress periods, each with 12-time steps per month and a multiplier of 1, resulting in a simulation period of 6209 days.

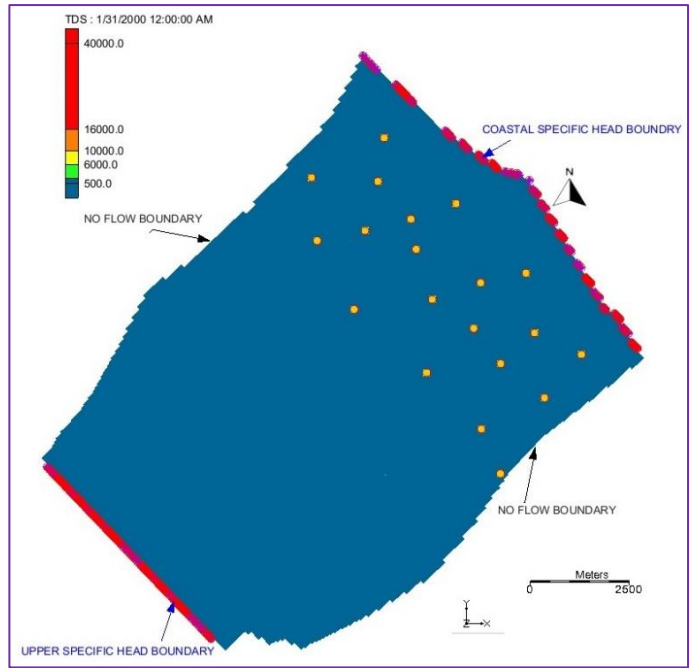
Overuse of groundwater has led groundwater levels to fall as a result of the deterioration of the quantity and quality of available surface water. Salinity intrusion mainly resulted due to over pumping of groundwater (Berkic & Serzic, 2021, Abdalla, 2016). If transient conditions were not taken into account, coastal aquifers in semi-arid locations with inadequate groundwater recharge, salinity intrusion due to groundwater abstraction pumping could have been underestimated. SWI caused by freshwater pumping from coastal aquifers can be influenced by several factors, including the location and pumping rates of wells, as well as aquifer characteristics such as hydraulic conductivity and porosity, the ratio of aquifer length to height, the density contrast between freshwater and saltwater, and the recharge condition (Stoeckl et al., 2019).

Seawater intrusion occurs when the amount of water abstracted from aquifers connected to the sea exceeds the recharge rate. This phenomenon is particularly severe along the Batinah coast in Northern Oman, where significant agricultural land has become unusable over the past 25 years. Figures 4-7 to 4-10 (a & b) show the salinity contour maps for the year 2000, 2005, 2010 and 2016 respectively for the observed values of the TDS by the MRMWR in Wadi Jizi and that by the model simulation. All the map shows the approximate trend with some discrepancies. As per Figures 4-7 (a & b), in the year 2000 salinity intrusion of around 2.0 km (TDS 1300 - 4800 mg / L) shows on the right-hand corner of the ministry's salinity contour map, whereas, in the model simulation it lies in the range of < 1300 mg/L for the whole modelled area. This may be due to the lack of salinity observation data and not collected in the same month for every year.



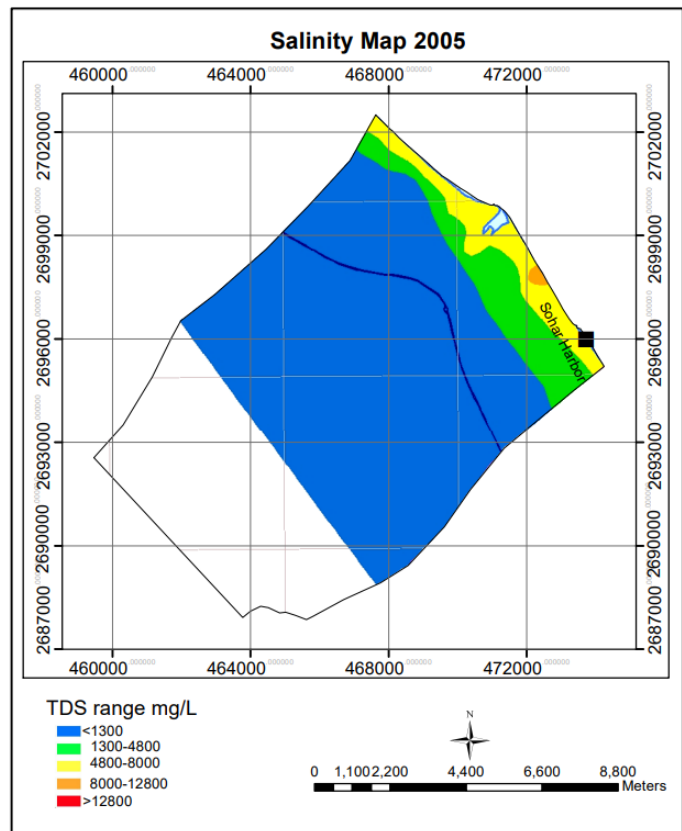
(a)



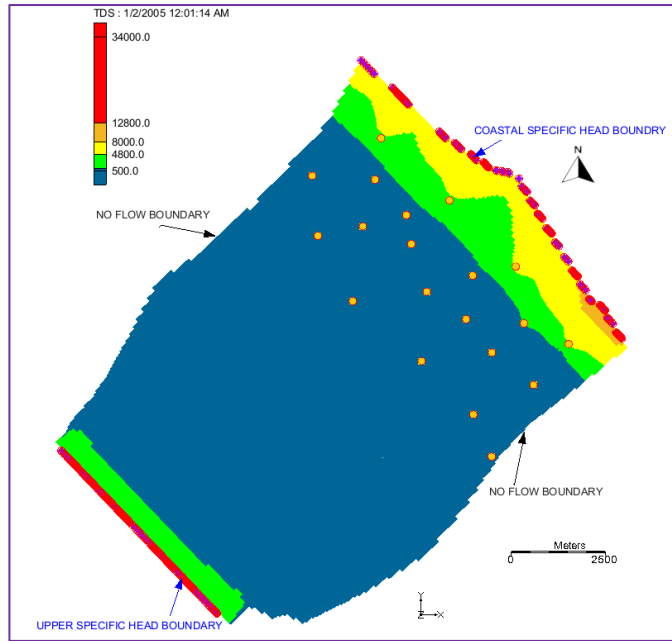


(b)

Figure 4-7 Salinity contour map year 2000 (a) Ministry map (b) Model simulation

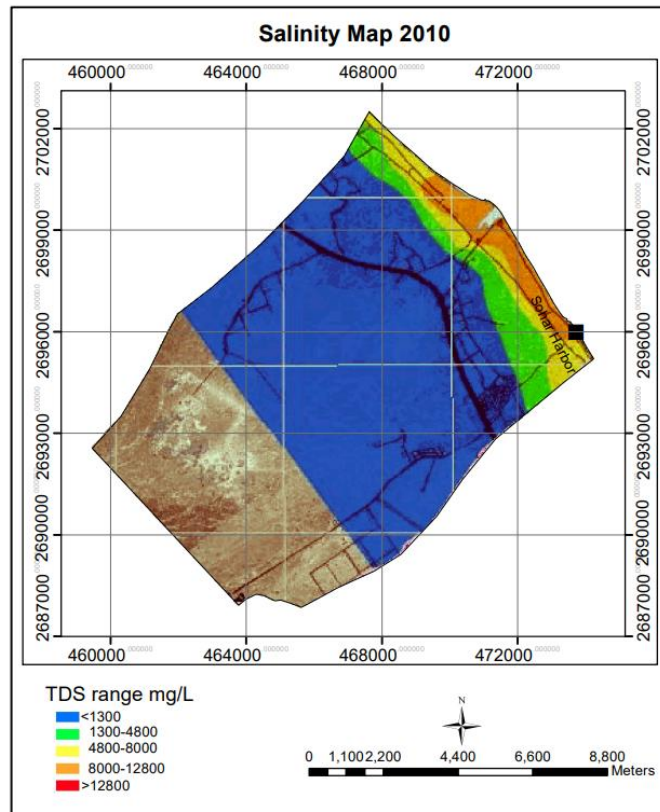


(a)

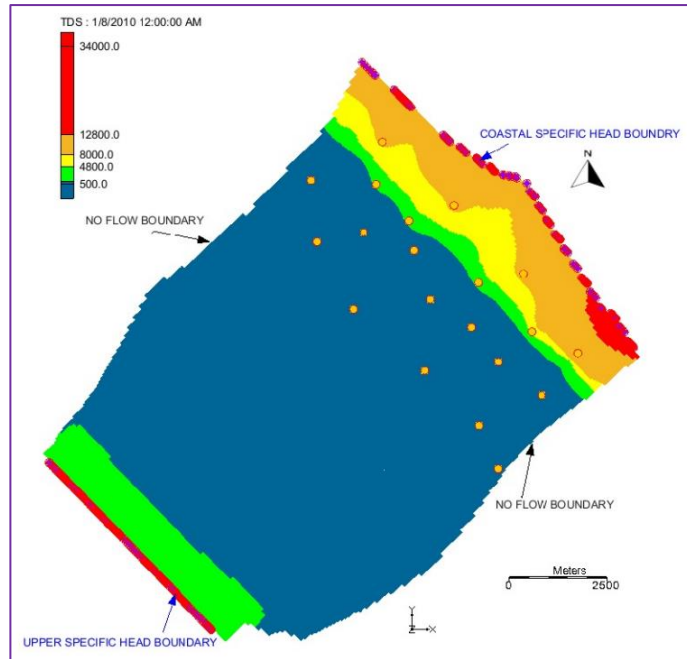


(b)

Figure 4-8 Salinity contour map year 2005 (a) Ministry map (b) Model simulation

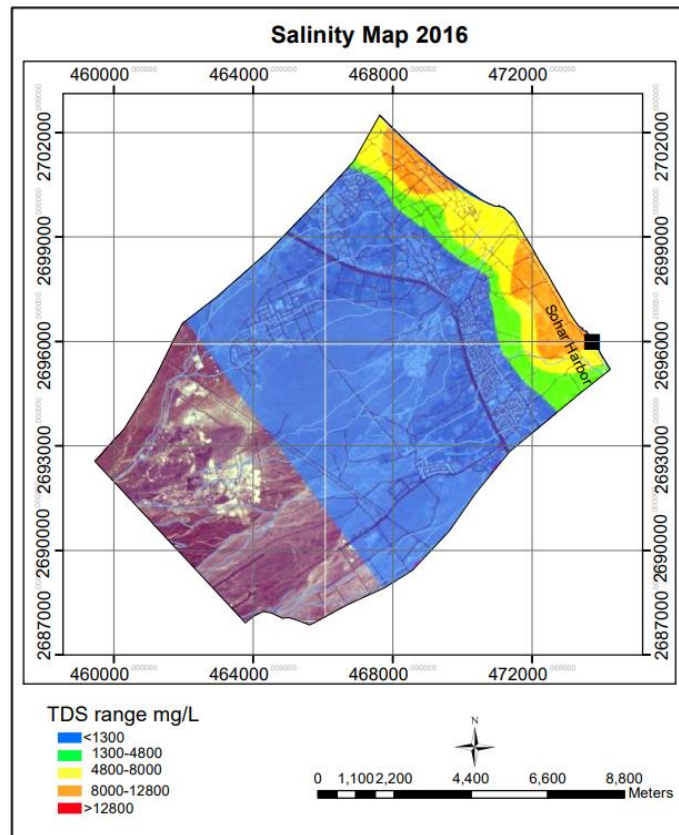


(a)

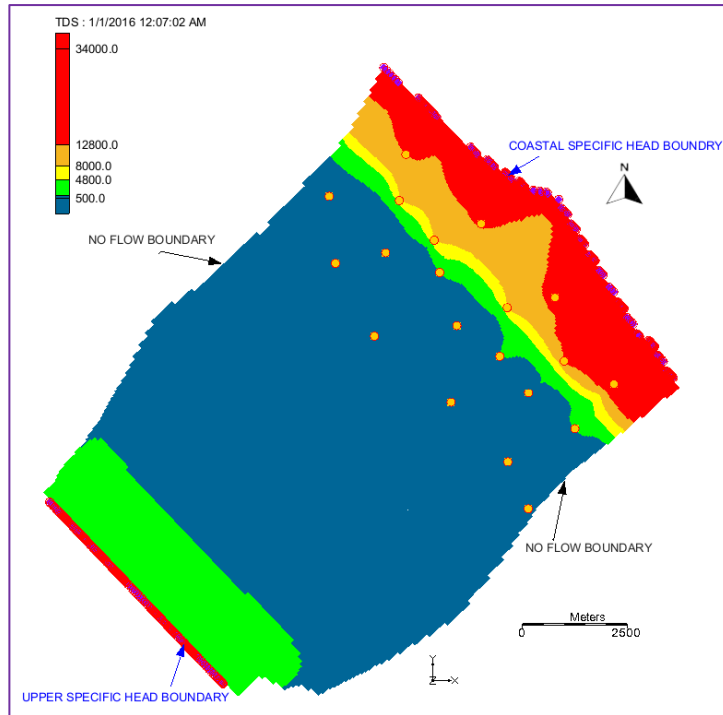


(b)

**Figure 4-9 Salinity contour map year 2010 (a) Ministry map (b) Model simulation**



(a)



(b)

**Figure 4-10 Salinity contour map year 2016 (a) Ministry map (b) Model simulation**

Figures 4-8 (a & b) which shows comparison of observed and simulated salinity value (2005) shows almost the same trend except some extra distance (1.30 km) covered by the salinity intrusion (4800 - 8000 mg/L) when simulated with the model as well as start of salinity intrusion (8000 -12800 mg/L) on the right-hand side of the model domain which intrudes around 0.30 km. While comparing Figures 4-9 (a & b) salinity intrusion (8000 -12800 mg/L) seems to move inland at an average of 1.35 km whereas on the right-hand side boundary it intrudes at a distance of 0.60 km having salinity more than 12800 mg/L. The intrusion of salinity is more severe near the location in the pumping well proximity which can also be observed in all the salinity computed maps. Figures 4-10 (a & b) which shows comparison of observed and simulated salinity value (2016) shows a steep rise in the value of salinity in comparison with the observed values. Salinity of more than 12800 mg/L intrudes at an average distance of 1.42 km as simulated by the model. The same intensity of salinity is not seen at the center of the model due to unavailability of the pumping wells at

that location. Salinity (>500 mg/L) also seems to intrude inland from the upper specific head boundary to the middle region of the study domain. This was attributed to the corresponding salinity value allotted and applied pertaining to nearest available observation well NJ-3 to this boundary. The water heads of the same well was also applied to the boundary.

#### **4.7 Impact of Pumping rates on Sea Water intrusion**

Over-exploitation of groundwater basins for industrial or agricultural use, resulted in dropping water tables and intrusion of seawater. The risk of seawater intrusion is higher during non-rainy seasons, even with relatively lower groundwater withdrawal, as compared to the rainy season (Prusty & Farooq, 2020). Because of the expansion in population and people's living conditions, the trend of groundwater consumption is increasing day by day. The developed model was used to assess the impact of pumping on salinity intrusion. To study the pumping impact scenario considering baseline pumping rate of the year 2017 and an increase of 10%, 20% & 30% were considered in the baseline pumping rates of 2017 and a reduction of 5% & 10% were considered in the baseline pumping of the year 2017 for all the 22 pumping wells used in the model domain. The pumping scenarios were considered for a period between 2018 – 2040.

The groundwater levels simulated for all pumping scenarios were compared to the levels obtained under normal pumping rates at different wells, as illustrated in Figure 5-5. It was obvious that salinity will move inland with the increase in the pumping rates and retreat back on reducing the pumping rates and the same was observed when the increments and the reduction of the pumping rates simulated with the help of a developed model. The distance of salinity intrusion was measured in all scenarios at the pumping well locations Well-12, Well-18 and Well-19 located in the left, centre and right-hand side respectively positioned in zone-1 (close to coastal boundary) in the model domain.

##### **4.7.1 Pumping @ baseline pumping rate of 2017**

In this case, the rate of water abstraction as used in the year 2017 considered to remain constant from the year 2018 till 2040. Table 4-7

shows the observed salinity in the year 2016 and computed salinity in the year 2030 and 2040.

**Table 4-6 Observed and computed salinity (Base pumping rates)**

Salinity Monitoring Well ID	Observed salinity (mg /L)	Computed salinity (mg /L)	
	2016	2030	2040
NCH -83	479	18072	20615
NCH -88	696	20968	23499
NCH -92	763	17740	20889
NCH -98B	864	17304	21662
NCH -85	928	18148	20753
NCH -91	966	18357	21213
NCH -99	1357	1637	1212
NCH -89B	1805	22015	24321
NS -8	1984	21495	24110
NCH -96	2138	25957	27949
NS -1	2624	27665	29394
NCH -80	2861	22260	24422
NCH-95	3334	23880	26176
NS -12	4160	22664	24809
CHS -165B	4870	24887	27244
CHS -164	5805	24724	26864
NCH -84	7584	22059	24342
NS -4	9088	24608	26733
NS -5W	12550	23857	26102
NS -10B	5498	22912	25124

Figures 4-11 to 4-13 shows the predicted salinity intrusion contours in the Jizi aquifer for the year 2025, 2030 and 2040 respectively. From the salinity contour simulated by the model, it can be clearly seen that the saline water having TDS (>12800 mg/L) intruded landward side by an average distance

of 2.19 km in the year 2025. The same intensity of salinity intruded inland by an average distance of 2.39 km and 2.56 km computed for the year 2030 and 2040 respectively. It means that salinity (>12800 mg/L) in the year 2040 intrudes 1.14 km inland when compared with the year 2016 if the pumping rates maintained at the base rates considered in 2017.

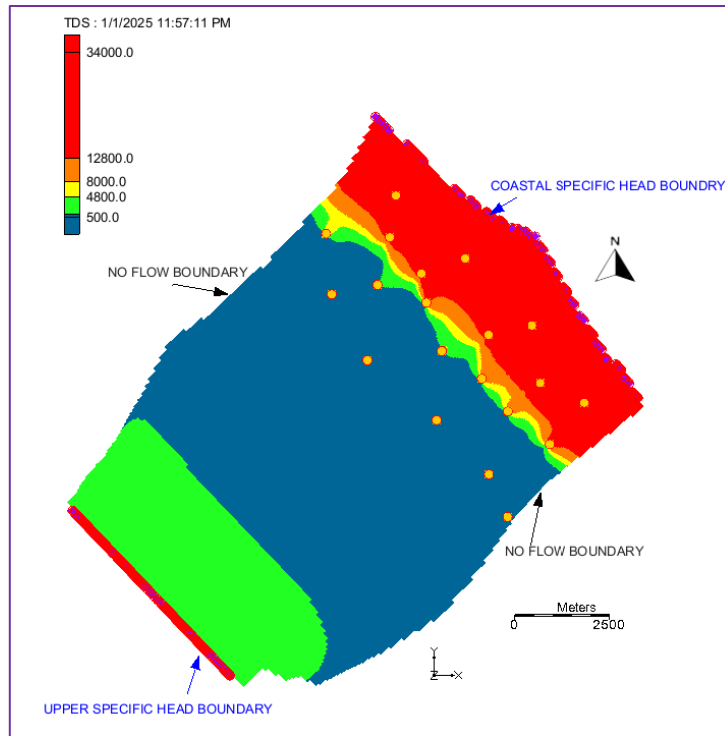


**Figure 4-11: Salinity contour in the Year 2025 during baseline pumping rates of 2017**

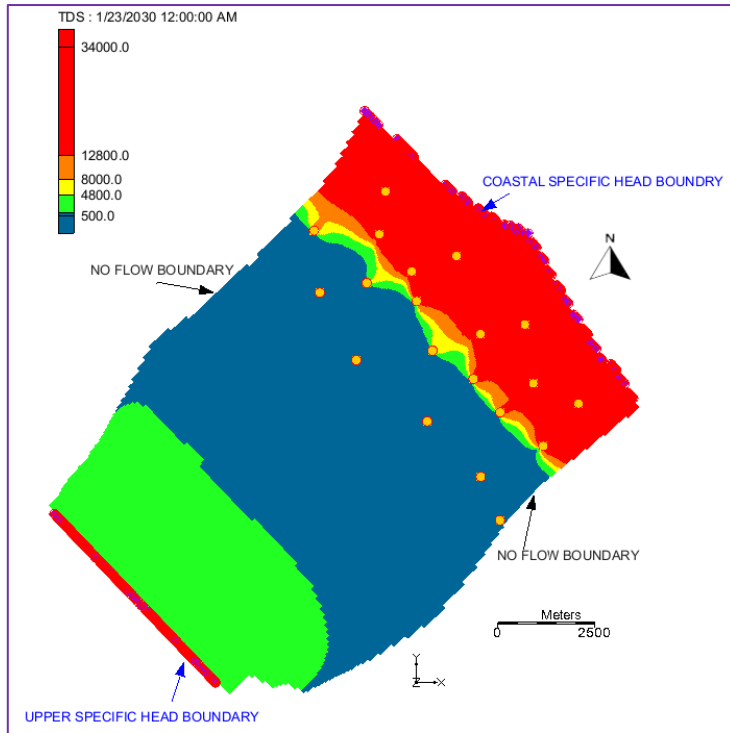


**Figure 4-12: Salinity contour in the Year 2030 during baseline pumping rates of 2017**

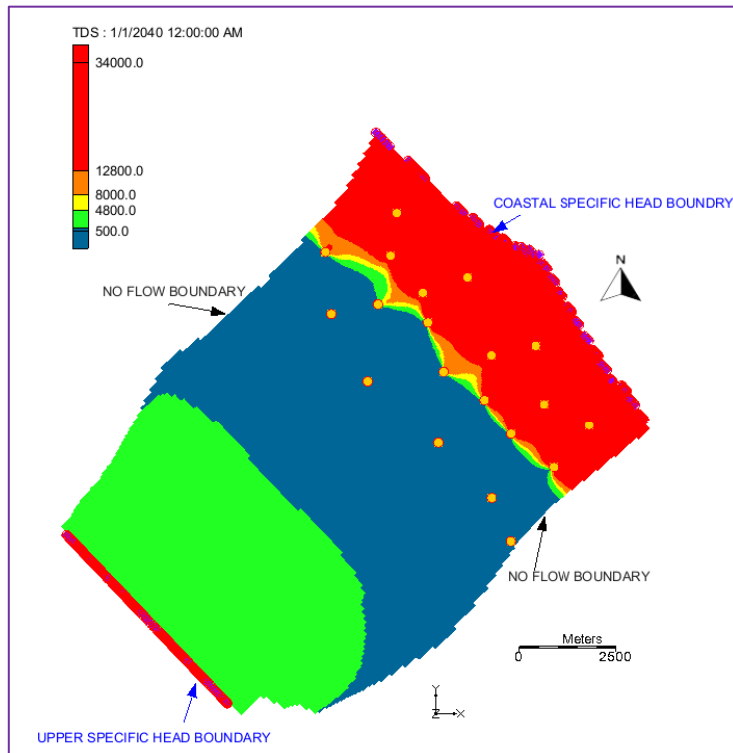


**Figure 4-13: Salinity contour in the Year 2040 during baseline pumping rates of 2017**



#### 4.7.2 Pumping Increment @ 10%

The calibrated model was used to predict salinity intrusion up to the year 2040. The predicted salinity intrusion contours in the Al Jizi aquifer for the year 2025, 2030 and 2040 are shown in Figures 4-14 to 4-16. It is evident from the salinity contour that the saline water having TDS (>12800 mg/L) intruded landward side by an average distance of 2.20 km. Salinity intrusion of the same intensity continue further inland by 2.42 km and 2.57 km in the year 2030 and 2040 respectively. Salinity (>12800 mg/L) in the year 2040 intruded 1.41 km inland when compared with the year 2016.

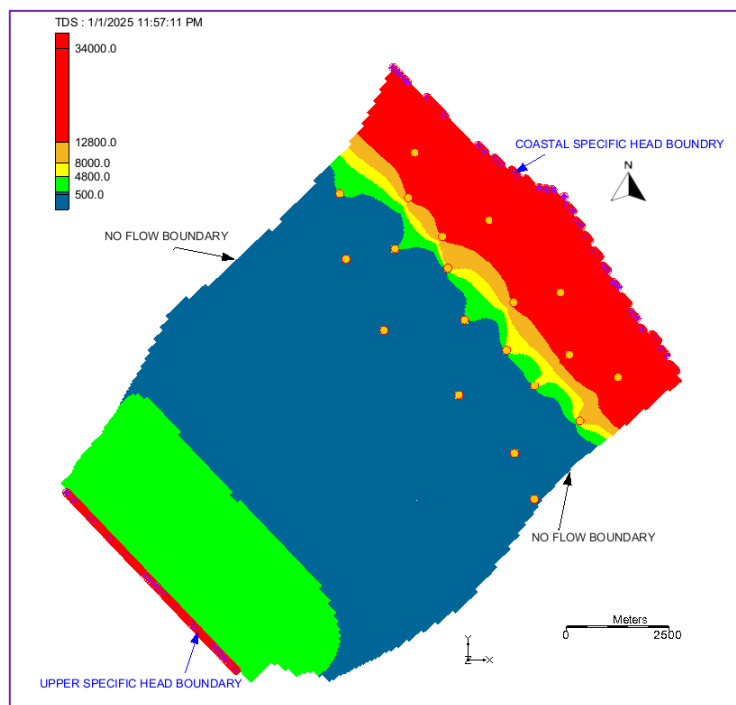


**Figure 4-14: Salinity contour in the Year 2025 during pumping increment @10%**

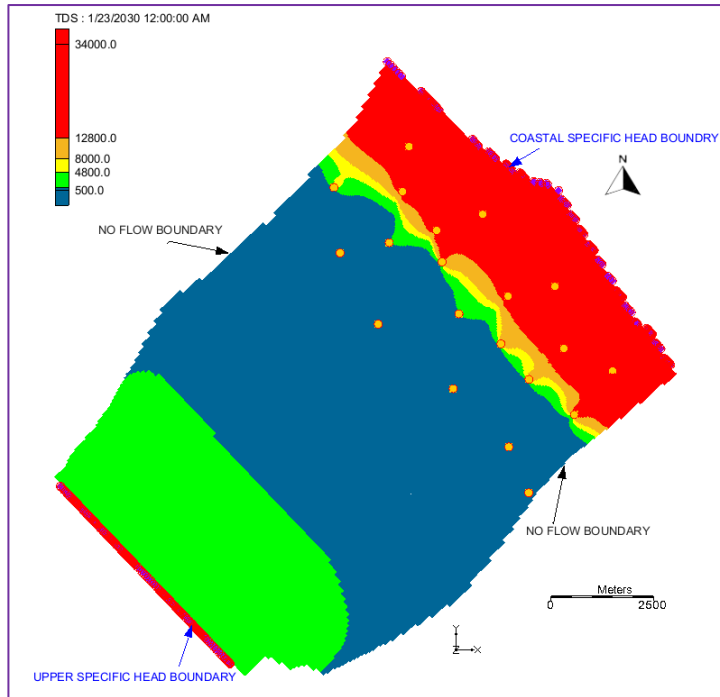


**Figure 4-15: Salinity contour in the Year 2030 during pumping increment @10%**

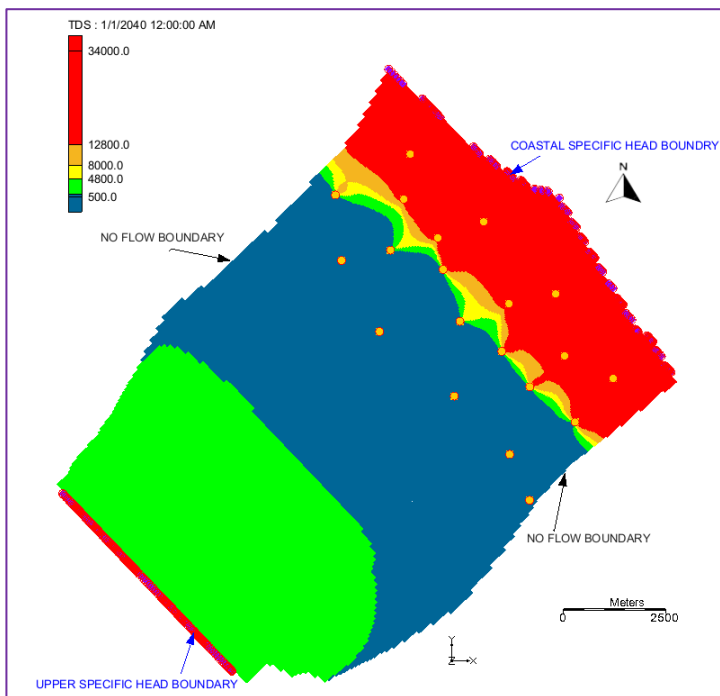


**Figure 4-16: Salinity contour in the Year 2040 during pumping increment @10%**

### 4.7.3 Pumping Increment @ 20%

Figures 4-17 to 4-19 shows the predicted salinity intrusion contours in the Jizi aquifer for the year 2025, 2030 and 2040. From the salinity contour simulated by the model it can be clearly seen that the sea water having TDS (>12800 mg/L) intruded landward side by an average distance of 2.35 km. The same intensity of salinity intruded inland by an average distance of 2.58 km and 2.65 km computed for the year 2030 and 2040 respectively. It means that salinity (>12800 mg/L) in the year 2040 intrudes 1.23 km inland when compared with the year 2016 if the pumping increased by 20% of its base rate of 2017.

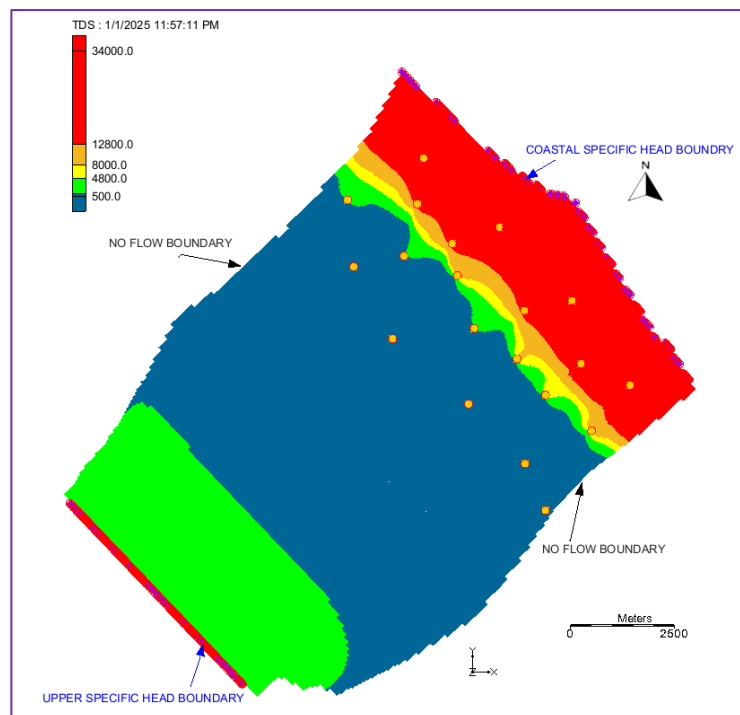


**Figure 4-17: Salinity contour in the Year 2025 during pumping increment @20%**

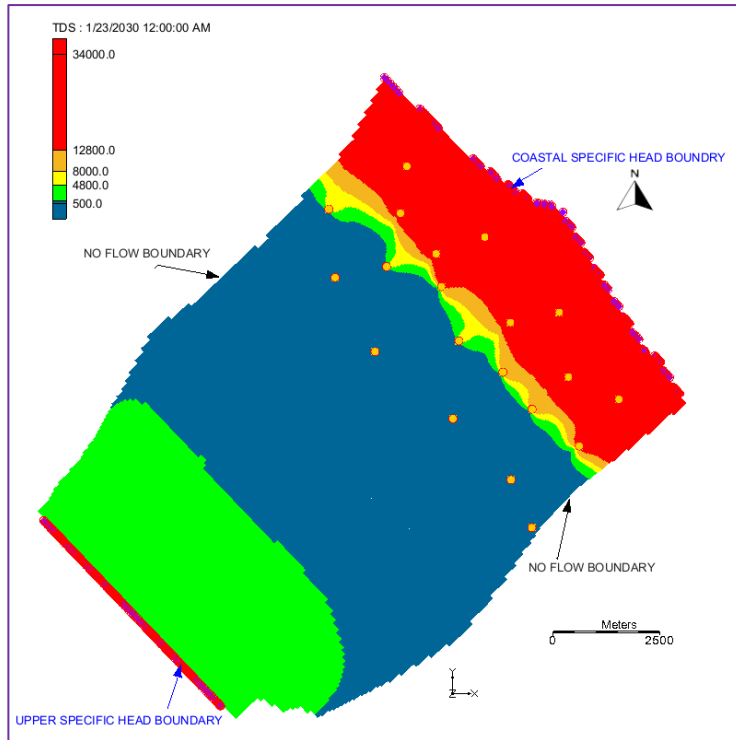


**Figure 4-18: Salinity contour during the Year 2030 pumping increment @20%**

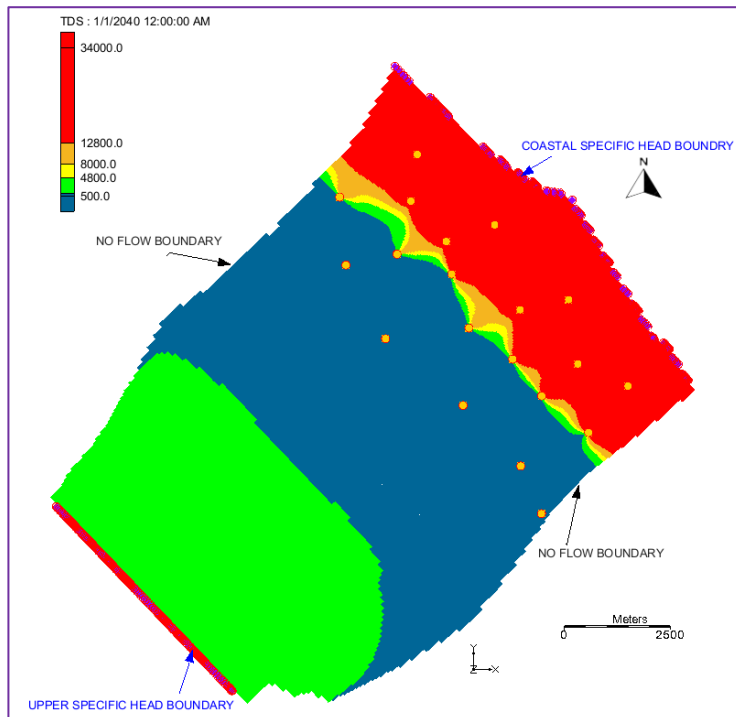


**Figure 4-19: Salinity contour in the Year 2040 during pumping increment @20%**

#### 4.7.4 Pumping Increment @ 30%

The predicted salinity condition in the Wadi Jizi aquifer for the years 2025, 2030 and 2040 is shown in Figures 4-20 to 4-22. It is evident from the salinity contour that the saline water having TDS ( $>12800$  mg/L) intruded landward side by an average distance of 2.47 km in the year 2025. Salinity intrusion of the same intensity continues further inland by 2.69 km and 2.37 km in the year 2030 and 2040 respectively. Salinity ( $>12800$  mg/L) in the year 2040 intruded 1.29 km inland when compared with the year 2016.

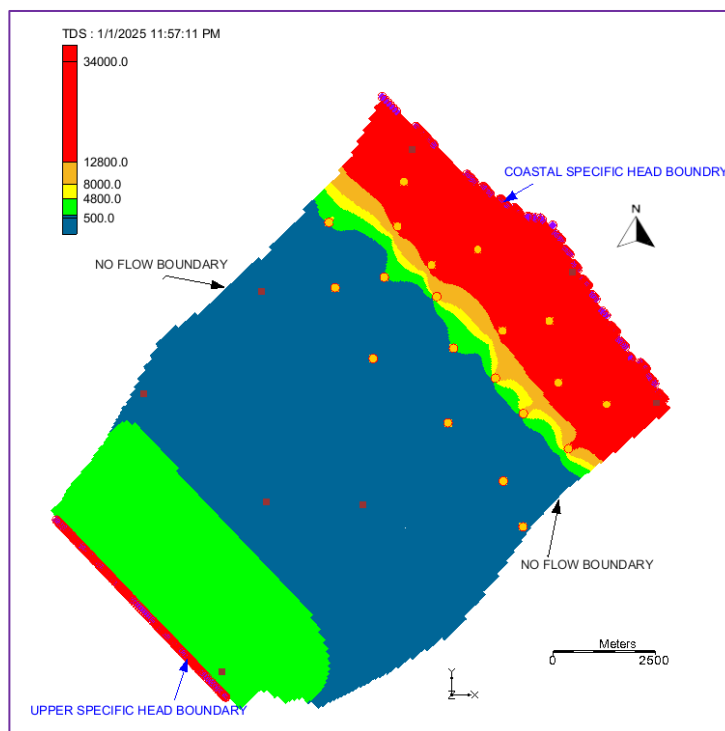


**Figure 4-20: Salinity contour in the Year 2025 during pumping increment @ 30%**

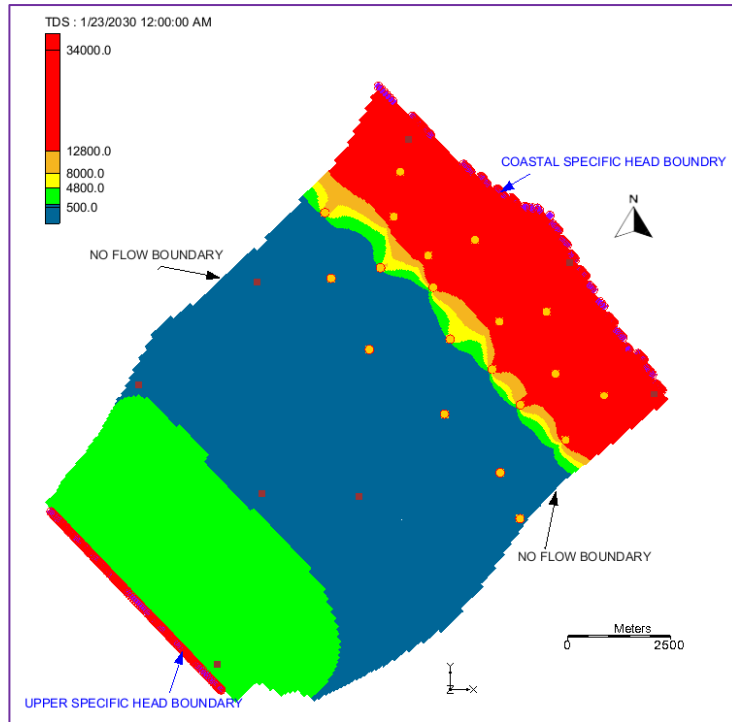


**Figure 4-21: Salinity contour in the Year 2030 during pumping increment @ 30%**

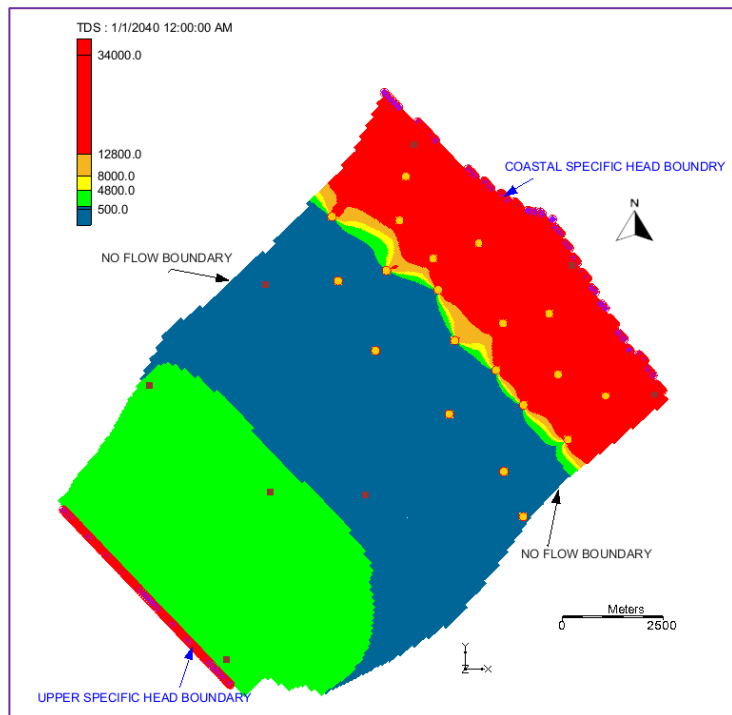


**Figure 4-22: Salinity contour in the Year 2040 during pumping increment @ 30%**

#### 4.7.5 Pumping Reduction @ 5%

It is obvious that salinity intrusion will retreat or seize if the pumping rates reduced from the current rates of the year 2017, the same is simulated and shown in the Figures 4-23 to 4-25 in the Wadi Jizi aquifer for the year 2025, 2030 and 2040 when pumping rates were reduced by 5% of the base pumping rates of 2017, for all the 22 wells in the model domain. From the salinity contour simulated by the model it can be clearly seen that the seawater having TDS (>12800 mg/L) intruded landward by an average distance of 1.12 km. The same intensity of salinity intruded inland by an average distance of 2.19 km and 2.41 km computed for the year 2030 and 2040 respectively. Salinity (>12800 mg/L) in the year 2040 intrudes around 1km inland when compared with the year 2016.

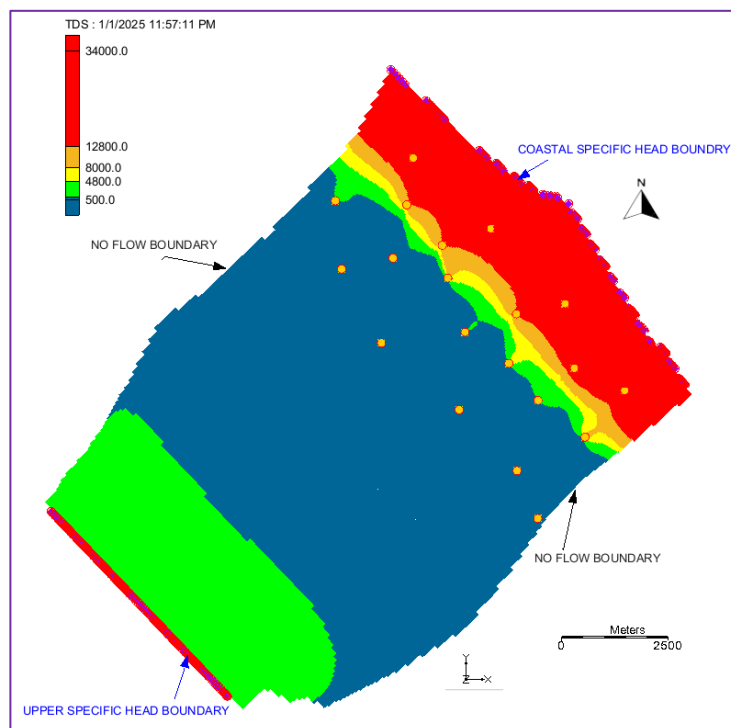


**Figure 4-23: Salinity contour in the Year 2025 during pumping reduction @ 5%**

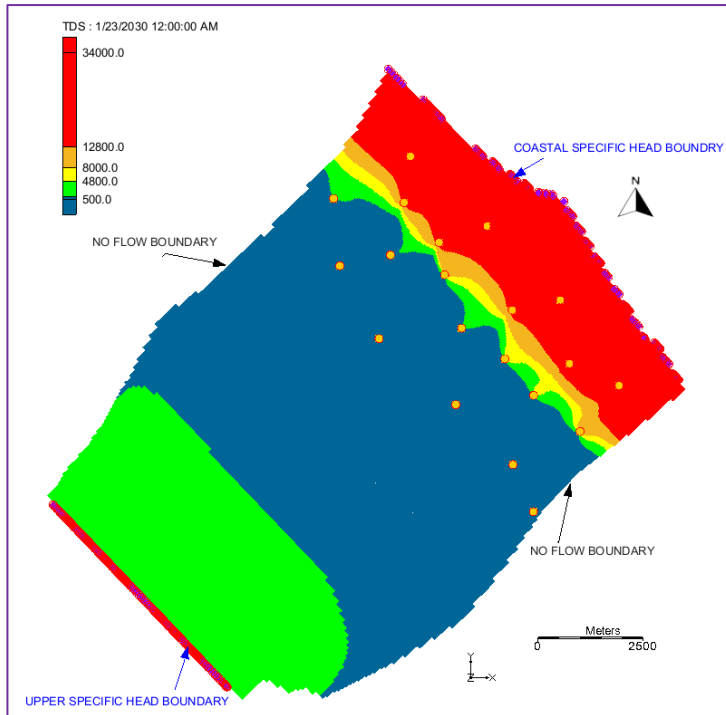


**Figure 4-24: Salinity contour in the Year 2030 during pumping reduction @ 5%**

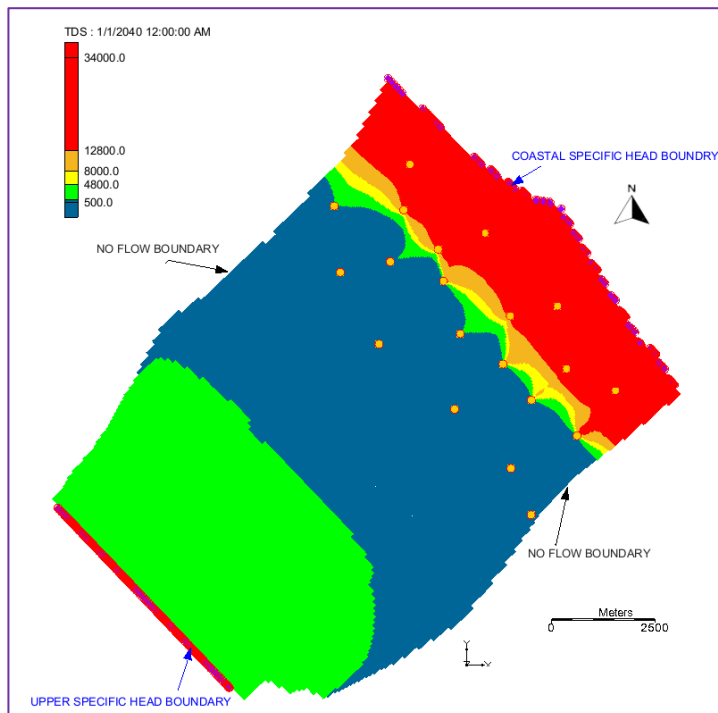


**Figure 4-25: Salinity contour in the Year 2040 during pumping reduction @ 5%**



#### 4.7.6 Pumping Reduction @ 10%

Figures 4-26 to 4-28 shows the predicted salinity intrusion contours in the Jizi aquifer for the year 2025, 2030 and 2040 due to 10% reduction in the base pumping rates. From the salinity contour simulated by the model, it can be clearly seen that the saline intrusion (TDS >12800 mg/L) intruded landward side by an average distance of 1.99 km. The same intensity of salinity intruded inland by an average distance of 2.12 km and 2.15 km computed for the year 2030 and 2040 respectively. It means that salinity (TDS >12800 mg/L) in the year 2040 intrudes 1.03 km inland when compared with the year 2016 if the pumping reduced by 10% of the year 2017 base rates for all the wells.

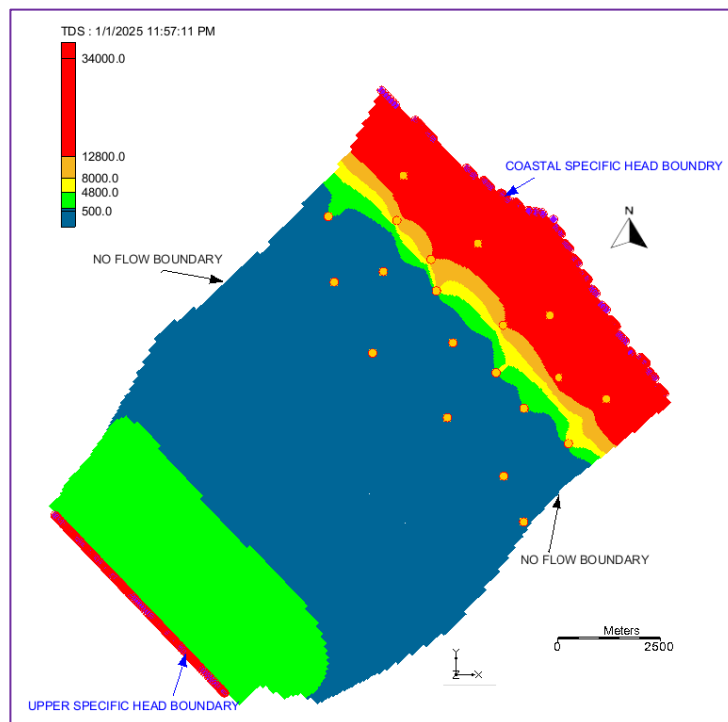


**Figure 4-26: Salinity contour in the Year 2025 during pumping reduction @ 10%**

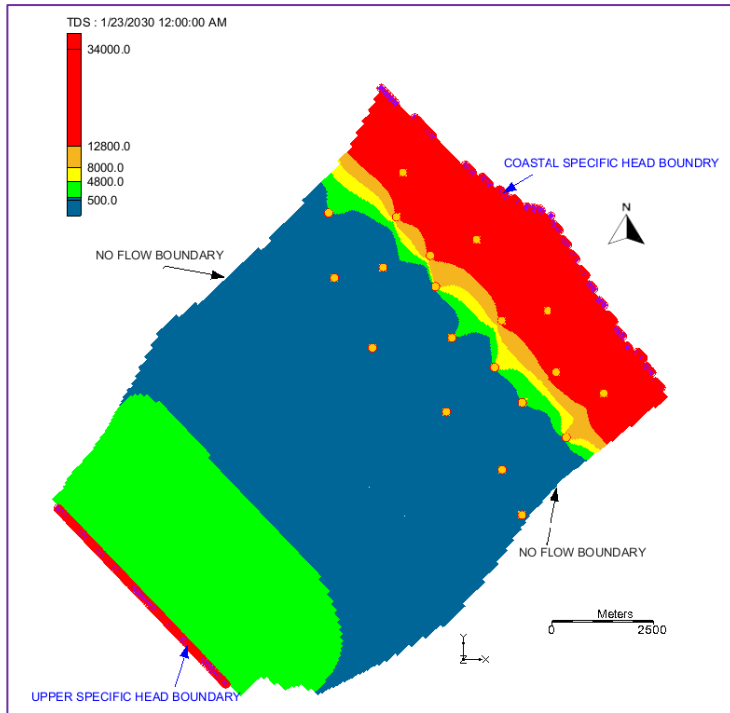


**Figure 4-27: Salinity contour in the Year 2030 during pumping reduction @ 10%**

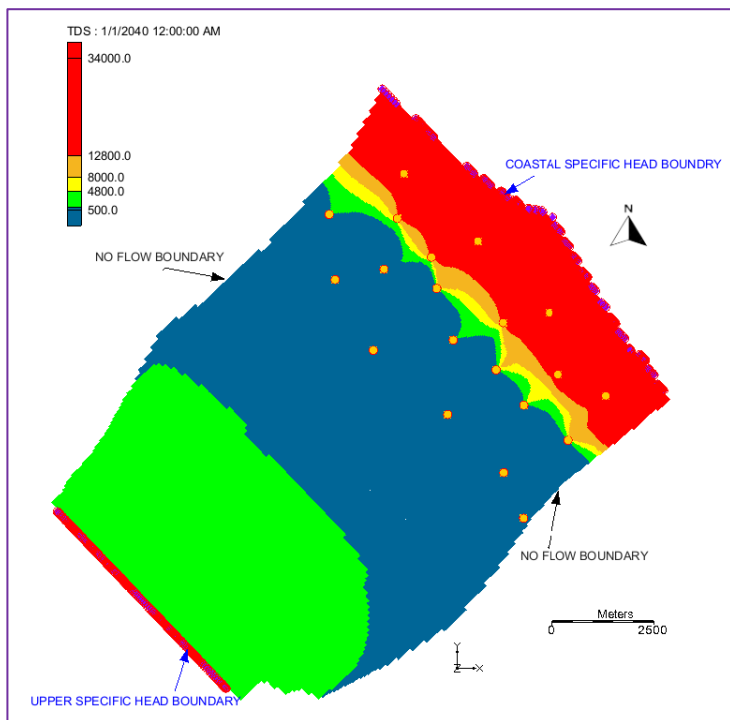


**Figure 4-28: Salinity contour in the Year 2040 during pumping reduction @ 10%**

#### **4.8 The Impact of Climate Change on the Intrusion of Seawater**

Coastal aquifers face an increased risk as a result of rising sea levels due to global climate change. Managing saltwater intrusion in coastal aquifers is considered a highly challenging environmental issue worldwide. Scientists have concentrated on the mechanism, the mathematical model, and the problems of addressing, forecasting, and preventing seawater infiltration (Brkic & Serzic, 2021).

The MT3DMS model was utilized to simulate the intrusion of saltwater into the Wadi Jizi aquifer under different scenarios of Sea Level Rise (SLR) caused by climate change. The prediction of the SLR as per IPCC (Inter Governmental Panel on Climatic Change) and the other possible changes in the sea level (+0.25 m, +0.50 m and – 0.25 m with respect to the base sea level) were considered to simulate the possible sea water intrusion in the study area. The same boundary conditions used for calibrating and validating the model are used in these predictive simulations. The pumping rates those considered in the year 2017 kept constant and continued till 2040.

##### **4.8.1 Sea level rise as per IPCC prediction**

In this scenario, the sea level rise is considered as per Representative concentration pathway (RCP) - 8.5, as mentioned in the annual report no. 5 of IPCC. As per RCP (8.5), a gradual increase of 0.31m (0.26 m – 0.42 m) is applied to the base sea level (0.65 m) considered for the transient model. The predictive scenario considered and applied gradually from 2018 - 2040. The salinity contours for the years 2025, 2030 and 2040 are studied to see the impact of sea level as per IPCC prediction of sea level rise in the region. From the salinity contour simulated by the model (Figures 4-29 to 4-31), it can be clearly seen that the saline intrusion (TDS >12800 mg/L) intruded landward side by an average distance of 2.48 km in the year 2025. The same intensity of salinity intruded inland by an average distance of 2.62 km and 2.70 km computed in the year 2030 and 2040 respectively. It means that salinity (TDS >12800 mg/L) in the year 2040 intrudes 0.68 km inland when compared with the year 2016.

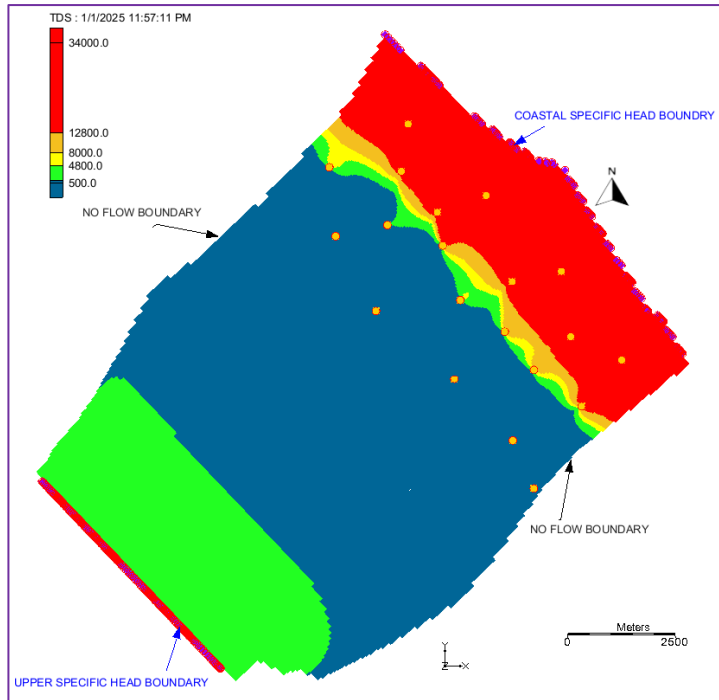


**Figure 4-29: Salinity contour in the Year 2025 during Sea level rise as per IPCC**

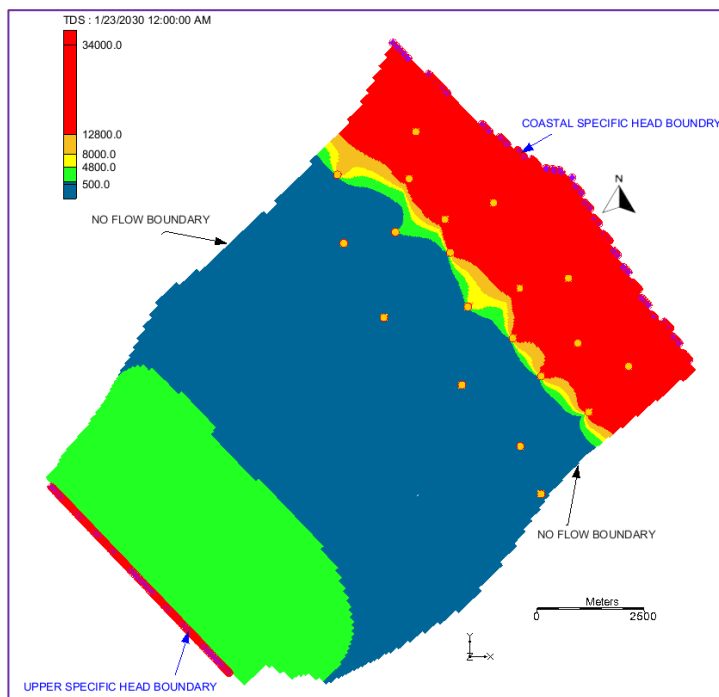


**Figure 4-30: Salinity contour in the Year 2030 during Sea level rise as per IPCC**

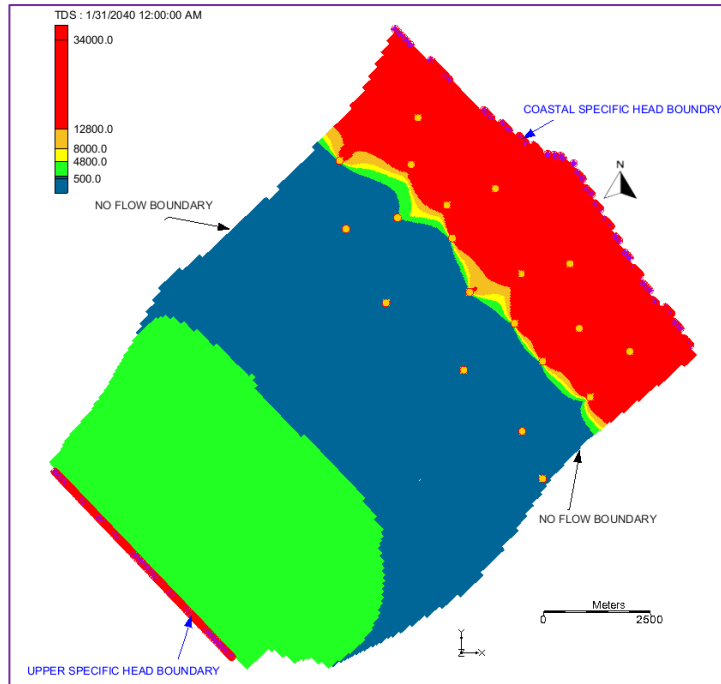


**Figure 4-31: Salinity contour in the Year 2040 during Sea level rise as per IPCC**

#### **4.8.2 Sea level rise @ +0.25m to the base sea level**

In this scenario, a rise of 0.25 m is added to the base sea level (0.65 m) which was considered for the transient model. This predictive scenario is considered and applied from the year 2018 - 2040. The salinity contours for the years 2025, 2030 and 2040 are studied to see the impact of sea level in the Wadi Jizi aquifer. As shown in the Figures 4-32 to 4-34, the saline intrusion (TDS >12800 mg/L) intruded landward side by an average distance of 2.46 km in the year 2025 as computed by the model simulation. Same intensity of salinity intruded inland by an average distance of 2.63 km and 2.71 km computed in the year 2030 and 2040 respectively. That means salinity (TDS >12800 mg/L) in the year 2040 intrudes 0.69 km inland when compared with the year 2016 salinity intrusion value.

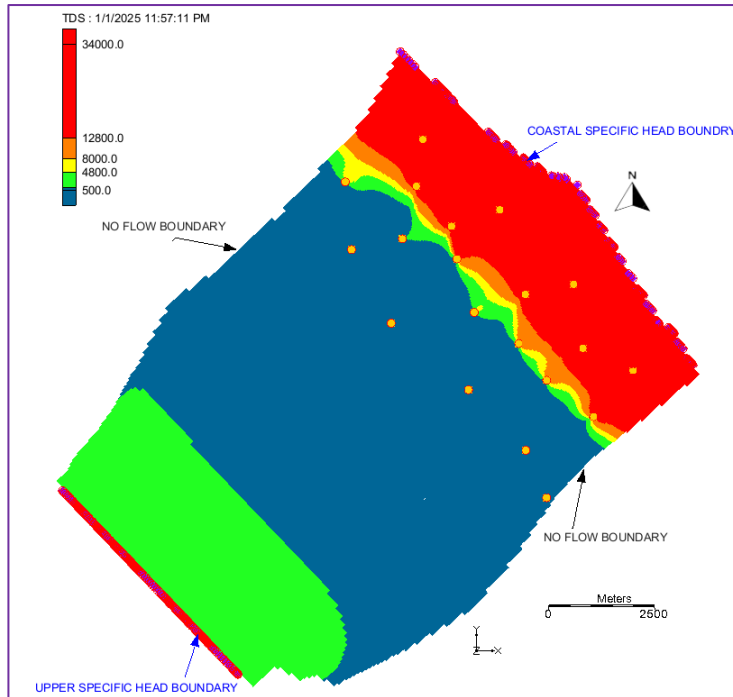


**Figure 4-32: Salinity contour in the Year 2025 during Sea level rise @ +0.25m**

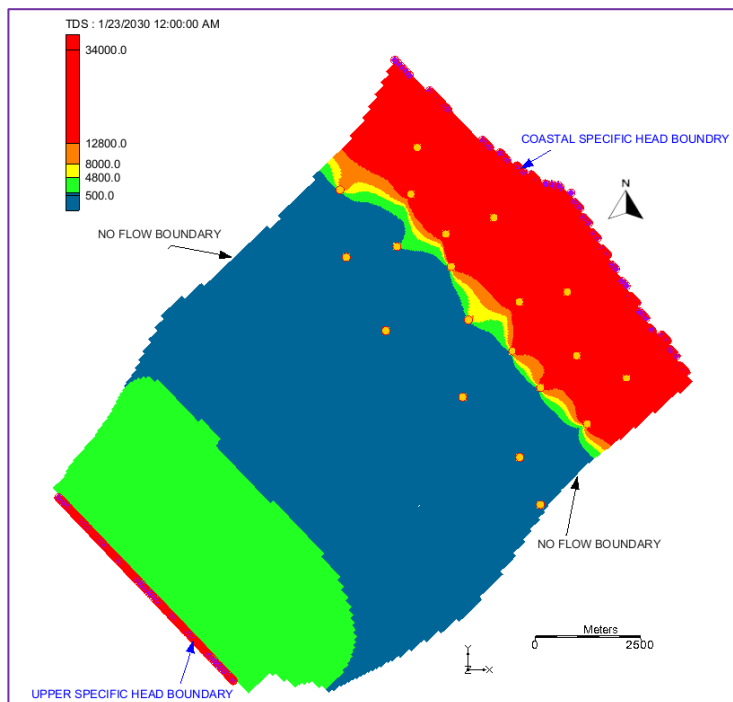


**Figure 4-33: Salinity contour in the Year 2030 during Sea level rise @ +0.25m**

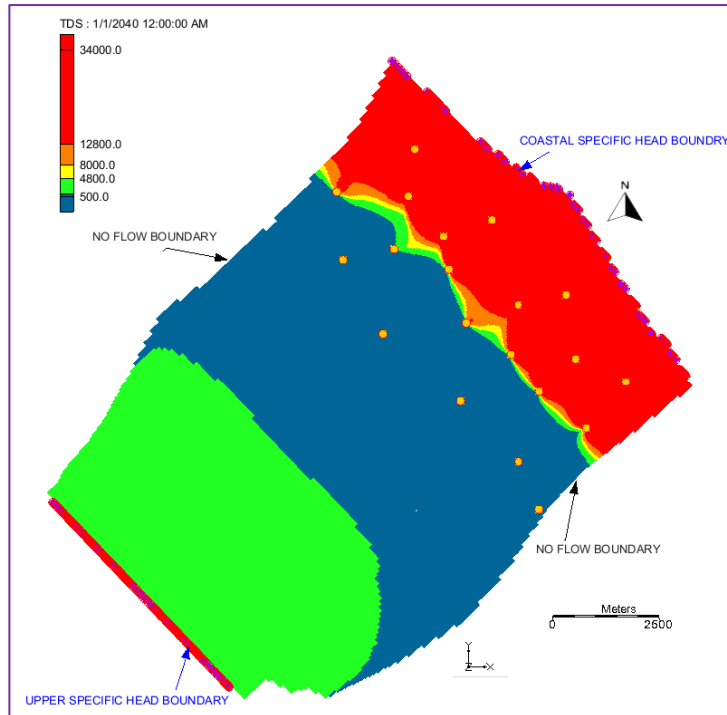


**Figure 4-34: Salinity contour in the Year 2040 during Sea level rise @ +0.25m**

#### **4.8.3 Sea level rise @ +0.50 m to the base sea level**

A rise of 0.50 m is added to the base sea level (0.65 m) which was considered for the transient model for this stage of sea level rise simulation and prediction. This predictive scenario is considered and applied from the year 2018 -2040 as well. The salinity contours for the years 2025, 2030 and 2040 are studied to see the impact of sea level in the Wadi Jizi aquifer. As shown in Figures 4-35 to 4-37, salinity (TDS >12800 mg/L) intruded land by an average distance of 2.48 km in the year 2025 as computed by the model simulation. The same intensity of salinity intruded inland at an average distance of 2.61 km and 2.71 km computed in the years 2030 and 2040 respectively. It has been observed that salinity (TDS >12800 mg/L) in the year 2040 intrudes 0.68 km inland when compared with the salinity intrusion values of the year 2016.

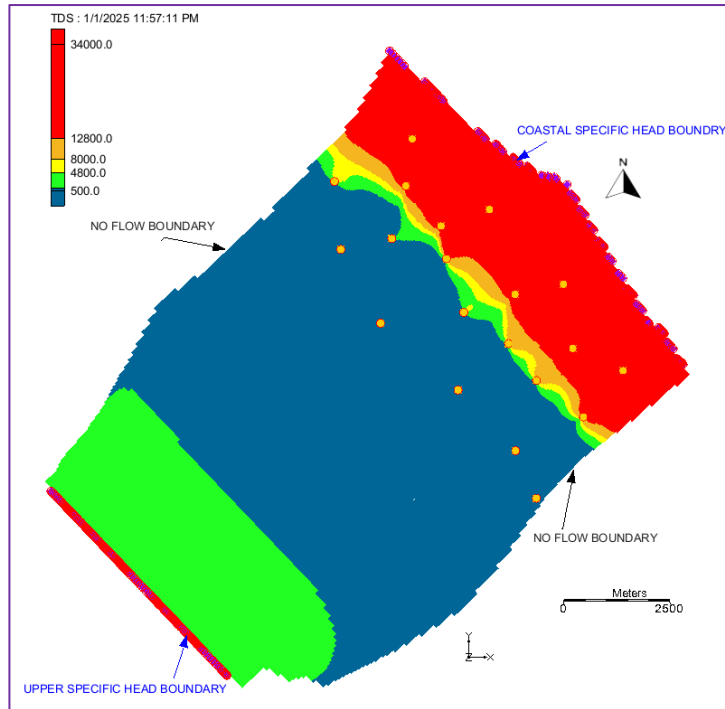


**Figure 4-35: Salinity contour in the Year 2025 during Sea level rise @ +0.50m**

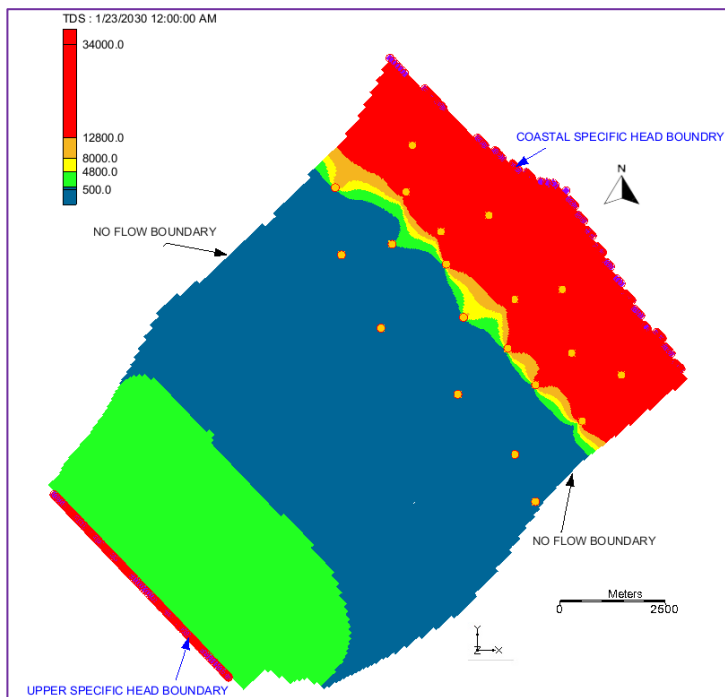


**Figure 4-36: Salinity contour in the Year 2030 during Sea level rise @ +0.50m**



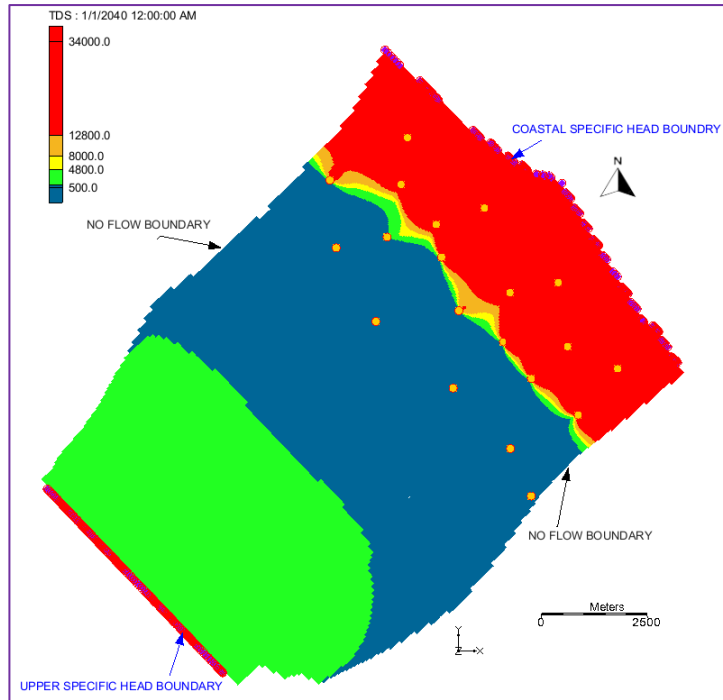


**Figure 4-37: Salinity contour in the Year 2040 during Sea level rise @ +0.50m**

#### **4.8.4 Sea level rise @ -0.25 m to the base sea level**

A reduction of 0.25 m is considered to the base sea level (0.65 m) which was considered for the transient model for this stage of sea level rise simulation and prediction period of 2018 -2040. The computed salinity contours for the years 2025, 2030 and 2040 are studied to see the impact of sea level in the Wadi Jizi aquifer. As shown in the Figures 4-38 to 4-40, salinity intrusion (TDS >12800 mg/L) intruded land by an average distance of 2.56 km in the year 2025 as computed by the model simulation. Same intensity of salinity intruded inland at an average distance of 2.64 km and 2.70 km computed in the year 2030 and 2040 respectively. It has been observed salinity (TDS >12800 mg/L) in the year 2040 intrudes 0.68 km inland when compared with the salinity intrusion values of the year 2016 but the salinity in the year 2025 intrudes more inland in comparison to other conditions of sea level rise.

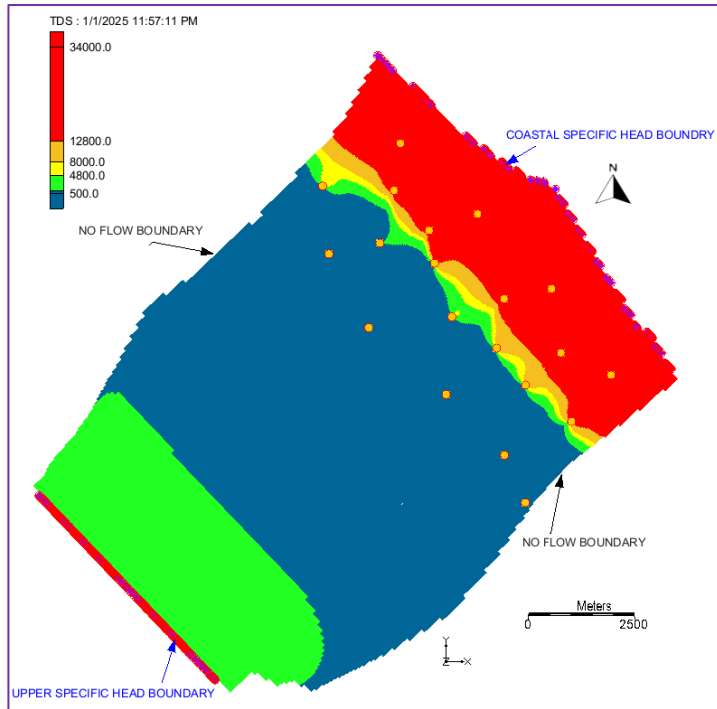


**Figure 4-38: Salinity contour in the Year 2025 during Sea level rise @ - 0.25m**

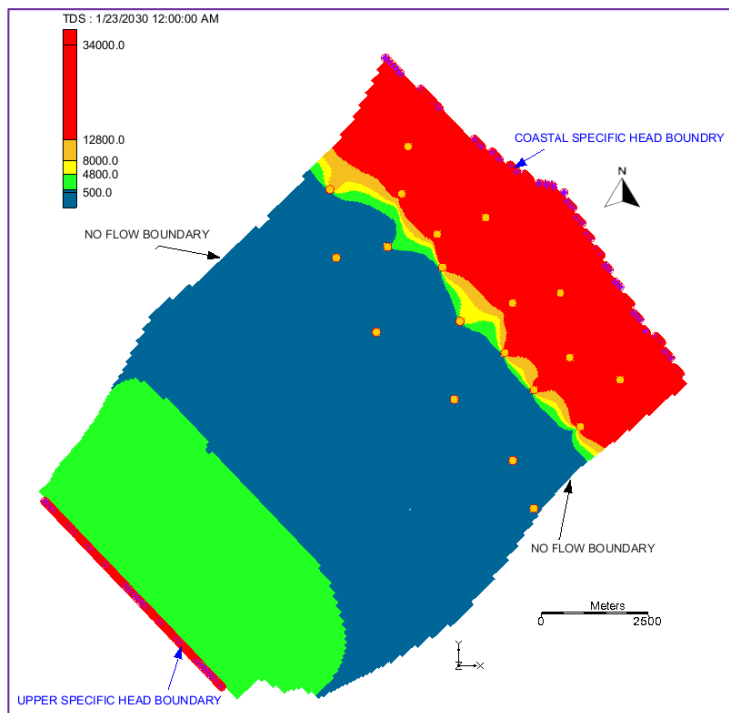


**Figure 4-39: Salinity contour in the Year 2030 during Sea level rise @ - 0.25m**

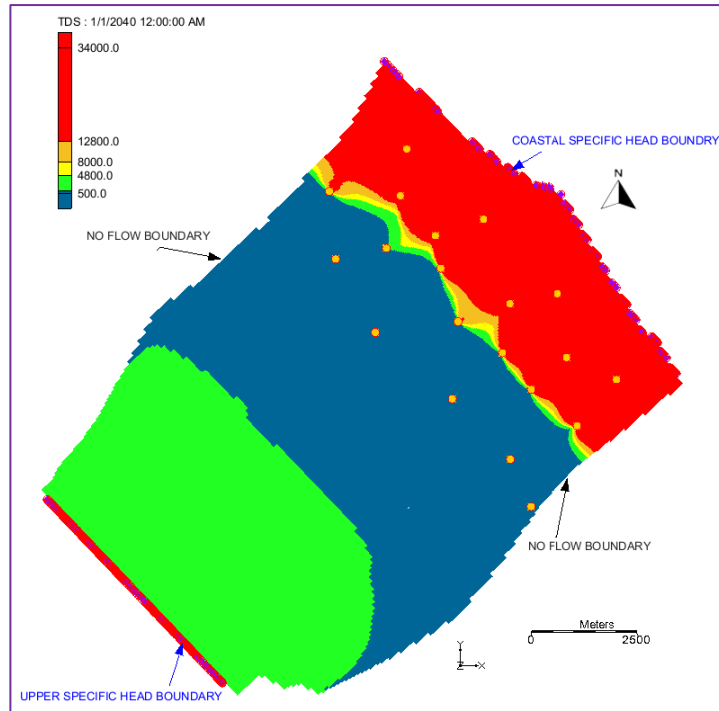


**Figure 4-40: Salinity contour in the Year 2040 during Sea level rise @ - 0.25m**

**Table 4-7 Predictive scenarios and respective salinity intrusion distance**

Scenario Type	Description of the Scenario	Predicted average salinity intrusion inland (km)	
		2030	2040
<b>Pumping increment and reduction</b>	Pumping at baseline pumping rates of 2017	2.39	2.56
	Pumping increment of 10% to the baseline pumping rate of 2017	2.42	2.57
	Pumping increment of 20% to the baseline pumping rate of 2017	2.58	2.65
	Pumping increment of 30% to the baseline pumping rate of 2017	2.69	2.73
	Pumping reduction of 5% to the baseline pumping rate of 2017	2.19	2.41
	Pumping reduction of 10% to the baseline pumping rate of 2017	2.12	2.15
<b>Sea Level Rise due to climatic changes</b>	Sea level rise as per IPCC prediction	2.60	2.63
	Sea level rise @ + 0.25m to the base sea level	2.60	2.65
	Sea level rise @ + 0.50 m to the base sea level	2.61	2.70
	Sea level rise @ - 0.25 m to the base sea level	2.52	2.59

The results of all the predictive scenarios considered under the pumping rates and sea level rise due to climatic changes are summarized in Table 4-8. An increase in the abstraction rates of approximately 20% in the base pumping rate of 2017 will cause almost the same extent of seawater intrusion as that by a sea level rise as per IPCC predictions.

#### **4.9 Management implications of the research**

The inflow and outflow characteristics of the Wadi Al-Jizi aquifer are dynamic groundwater systems that are regularly changing. Large-scale groundwater abstraction in the area which is known for its agricultural and industrial activities with the growing population which requires huge quantities of potable water has disrupted the equilibrium that may have formerly existed between fresh and salt water. Over the past four decades, this aquifer has been overexploited causing seawater to encroach inland as evident by the observations by the authorities and numerical simulations carried out in the present study.

The developed model will be helpful in implementing new policies and develop new recharge facilities in an area suffering from acute shortage of surface water resources and depleting groundwater table. The solute transport model results depicted a clear picture of salinity intrusion at an alarming pace. From the numerical simulations, it can be clearly observed that the salinity intrusion near the vicinity of pumping wells decelerated and halted for a certain duration before it proceeded further inland. The reason is the pumping wells act as a barrier to salinity intrusion due to the cone of depression generated by the pumping. The answers provided by the modeling process may help the decision-makers and local authorities to address a number of queries, including:

- Determining the start date of the seawater intrusion in the aquifer and tracking its progression with respect to time;
- Identifying the salinity-invaded zones and assessing their degree of salinity;
- Quantifying the seawater intrusion volume as well as the other elements of the hydraulic mass balance.

Additional field investigations, continuous monitoring, and improved characterization of the aquifer and soil are needed to gain a better understanding of saltwater contamination mechanisms and the interactions between the soil zone, the aquifer, and the sea. This information is necessary to make progress in effectively managing and mitigating saltwater intrusion in the investigated aquifer. Due to the persistent negative mass balance in the aquifer, seawater intrusion results in a slow recovery of groundwater quality. Pumping demand and quality standards need to be balanced. When the end goal is to improve the quality of the already-polluted aquifer, it is difficult to maintain this balance. Some actions are required to help continue pumping while enhancing the aquifer's recovery. The measures that can be implemented are categorized into four groups: i) measures to reduce demand and abstraction rate (e.g., pumping minimization, water conservation) (Sherif et al. 2012) ii) measures to increase recharge rate (e.g., artificial recharge with treated wastewater)(Sana et al. 2013), iii) relocation of pumping wells and other engineering solutions (e.g., seawater intrusion barriers, pumping of saline water from the aquifer ( Hussain et al. 2019; Kacimov et al. 2009), and iv) raising public awareness about water scarcity, conservation, and the impacts of reckless water consumption.

## **CHAPTER 5      CONCLUSIONS AND SCOPE FOR FUTURE WORK**

### **5.1 Conclusion**

#### **Groundwater flow**

Groundwater flow models are very important management and prediction tools which may facilitate the policy maker to precisely analyse the current situation and arrange sustainable pumping schedules. These models will also help in implementing new policies and develop new recharge facilities in an area suffering from acute shortage of surface water resources and depleting groundwater table. MODFLOW was used to study the groundwater flow system of Wadi Al-Jizi in Al Batinah region facing a persistent water deficit since early 90s. The model was initially calibrated for hydraulic conductivity and vertical anisotropy using the field observation values and then validated for another set of data before using it for future predictions of pumping rates and sea level rise due to climatic changes. Sensitivity analysis depicted that the model was sensitive to the variation in hydraulic conductivity which is the most important geo-hydrogeological parameter used in the model. The transient groundwater flow simulation confirmed a reduction in the groundwater elevation with a maximum decline of 3.82m for an observation well located in the model domain. The scenarios of increased pumping rates by 10%, 20% and 30% and reduced pumping rates by 5% and 10% were considered in predictive simulation. According to the model, if the current rate of groundwater abstraction persists, the water table in the study area is expected to fall by an average of 2.0 meters over the next 22 years. If the pumping is reduced by 10% of the year 2017 value, the water level may be increased by approximately 0.5m and help in mitigating the seawater intrusion.

#### **Transient Salinity intrusion**

Saline water intrusion occurs along the entire width of the model domain at all depths from the northeast boundary of the coastal zone in Wadi Al-Jizi aquifer.

The maps of salinity showed that the boundary between saltwater and freshwater varies over time due to the impact of seasonal recharge patterns and consequent fluctuations in the groundwater table. The historical data of most wells in the plain aquifer indicates an increase in total dissolved solids (TDS) levels in groundwater, suggesting a potential threat to groundwater quality due to contamination, especially from seawater intrusion. A growing yearly shortfall also demonstrates the aquifer's perilous state in terms of salinity invasion. If the base pumping of 2017 to be continued up to 2040, salinity intrusion (TDS >12800 mg/L) will intrude by an average distance of 0.80km inland. The gap is anticipated to grow in the following years. For the year 2040, the salinity intrusion (TDS >12800 mg/L) will encroach inland at an average distance of 1.41 m, 1.23 m and 1.29 m by increasing the abstraction rate by 10%, 20% and 30% respectively to the base pumping rate. On the contrary, on reducing the pumping rates by 5% and 10%, the saline wedge will retreat back and intrude 1.30 km and 1.0 km, respectively in the year 2040. If excessive pumping is not controlled and high abstraction rates are allowed to continue, the groundwater in the coastal aquifers will be hugely stressed. Sea level rise due to IPCC scenario showed intrusion of saline wedge (TDS >12800 mg/L) at 0.70 km in the year 2040 when compared with the results of year 2016 intrusions of the model simulation. The rise of Sea-level by 0.25 m and 0.50 m also showed somewhat same results as IPCC scenario, but the drop in the sea-level by 0.25m in the year 2040 would result in the salinity intrusion by more than 100m (measured 0.80km) when compared with the salinity intrusion of the year 2016. The growing annual shortfall illustrates the precarious state of the aquifer in relation to seawater intrusion. The discharge of freshwater into the sea is decreasing, leading to the inland encroachment of seawater. It is anticipated that the shortfall will continue to increase in the upcoming years.

The validated and calibrated model is currently being employed to examine different scenarios of pumping and sea-level rise, with the aim of offering recommendations for water resources planning and management based on the simulation outcomes. The groundwater simulation model developed in this study has the potential to assist decision-makers in effectively managing the groundwater resources of the Wadi Al-Jizi coastal aquifer. Improved

groundwater development and aquifer management measures (excessive pumping, monitoring and rationing schemes, use of desalinated water, recharging aquifers with recycled water) would be necessary to safeguard rapidly contaminated fresh groundwater aquifers from saline intrusion.

## **5.2 Future scope for work**

Future works may increase the potential and the reliability of the proposed approaches as follows:

The developed model was used for the prediction of the groundwater elevations and groundwater quality in the study area can also be used for the water resources planning and management. The water quality data (TDS) in the study area was not properly monitored and measured and incompatible with the seriousness of the problem. The collected data was scarce and lacks the details by virtue of the depth of aquifer. The concerned agencies should substantially improve the data segment of the water levels and water quality to improve the future study results. An average value of the salinity was measured in the salinity monitoring wells once in four years which was used for the model study. The collected data did not cover the entire depth of the well to give a vertical profile of salinity along the depth of the monitoring well. Therefore, simulation of the water quality with respect to the well profile was not possible and the depth and extent of salt wedge could not be computed.

Further study could be conducted by considering more numbers of zone for both groundwater and salinity intrusion model. It is also suggested that additional field investigations should be conducted in the Al Batinah coastal plain to validate the model results. For simplification, input parameters such as hydraulic conductivity, specific yield, and storage should be employed based on field situations rather than averaging throughout the entire model region. Although a finer grid than used in the previous studies has been considered in this work, it is advisable to construct much finer grids at the pumping well locations and the rest of the model domain to achieve more precise results. The study can also be supported by the experimental work.



## REFERENCES

1. Abdalla, F. (2016). Ionic ratios as tracers to assess seawater intrusion and to identify salinity sources in Jazan coastal aquifer, Saudi Arabia. *Arabian Journal of Geoscience* 9: 40. DOI 10.1007/s12517-015-2065-3.
2. Abderrahman, W.A., & Rasheeduddin, M. (2001). Management of groundwater resources in a coastal belt aquifer system of Saudi arabia. *Water International*, 26:1, 40-50, DOI: 10.1080/02508060108686885.
3. Abd-Elhamid, H. F., & Javadi, A. A. (2011a). A cost-effective method to control seawater intrusion in coastal aquifers. *Water Resources Management*, 25:2755–2780, ISSN: 09204741; DOI: 10.1007/s11269-011-9837-7.
4. Abd - Elhamid, H. F., Javadi, A., & Qahman, K.A. (2015). Impact of sea level rise and over-pumping on seawater intrusion in Gaza aquifer (Palestine). *Journal of Water and Climate Change*, 2(1), pp.19–28. DOI: 10.2166/wcc.2015.055.
5. Abrams,W. Ghoneim, E., Shew, R., LaMaskin,T., Al-Bloushi,K., Hussein, S., AbuBakr, M, Al-Mulla, E., Al-Aware, M., & El-Baz, F. (2018). Delineation of groundwater potential (GWP) in the northern United Arab Emirates and Oman using geospatial technologies in conjunction with Simple additive weight (SAW), Analytical hierarchy process (AHP), and Probabilistic frequency ratio (PFR) techniques. *Journal of Arid Environments*: 157, pp.77-96.
6. Abulibdeh, A., Al Awadhi, T. Al Bolushi, A., & Abdelghani, M. (2021). Spatiotemporal mapping of groundwater salinity in Al-Batinah, Oman. *Groundwater for Sustainable Management*, Vol. 12. <https://doi.org/10.1016/j.gsd.2021.100551>.
7. Agarwal, R., & Garg, P. K. (2016). Remote Sensing and GIS based groundwater potential & recharge zones mapping using multi-criteria decision-making technique. *Water Resource Management* 30:243–260.DOI 10.1007/s11269-015-1159-8.
8. Al-Barwani, A. (2012). Effective flood management in the Sultanate of Oman. *The Second International Conference on Water Resources (ICWR-2012)*, Langkawi, Malaysia.

9. Al-Barwani, A., & Helmi, T. (2006). Sea water intrusion in coastal aquifer: A case study for the area between As Seeb and As Suwaiq (1984–2005). *International Conference on Economic Incentives and Water Demand Management*. United Nations Education Scientific and Cultural Organization (UNESCO), France.
10. Al-Damkhi, A.M., Al-Fares, R.A., Al-Khalifa, K.A., & Abdul-Wahab, S.A. (2009). Water issues in Kuwait: a future sustainable vision. *International Journal of Environmental Studies*, 66:5, 619-636, DOI: 10.1080/00207230903097552.
11. Al-Hassoun, S.A., & Mohammad, T.A. (2011). Prediction of water table in an alluvial aquifer using MODFLOW. *Pertanika Journal of Science & Technology 19* (1): 45 – 55. ISSN: 0128-7680.
12. Al-Maktoumi, A., Zekri, S., El-Rawy, M., Abdalla, O., Al-Wardy, M. Al-Rawas, G., & Charabi, Y. (2018). Assessment of the impact of climate change on coastal aquifers in Oman. *Arabian Journal of Geosciences 11*: 501. <https://doi.org/10.1007/s12517-018-3858-y>.
13. Al-Muhaylan, M.R., Ghumman, A.R., Al-Salamah, I.S., Ahmad, A., Ghazaw, Y.M., Haider, H., & Shafiquzzaman, M. (2020). Evaluating the impacts of pumping on aquifer depletion in arid regions using MODFLOW, ANFIS and ANN. *Water 2020*, 12, 2297; DOI:10.3390/w12082297.
14. Al-Naeem, A.A. (2014). Effect of excess pumping on groundwater salinity and water level in hail region of Saudi Arabia. *Research Journal of Environmental Toxicology 8* (3): 124-135. ISSN 1819-3420 / DOI: 10.3923/rjet.2014.124.135.
15. Al-Salamah, I.S., Ghazaw, Y.M., & Ghumman, A.R. (2011). Groundwater modeling of Saq aquifer Buraydah Al Qassim for better water management strategies. *Environment Monitoring Assessment*, 173:851–860. DOI 10.1007/s10661-010-1428.
16. Al-Taani, A.A., Batayneh, A., Mogren, S., Nazzal, Y., Ghrefat, H., Zaman, H., & Elawadi, E. (2013). Groundwater quality of coastal aquifer systems in the eastern coast of the Gulf of Aqaba, Saudi Arabia. *Journal of Applied Science and Agriculture*, 8(6): 768-778.

17. Al-Wathaf, Y., & El Mansouri, B. (2012). Hydrodynamic modelling for groundwater assessment in Sana'a Basin, Yemen. *Hydrogeology Journal*. DOI: 10.1007/s10040-012-0879-6.
18. Al-Weshah, R.A., & Yihdego, Y. (2016). Flow modelling of strategically vital freshwater aquifers in Kuwait. *Environmental Earth Science* 75:1315 DOI 10.1007/s12665-016-6132-1.
19. Anil Kumar, K.S, Prijub, C.P., & Narasimha Prasad, N.B. (2015). Study on saline water intrusion into the shallow coastal aquifers of Periyar river basin, Kerala using Hydro chemical and Electrical resistivity methods. *International Conference on Water Resources, Coastal and Ocean Engineering (ICWRCOE 2015) Aquatic Procedia* 4, 32 – 40.
20. Baalousha, H.M. (2016). Development of a groundwater flow model for the highly parameterized Qatar aquifers. *Modeling Earth Systems & Environment*, 2, 67. DOI 10.1007/s40808-016-0124-8.
21. Baalousha, H.M., Fahs, M., Ramasomanana, F., & Younes, A. (2019). Effect of pilot-points location on model calibration: Application to the Northern karst aquifer of Qatar. *Water* 2019, 11, 679; doi:10.3390/w11040679.
22. Baawain, M.S., Sana, A., & Al-Yahyai R. (2012). Sustainable and beneficial options for reusing of “Haya water” treated wastewater: Phase 1 – Exploratory study. Final Report, Haya Water (Oman Wastewater Services Company).
23. Bear, J., Cheng, A., Sorek, S., Ouazar, D., & Herrera, I. (1999). *Seawater intrusion in coastal aquifers: concepts, methods, and practices*. Environmental Science, Springer Netherlands, pp. 127-161. <https://doi.org/10.1007/978-94-017-2969-7>
24. Bekhit H.M. (2015). Sustainable groundwater management in coastal aquifer of Sinai using evolutionary algorithms. *7<sup>th</sup> Groundwater Symposium of the International Association for Hydro-Environment Engineering and Research (IAHR)*, Procedia Environmental Sciences 25, pp.19-27.

25. Bhagwat, T. N., Hegde, V. S., & Shetty, A. (2018). Application of Remote sensing and GIS for identification of potential groundwater recharge sites in Semi-arid regions of Hard-rock terrain, in north Karnataka, south India. *Sustainable Water Resources Management*, DOI 10.1007/s40899-018-0244-6.
26. Bobba, A., Singh, V., Berndtsson, R., & Bengtsson, L. (2000). Numerical simulation of saltwater intrusion into Laccadive Island aquifers due to climate change. *Journal of the Geological Society of India*, Vol. 55, pp. 589-612.
27. Bocanegra, E., Jr. Da Silva, G.C., Custodio, E., Manzano, M., & Montenegro, S. (2010). State of knowledge of coastal aquifer management in south America. *Hydrology Journal* 18, pp. 261-267, DOI: 10.1007/s10040-009-0520-5.
28. Bolster, D.T., Tartakovsky, D.M., & Dentz, M. (2007). Analytical models of contamination transport in coastal aquifers. *Advances in Water Resources*, 30, 1962-1972. DOI: 10.1016/j.advwatres.2007.03.007.
29. Brkic, M., & Serzic, V. (2021). Modelling of seawater intrusion into coastal aquifers in laboratory conditions. Electronic collection of papers of the Faculty of Civil Engineering, e-ZBORNIK 21/2021. <https://doi.org/10.47960/2232-9080.2021.21.11.29>
30. Chitrakar, P., & Sana, A. (2015). Groundwater flow and solute transport simulation in eastern Al Batinah coastal plain, Oman: Case study. *Journal of Hydrologic Engineering*, ASCE.ISSN: 1084-0699/050150020 (11).
31. Choudri, B.S., Baawain, M.S., & Ahmed, M. (2015). Review of water quality and pollution in coastal areas of Oman. *Pollution Research*, 34:2, 229-239. ISSN 0257–8050.
32. Chowdhury, S. J., Rahaman, M., Riad. A., Ali, M. S., & Mazumder, Q. H. (2019). Delineation of groundwater potential zones of Atrai–Sib river basin in north-west Bangladesh using Remote sensing and GIS techniques. *Sustainable Water Resources Management*, 5, 689–702, <https://doi.org/10.1007/s40899-018-0240-x>.

33. Chun, J.A., Lim, C., Kim, D., & Kim, J.S. (2018). Assessing impacts of climate change and sea-level rise on seawater intrusion in a coastal aquifer. *Water* 2018, 10, 357. doi:10.3390/w10040357.
34. Dale, R.H. (1983). *Salinity survey of the Batinah*. Source: Library of the General Directorate of Regional Municipality, Environment and Water Resources in North of Al Batinah (GDRMEWRNB), Ref. 9, Sohar, Oman.
35. Davison, D. W. Jr. (1986). *Change in groundwater quality along the Batinah coast 1983 to 1986*. Council for Conservation of Environment and Water Resources (CCEWR). Source: Library of the General Directorate of Regional Municipality, Environment and Water Resources in North of Al Batinah. Ref.157. Sohar.
36. Dibaj, M., Javadi, A.A., Akrami, M., Yuan K.K., Farmani, R., Tan, Y.C., & Chen, A.S. (2020). Modelling seawater intrusion in the Pingtung coastal aquifer in Taiwan, under the influence of sea-level rise and changing abstraction regime. *Hydrogeology Journal*. <https://doi.org/10.1007/s10040-020-02172-4>.
37. EL Hamidi, M.J., Larabi, A., & Faouzi, M. (2021). Numerical Modeling of Saltwater Intrusion in the Rmel-Oulad Ogbane Coastal Aquifer (Larache, Morocco) in the Climate Change and Sea-Level Rise Context (2040). *Water* 2021, 13, 2167. <https://doi.org/10.3390/w13162167>.
38. FAO (2009). *Groundwater management in Oman*, Draft Synthesis Report. Food and Agriculture Organization of the United Nations. Rome.
39. Ghazaw, Y.M., Gumman, A.R., Al-Salamah, I., & Khan, Q.U.Z. (2014). Investigations of impact of recharge wells on groundwater in Buraydah by numerical modeling. *Arabian Journal for Science and Engineering*, 39, 713–724. DOI 10.1007/s13369-013-0690-2.
40. Ghoraba, S.M., Zyedan, B.A., & Rashwan, I.M.H. (2013). Solute transport modelling of the groundwater for quaternary aquifer quality management in middle delta, Egypt. *Alexandria Engineering Journal* 52, 192-207.
41. Hani, S., Toumi, F., Bougherira, N., Shahrour, I., & Hani, I. (2023). Numerical simulation of seawater intrusion in the lower Seybouse aquifer

- system, Algeria. *Acque Sotterranee - Italian Journal of Groundwater*, 12(2), 09 – 17. <https://doi.org/10.7343/as-2023-635>.
42. Hussain, M.S., Elhamid, H.F. A., Javadi, A.A., & Sherif, M.M. (2019). Management of seawater intrusion in coastal aquifers: A review. *Water* 2019, 11, 2467. doi:10.3390/w11122467.
  43. Hussain, M.S., Javadi, A. A., & Sherif, M. M. (2015). Three-dimensional simulation of seawater intrusion in a regional coastal aquifer in UAE. *Procedia Engineering*, 119, 1153 – 1160. <http://dx.doi.org/10.1016/j.proeng.2015.08.965>.
  44. Hydroconsult (1985). *Preliminary soil and groundwater survey in the Batinah region: Part 1 Groundwater*. Ministry of Agriculture and Fisheries (MAF), Oman. Source: Library of the Ministry of Regional Municipality, Environment and Water Resources (MRMEWR). Ref.3549. Ruwi, Muscat.
  45. Izady A, Abdalla O, Joodavi A., & Chen M. (2017a). Groundwater modeling and sustainability of a transboundary hardrock–alluvium aquifer in north Oman mountain. *Water*, 9(3), 161. <https://doi.org/10.3390/w903016>.
  46. Japan International Cooperation Agency (JICA) (1986). *Hydrologic observation project in the Batinah coast*. Volume-1. Source: Library of the General Directorate of Regional Municipality, Environment and Water Resources in North of Al Batinah.
  47. Kacimov, A.R., Sherif, M.M., Perret, J.S., & Al-Mushikhi, A. (2009). Control of sea water intrusion by saltwater pumping: Coast of Oman. *Hydrogeology Journal*, 17, 541-558. DOI: 10.1007/s10040-008-0425-8.
  48. Khublaryan, M.G., Frolov, A.P., & Yushmanov, I.O. (2008). Seawater intrusion into coastal aquifer. *Water Resources*, 35, 274-286. ISSN 0097-8078
  49. Khorri, J. (2003). Sustainable development and management of water resources in the Arab region. *Developments in Water Science*, 50, 199-220.
  50. Kresic, N. (1997). *Quantitative solutions in hydrogeology and groundwater modelling*. Lewis Publishers, CRC Press Company, USA. ISBN: 1-55670-219-4.

51. Kwarteng, A. Y., Dorvlo, A. S., & Kumar, G. T. V. (2009). Analysis of a 27-year rainfall data (1977–2003) in the sultanate of Oman. *International Journal of Climatology*, 29, 605–617.
52. Lachaal, F., & Gana, S. (2016). Groundwater flow modeling for impact assessment of port dredging works on coastal hydrogeology in the area of Al-Wakrah (Qatar). *Modeling Earth Systems & Environment*, 2, 1–15. <https://doi.org/10.1007/s40808-016-0252-1>
53. Lakey, R., Easton, P., & Hinai, A. H. (1995). Eastern Batinah water resources assessment. *The International Conference on Water Resources Management in Arid Countries Proceedings*. Muscat. Sultanate of Oman. The library of the General Directorate of Regional Municipality, Environment and Water Resources in North of Al Batinah, Sohar, Oman.
54. Lathashri, U.A., & Mahesha, A. (2015). Simulation of saltwater intrusion in a coastal aquifer in Karnataka, India. *The International Conference on Water resources, Coastal and Ocean engineering (ICWRCOE 2015) Aquatic Procedia* 4, pp 700 - 705, DOI: 10.1016/J.aqpro.2015.02.090.
55. Magesh, N. S., Chandrasekar, N., & Soundranayagam, J. P. (2012). Delineation of groundwater potential zones in Theni district, Tamil Nadu, using Remote sensing, GIS and MIF techniques. *Geoscience Frontiers*, 3, 189-196.
56. Mazzonia, A., Heggy, E., & Scabbia, G. (2018). Forecasting water budget deficits and groundwater depletion in the main fossil aquifer systems in north Africa and the Arabian Peninsula. *Global Environmental Changes*, 53, 157 -173. <https://doi.org/10.1016/j.gloenvcha.2018.09.009>.
57. McDonald, M. G., & Harbaugh, A. W. (1988). *A modular three-dimensional finite difference groundwater flow model technique of water resources investigations of United States geological survey*. Vol. 6, U.S. Geological Survey, Denver, 586.
58. McDonald, M. G., Harbaugh, A. W., Banta, E. R., & Hill, M. C. (2000). *MODFLOW-2000, U.S. geological survey modular ground-water model—User guide to modularization concept and the groundwater flow process*. U.S. Geological Survey Open-File Rep. 00-92, Reston, VA, 121.

59. Ministry of Agriculture and Fisheries (MAF) and International Center for Biosaline Agriculture (ICBA) (2012). *Oman salinity strategy - Assessment of salinity problem: Annex-1*. Muscat, Sultanate of Oman.
60. Ministry of Regional Municipality & Water Resources (MRMWR) (2008). *Water resources in Oman*. Report issued on the Occasion of the Expo Zaragoza – 2008, Sultanate of Oman.
61. Ministry of Water Resources (MWR) (1996). *Seawater intrusion beneath the Batinah coast. The Batinah coast salinity intrusion periodical monitoring results 1983 – 1995*. Source: Library of the General directorate of regional municipality, environment and water resources in north of Al Batinah, Sohar.
62. Ministry of Water Resources (MWR) (2000). *Al Batinah salinity report 97–99*. Source: Library of the General directorate of regional municipality, environment and water resources in north of Al Batinah, Sohar.
63. Mogren, S. (2015). Saltwater intrusion in Jizan coastal zone, southwest Saudi Arabia, inferred from Geoelectric resistivity survey. *International Journal of Geosciences*, 6, 286-297. <http://dx.doi.org/10.4236/ijg.2015.63022>.
64. Mondal, N.C., Singh, V.P., Singh, S., & Singh, V.S. (2011). Hydro chemical characteristic of coastal aquifer from Tuticorin, Tamil Nadu, India. *Environmental Monitoring Assessment*, 175, 531 -550. DOI: 10.1007/s10661-010-1549-6.
65. Nag, S. K., & Kundu, A. (2018). Application of Remote sensing, GIS and MCA techniques for delineating groundwater prospect zones in Kashipur block, Purulia district, West Bengal. *Applied Water Science*, 8, 38. <https://doi.org/10.1007/s13201-018-0679-9>
66. Nofal, E.R., Amer, M.A., El- Didy, S.M., & Fekry, A.M. (2015). Delineation and modelling of seawater intrusion into Nile delta aquifer: A new perspective. *Water Science*, 29, 156–166. DOI: 10.1016/j.wsj.2015.11.003.
67. Oman Observer (2017, Nov. 11). Al Batinah key to achieving food security. Oman Observer.



<https://www.omanobserver.om/article/69050/Local/al-batinah-key-to-achieving-food-security> (Assessed on Aug. 2022).

68. Perera, E.D.P., Jinno, K., Tautsumi, A., & Hiroshiro, Y. (2010). A numerical study of saline contamination of a coastal aquifer. *Proceedings of the Institution of Civil Engineers Water Management*, 163, 367-375. DOI: 10.1680/wama.2010.163.7.367
69. Pramada, S.K., & Mohan, S. (2015). Stochastic simulation of seawater intrusion into freshwater aquifers. *International Conference on Water resources, Coastal and Ocean Engineering*, Aquatic Procedia 4, 87 – 94.
70. Praveena, S.M., & Aris, A. Z. (2010). Groundwater resources assessment using numerical model: A case study in low-lying coastal area. *International Journal of Environmental Science & Technology*, 7, 135-146. ISSN: 1735-1472
71. Prusty, P., & Farooq, S.H. (2020). Seawater intrusion in the coastal aquifers of India - A review. *Hydro-Research*, 3, 61-74. <https://doi.org/10.1016/j.hydres.2020.06.001>.
72. Ranjan, P., Kazama, S., Sawamoto, M., & Sana, A. (2008). Global scale evaluation of coastal fresh groundwater resources. *Ocean and Coastal Management*, 52, 197 – 206. <http://dx.doi.org/10.1016/j.ocecoaman.2008.09.006>.
73. Razack, M., Jalludin, M. & Gaba, A.H. (2019). Simulation of climate change impact on a coastal aquifer under arid climate. The Tadjourah aquifer (Republic of Djibouti, Horn of Africa). *Water*, 19, 11, pp.2347. 10.3390/w11112347. hal-03279084.
74. Sana, A., & Baawain, M. (2012). Verification of a turbulence model for rough oscillatory boundary layers. *Proceedings of 10<sup>th</sup> International Congress on Advances in Civil Engineering (ACE 2012)*, Ankara, Turkey.
75. Sana, A., & Baawain, M. (2011). Assessment of seawater quality along northern coast of Oman. *Proceedings of 6<sup>th</sup> International Conference on Asian and Pacific and Coasts (APAC 2011)*, Hong Kong, 2002-2009.
76. Sana, A. Baawain, M., & Al Sabti, A. (2013). Feasibility study of using treated wastewater to mitigate seawater intrusion along northern coast of

- Oman. *International Journal of Water Resources and Arid Environments*, 3, 56-63. ISSN 2079-7079.
77. Sana, A., & Al Shibli, S.H. (2003). Modelling of seawater intrusion into a coastal aquifer in the sultanate of Oman. *Proceedings of 30<sup>th</sup> Congress of International Association for Hydro-Environment Research (IAHR 2003)*, Thessaloniki, Greece, 581-588.
  78. Sana, A., & Baawain, M. (2014). Groundwater modelling of coastal plain aquifer in southern Oman. *Proceedings of 19<sup>th</sup> IAHR – APD Congress 2014*, Hanoi, Vietnam.
  79. Sharan, A. Datta, B., & Lal, A. (2023). Integrating numerical modelling and scenario-based sensitivity analysis for saltwater intrusion management: case study of a complex heterogeneous island aquifer system. *Environ Monit Assess*, 195:553. <https://doi.org/10.1007/s10661-023-11159-z>.
  80. Senanayake, I. P., Dissanayake, D.M.D.O.K, Mayadunna B. B., & Weerasekera, W. L. (2016). An approach to delineate groundwater recharge potential sites in Ambalantota, Sri Lanka using GIS techniques. *Geoscience Frontiers*, 7, 115-124. <http://dx.doi.org/10.1016/j.gsf.2015.03.002>
  81. Shammass, M. I., & Jacks, G. (2007). Seawater intrusion in the Salalah plain aquifer, Oman. *Environmental Geological Journal*, 15, 24. DOI:10.1007/s00254-007-0673-2.
  82. Shamrukh, M., Al-Muraikhi, A.A., & Al-Hamar, Y.I. (2012). Exploring of deep groundwater in the southwest aquifer of Qatar. *The 10<sup>th</sup> Gulf Water Conference*. DOI: 10.13140/2.1.3191.5521.
  83. Sherif, M. M., Kacimov, A., Javadi, A. A., and Ebraheem, A. (2012). Modelling groundwater flow and seawater intrusion in the coastal aquifer of wadi Ham, UAE. *Water Resources Management: An International Journal, Published for the European Water Resources Association (EWRA)*, 36, 751-774. DOI: 10.1007/s11269-011-9943-6.
  84. Shibli, S. H. (2002). Modelling of saltwater intrusion in wadi Al Jizi aquifer. Master's Thesis, SQU, Sultanate of Oman.

85. Sindhu, G., Ashita, M., Jairaj, P.G., & Raghunath, R. (2012). Modelling of coastal aquifer of Trivandrum. *Procedia Engineering*, 38, 3434 – 3448  
DOI: 10.1016/j.proeng.2012.06.397.
86. Singhal, B.B.S., & Gupta R.P. (2010). *Applied hydrogeology of fractured rocks*. Springer Science. DOI: 10.1007/978-90-481-8799-7\_12.
87. Sowe, M.A., Sadhasivam, S., Mohamed, M.M., & Mohsen, S. (2019). Modeling the mitigation of seawater intrusion by pumping of brackish water from the coastal aquifer of wadi Ham, UAE. *Sustainable Water Resources Management*, 5, 1435–1451. <https://doi.org/10.1007/s40899-018-0271-3>.
88. Stocker, T.F., Qin, D., Plattner, G.-K., Tignor, M., Allen, S.K., Boschung, J., Nauels, A., Xia, Y., Bex, V., & Midgley, P.M., (2013). *Summary for Policymakers in Climate Change 2013: The Physical Science Basis*. Contribution of working group I to the fifth assessment report of the Intergovernmental Panel on Climate Change (IPCC), Cambridge University Press: Cambridge, UK; New York, USA.
89. Stoeckl, L., Walther, M., & Morgan, L.K. (2019). Physical and numerical modelling of post-pumping seawater intrusion. *Hindawi Geofluids*, 2019, Article ID 7191370. <https://doi.org/10.1155/2019/7191370>.
90. Supreme Council for Planning (2019). First voluntary national review of the sultanate of Oman 2019 Draft Copy, *United Nations High-Level Political Forum on Sustainable Development*, Sultanate of Oman.
91. Tabinas, Z.M. (2014, 25 Nov.) Over-extraction of Cebu’s groundwater and its consequences, Retrieved 25<sup>th</sup> Dec. 2020 from <https://sweetscienceyspirit.wordpress.com/2014/11/25/over-extraction-of-groundwater-and-its-consequences>.
92. UN-ESCWA and BGR (United Nations Economic and Social Commission for Western Asia; Bundesanstalt für Geowissenschaften und Rohstoffe) (2013). *Inventory of Shared Water Resources in Western Asia*, Beirut.
93. Waikar, M. L., & Nilawar, A. P. (2014). Identification of groundwater potential zone using Remote sensing and GIS technique. *International Journal of Innovative Research in Science, Engineering and Technology*, 3, 12163-12174.ISSN: 2319-8753.

94. World Health Organization (WHO) (1997). *Comprehensive assessment of the freshwater resources of the world*. WHO, Geneva, pp.34.
95. Weyhenmeyer, C. E., Stephen, J. B., & Niklaus, W. H. (2002). Isotope study of moisture sources, recharge areas, and groundwater flow paths within the Eastern Batinah coastal plain, Sultanate of Oman. *Water Resources Research*, 38, 1184. DOI: 10.1029/2000WR000149.
96. Yeh, H. F., Cheng, Y. S., Lin, H. I., & Lee, C. H. (2016). Mapping groundwater recharge potential zone using a GIS approach in Hualian river, Taiwan. *Sustainable Environment Research*, 26, 33-43. <http://dx.doi.org/10.1016/j.serj.2015.09.005>
97. Young, M. E., Bruign, R.G.M., & Al Ismaily, A. S. (1998). Exploration of an alluvial aquifer in Oman by time-domain electromagnetic sounding. *Hydrogeology Journal*, 6, 383–393. <http://dx.doi.org/10.1007/s100400050161>
98. Zheng, C., & Wang, P. P. (1999). MT3DMS:Transport model for simulation of advection, dispersion, and chemical reactions of contaminants in groundwater systems; *Documentation and User's Guide*. Vicksburg, Mississippi: United State Army Corps of Engineers.

## APPENDIX -A

**Table A-5-1 Al Khan station monthly rainfall data and recharge rates**

Time (month/year)	Rainfall (mm)	Avg. Wet/Dry	Recharge rate (m/d)	Interval	Remarks
1/1999	2.6	dry	0.0001516	1-31/1/1999	
2/1999	18.4	dry	0.0011881	1-28/2/1999	
3/1999	44	dry	0.0025662	1-31/3/1999	
9/1999	21.8	dry	0.0013138	1-30/9/1999	1/4 - 31/8/1999 = 0
11/1999	0.6	dry	3.616E-05	1 - 30/11/1999	1/10 - 31/10/1999 =0
7/2000	5	dry	0.0002916	1-31/7/2000	1/12/99 -30/6/2000 =0
9/2000	2.6	dry	0.0001567	1-30/9/2000	1/8 -31/8/2000 =0
10/2000	11.4	dry	0.0006649	1-31/10/2000	
12/2000	4.2	dry	0.000245	1-31/12/2000	1/11-30/11/2000 =0
1/2001	0.6	dry	3.499E-05	1-31/1/2001	
9/2001	4.2	dry	0.0002531	1-9/9/2001	1/2 - 31/8/2001=0
11/2001	1.2	dry	7.232E-05	1- 30/11/2001	1/10 - 31/10/2001=0
3/2002	21	dry	0.0012248	1 -31/3/2002	1/12/2001- 8/2/2002=0
4/2002	7	dry	0.0004219	1-30/4/2002	
5/2002	10.2	dry	0.0005949	1-31/5/2002	
7/2002	12.4	dry	0.0007232	1-31/7/2003	1/6 -30/6/2002=0
9/2002	2.8	dry	0.0001687	1-30/9/2002	1/8 -31/8/2002=0
11/2002	3.4	dry	0.0002049	1-30/11/2002	1/10 -31/10/2002=0
1/2003	2.4	dry	0.00014	1-31/1/2003	1/12 -31/12/2002=0
3/2003	0.2	dry	1.166E-05	1- 31/3/2003	
4/2003	15	dry	0.000904	1-30/4/2003	
7/2003	2.8	dry	0.0001633	1-31/7/2003	1/5 - 30/6/2003=0
8/2003	3.8	dry	0.0002216	1-31/8/2003	
10/2003	3.2	dry	0.0001866	1- 31/10/2003	1/9 -30/9/2003=0
11/2003	0.4	dry	2.411E-05	1-30/11/2003	
1/2004	0.8	dry	4.666E-05	1-31/1/2004	1/12 -31/12/2004=0
4/2004	0.4	dry	2.411E-05	1-30/4/2004	1/2 -31/3/2004=0
7/2004	6.4	dry	0.0003733	1-31/7/2004	1/5 -30/6/2004=0
10/2004	12	dry	0.0006999	1-31/10/2004	1/8 -30/9/2004=0
12/2004	10.5	dry	0.0006124	1-31/12/2004	1/11-30/11/2004=0
1/2005	5.8	dry	0.0003383	1-31/1/2005	
2/2005	12	dry	0.0007749	1-28/2/2005	
3/2005	6	dry	0.0003499	1-31/3/2005	
5/2005	1.2	dry	6.999E-05	1-31/5/2005	1/4-30/4/2005=0
6/2005	2.6	dry	0.0001567	1-30/6/2005	
7/2005	0.4	dry	2.333E-05	1-31/7/2005	

12/2005	2.6	dry	0.0001516	1-31/12/2005	1/8-30/11/2005=0
2/2006	28.4	wet	0.0018338	1-28/2/2006	1/1-31/1/2006=0
3/2006	1.6	wet	9.332E-05	1-31/3/2006	1/2-28/2/2006=0
6/2006	4	wet	0.0002411	1-30/6/2006	
8/2006	1.4	wet	8.165E-05	1-31/8/2006	1/7-31/7/2006=0
9/2006	30.6	wet	0.0018442	1-30/9/2006	
10/2006	32.2	wet	0.001878	1-31/10/2006	
12/2006	30	wet	0.0017497	1-31/12/2006	1-30/11/2006=0
1/2007	0.2	wet	1.166E-05	1-31/1/2007	
2/2007	5.8	wet	0.0003745	1-28/2/2007	
3/2007	99	wet	0.0057739	1-31/3/2007	
5/2007	2.6	wet	0.0001516	1-31/5/2007	1/4-30/4/2007=0
8/2007	27.2	wet	0.0015864	1-31/8/2007	1/7-31/7/2007=0
9/2007	4.8	wet	0.0002893	1-30/9/2007	
10/2007	2.8	wet	0.0001633	1-31/10/2007	
1/2008	30.4	dry	0.001773	1-31/1/2008	
2/2008	0.8	dry	5.166E-05	1-28/2/2008	
6/2008	0.6	dry	3.616E-05	1-31/7/2008	1/4-31/5/2008=0
7/2008	1.2	dry	6.999E-05	1-30/6/2008	
10/2008	0.6	dry	3.499E-05	1-31/10/2008	1/8-30/9/2008=0
3/2009	31	dry	0.001808	1-31/3/2009	1/11/2008- 8/2/2009=0
4/2009	13	dry	0.0007835	1-30/4/2009	
10/2009	0.8	dry	4.666E-05	1-31/10/2009	1/5-30/9/2009 =0
11/2009	0.2	dry	1.205E-05	1-30/11/2009	
3/2010	18	dry	0.0010498	1-31/3/2010	1/12/2009- /2/2010=0
4/2010	5.2	dry	0.0003134	1-30/4/2010	
6/2010	2.4	dry	0.0001446	1-30/6/2010	1-31/5/2010 =0
8/2010	0.2	dry	1.166E-05	1-31/8/2010	1-31/7/2010 =1
12/2010	0.6	dry	3.499E-05	1-31/10/2010	1/9-30/11/2010=0
1/2011	21.2	dry	0.0012364	1-28/2/2011	
2/2011	0.2	dry	1.291E-05	1-31/1/2011	
10/2011	3	dry	0.000175	1-31/10/2011	1/3-30/11/2010=0
11/2011	1	dry	6.027E-05	1-30/11/2011	
1/2012	1.4	dry	8.165E-05	1-30/1/2012	1/12 -31/12/2012=0
5/2012	20	dry	0.0012053	1-31/5/2012	1/2 -30/4/2012=0
7/2012	8	dry	0.0004666	1-31/7/2012	1-30/6/2012=0
8/2012	2	dry	0.0001166	1-31/8/2012	
9/2012	2.4	dry	0.0001446	1-30/9/2012	
10/2012	0.6	dry	3.499E-05	1-31/10/2012	
11/2012	1.8	dry	0.0001085	1-30/11/2012	
12/2012	4.2	dry	0.000245	1-31/12/2012	
1/2013	0.2	wet	1.166E-05	1-31/1/2013	
2/2013	5.8	wet	0.0003745	1-28/2/2013	
3/2013	13.8	wet	0.0008049	1-31/3/2013	
4/2013	73.4	wet	0.0044236	1-30/4/2013	
5/2013	1.6	wet	9.332E-05	1-31/5/2013	
11/2013	52.6	wet	0.00317	1-30/11/2013	1/6-31/10/2013=0

12/2013	4.6	wet	0.0002683	1-31/12/2013	
1/2014	0.6	wet	3.499E-05	1-31/1/2014	
2/2014	6.2	wet	0.0004003	1-28/2/2014	
3/2014	48.8	wet	0.0028461	1-31/3/2014	
4/2014	13.4	wet	0.0008076	1-30/4/2014	
7/2014	14.6	wet	0.0008515	1-31/7/2014	1/5-30/6/2014=0
8/2014	4.2	wet	0.000245	1-31/8/2014	
10/2014	0.2	wet	1.166E-05	1-31/10/2014	1-30/9/2014=0
11/2014	5.6	wet	0.0003375	1-30/11/2014	
12/2014	18.8	wet	0.0010965	1-31/12/2014	
1/2015	4	wet	0.0002333	1-31/1/2015	
7/2015	4.8	wet	0.0002799	1-31/7/2015	1/2- 30/6/2015=0
8/2015	28.2	wet	0.0016447	1-31/8/2015	
9/2015	52.2	wet	0.0031459	1-30/9/2015	
10/2015	38.8	wet	0.0022629	1-31/10/2015	
1/2016	5.8	wet	0.0003383	1-31/1/2016	1/11- 31/12/2015=0
2/2016	9	wet	0.0005611	1-28/2/2016	
3/2016	62.2	wet	0.0036277	1-31/3/2016	
4/2016	0.6	wet	3.616E-05	1-30/4/2016	
7/2016	1.2	wet	6.999E-05	1-31/7/2016	1/5-30/6/2016=0
8/2016	12.8	wet	0.0007465	1-31/8/2016	
10/2016	32.4	wet	0.0018897	1-31/10/2016	1-30/9/2016=0
1/2017	12.6	dry	0.0007349	1-31/1/2017	1/11- 31/12/2016=0
2/2017	0.6	dry	3.874E-05	1-28/2/2017	
3/2017	31.4	dry	0.0018313	1-31/3/2017	
4/2017	17	dry	0.0010245	1-30/4/2017	
5/2017	1.8	dry	0.000105	1-31/5/2017	
7/2017	12.4	dry	0.0007232	1-31/7/2017	1-30/6/2017=0
9/2017	1.2	dry	7.232E-05	1-30/9/2017	1-31/8/2017=0

**Table A-5-2 Abstraction by the pumping wells (2000-2008)**

Year of Pumping Well ID	2000	2001	2002	2003	2004	2005	2006	2007	2008
Well 1	-1474	-2900	-3500	-3600	-5500	-2400	-4600	-16000	-2940
Well 2	-1474	-2900	-3500	-3600	-5500	-2400	-4600	-16000	-2940
Well 3	-1474	-2900	-4100	-9000	-10200	-10000	-16560	-16000	-2940
Well 4	-1814	-4080	-10500	-9000	-10200	-10000	-16560	-9600	-6800
Well 5	-1814	-4080	-10500	-9000	-10200	-10000	-16560	-9600	-6800
Well 6	-1814	-4080	-10500	-9000	-10200	-10000	-16560	-9600	-6800
Well 7	-1814	-4080	-9800	-9000	-10200	-10000	-16560	-9600	-6500
Well 8	-1814	-4080	-9800	-8400	-8500	-10000	-4600	-9600	-6500
Well 9	-1814	-4080	-9800	-8400	-8500	-2400	-4600	-9600	-6500
Well 10	-1814	-4080	-9800	-8400	-8500	-2400	-4600	-9600	-6800
Well 11	-1814	-4080	-9800	-8400	-8500	-2400	-4600	-9600	-6800
Well 12	-1814	-4080	-9800	-9000	-10200	-10000	-16560	-9600	-6800
Well 13	-1814	-4080	-9800	-9000	-10200	-10000	-16560	-9600	-6800
Well 14	-1814	-4080	-9800	-9000	-10200	-10000	-16560	-9600	-6800
Well 15	-1814	-4080	-10500	-9000	-10200	-10000	-16560	-9600	-6800
Well 16	-1814	-4080	-10500	-9000	-10200	-10000	-16560	-9600	-6800
Well 17	-1814	-4080	-10500	-9000	-10200	-10000	-16560	-9600	-6800
Well 18	-1814	-4050	-10500	-9000	-10200	-10000	-16560	-9600	-6800
Well 19	-1814	-4050	-10500	-9000	-10200	-10000	-16560	-9600	-6800
Well 20	-1814	-4050	-10500	-9000	-10200	-10000	-16560	-9600	-6800
Well 21	-1814	-4050	-10500	-9000	-10200	-10000	-16560	-9600	-6800
Well 22	-1814	-4050	-10500	-9000	-10200	-10000	-16560	-9600	-6800

**Table A-5-3 Abstraction by the pumping wells (2009-2017)**

Year of Pumping Well ID	2009	2010	2011	2012	2013	2014	2015	2016	2017
Well 1	-7310	-5625	-5625	-7225	-9500	-7500	-7500	-7500	-5625
Well 2	-7310	-5625	-5625	-7225	-9500	-7500	-7500	-7500	-5625
Well 3	-7310	-5625	-5625	-7225	-9500	-7500	-7500	-7500	-5625
Well 4	-10370	-7777.5	-7777.5	-10200	-15000	-10370	-10370	-10000	-7500
Well 5	-10370	-7777.5	-7777.5	-10200	-15000	-10370	-10370	-10000	-7500
Well 6	-10370	-7777.5	-7777.5	-10200	-15000	-10370	-10370	-10000	-7500
Well 7	-10370	-7777.5	-7777.5	-10200	-15000	-10370	-10370	-10000	-7500
Well 8	-10370	-7777.5	-7777.5	-10200	-15000	-10370	-10370	-10000	-7500
Well 9	-10370	-7777.5	-7777.5	-10200	-15000	-10370	-10370	-10000	-7500
Well 10	-10370	-7777.5	-7777.5	-10200	-15000	-10370	-10370	-10000	-7500
Well 11	-10370	-7777.5	-7777.5	-10200	-15000	-10370	-10370	-10000	-7500
Well 12	-10370	-7777.5	-7777.5	-10200	-15000	-10370	-10370	-10000	-7500
Well 13	-10370	-7777.5	-7777.5	-10200	-15000	-10370	-10370	-10000	-7500
Well 14	-10370	-7777.5	-7777.5	-10200	-15000	-10370	-10370	-10000	-7500
Well 15	-10370	-7777.5	-7777.5	-10200	-15000	-10370	-10370	-10000	-7500
Well 16	-10370	-7777.5	-7777.5	-10200	-15000	-10370	-10370	-10000	-7500
Well 17	-10370	-7777.5	-7777.5	-10200	-15000	-10370	-10370	-10000	-7500
Well 18	-10370	-7777.5	-7777.5	-10200	-15000	-10370	-10370	-10000	-7500
Well 19	-10370	-7777.5	-7777.5	-10200	-15000	-10370	-10370	-10000	-7500
Well 20	-10370	-7777.5	-7777.5	-10200	-15000	-10370	-10370	-10000	-7500
Well 21	-10370	-7777.5	-7777.5	-10200	-15000	-10370	-10370	-10000	-7500
Well 22	-10370	-7777.5	-7777.5	-10200	-15000	-10370	-10370	-10000	-7500





## PLAGIRISM CERTIFICATE

1. We, Dr. Syed Mohammed Tauseef (Internal Guide) & Dr. Ahmed Sana (External Co-Guide) certify that the Thesis titled “**Customization of MODFLOW and MT3DMS Models for Integrated Water Resource Management in Coastal Aquifers in the Sultanate of Oman**” submitted by Scholar Mr. Javed Akhtar having SAP ID: 500055804 has been run through a Plagiarism Check Software and the Plagiarism Percentage is reported to be **11%**.

It may be noted that the report has been generated excluding the papers published by the scholar in open literature which are now available online. Also, there are multiple internet sources that have indexed the papers.

2. Akhtar, J., Sana, A. & Tauseef, S.M. Using MODFLOW to investigate the effect of persistent water deficit in Al-Jizi coastal aquifer, Sultanate of Oman. *Arab J Geosci* **15**, 1448 (2022). <https://doi.org/10.1007/s12517-022-10717-y>
3. Akhtar J, Sana A, Tauseef SM, Tanaka H. Numerical Modeling of Seawater Intrusion in Wadi Al-Jizi Coastal Aquifer in the Sultanate of Oman. *Hydrology*. 2022; 9(12):211. <https://doi.org/10.3390/hydrology9120211>
4. Akhtar, J., Sana, A., Tauseef, S.M. *et al.* Evaluating the groundwater potential of Wadi Al-Jizi, Sultanate of Oman, by integrating remote sensing and GIS techniques. *Environ Sci Pollut Res* **29**, 72332–72343 (2022). <https://doi.org/10.1007/s11356-021-17848-x>
5. Plagiarism Report generated by the Plagiarism Software is attached.

**Signature of the Internal Guide**

**Signature of External Co-Guide**

**Signature of the Scholar**

## SIMILARITY REPORT

### PhD Thesis

#### ORIGINALITY REPORT

<b>11</b> %	<b>10</b> %	<b>9</b> %	%
SIMILARITY INDEX	INTERNET SOURCES	PUBLICATIONS	STUDENT PAPERS

#### PRIMARY SOURCES

<b>1</b>	<b>ascelibrary.org</b> Internet Source	<b>1</b> %
<b>2</b>	<b>dr.ddn.upes.ac.in:8080</b> Internet Source	<b>1</b> %
<b>3</b>	<b>hdl.handle.net</b> Internet Source	<b>1</b> %
<b>4</b>	<b>www.researchgate.net</b> Internet Source	<b>1</b> %
<b>5</b>	<b>docplayer.net</b> Internet Source	<b>&lt;1</b> %
<b>6</b>	<b>www.hydroshare.org</b> Internet Source	<b>&lt;1</b> %
<b>7</b>	<b>"Groundwater in the Nile Delta", Springer Science and Business Media LLC, 2019</b> Publication	<b>&lt;1</b> %
<b>8</b>	<b>moam.info</b> Internet Source	<b>&lt;1</b> %
<b>9</b>	<b>Ahmed Al Barwani, Tariq Helmi. "Sea Water Intrusion in a Coastal Aquifer: A Case Study</b>	<b>&lt;1</b> %